

# HYDROLOGIC AND HYDRAULIC DESIGN OF CULVERTS AND BRIDGES

## A DISSERTATION

*Submitted in partial fulfillment of the  
requirements for the award of the degree  
of*  
**MASTER OF TECHNOLOGY**  
*in*  
**WATER RESOURCES DEVELOPMENT**

By

**VU THAI LONG**



**DEPARTMENT OF WATER RESOURCES DEVELOPMENT AND MANAGEMENT  
INDIAN INSTITUTE OF TECHNOLOGY ROORKEE  
ROORKEE -247 667 (INDIA)  
JUNE, 2006**

## CANDIDATE'S DECLARATION

I hereby declare that the dissertation titled “**Hydrologic and Hydraulic Design of Culverts and Bridges**” which is being submitted in partial fulfillment of the requirement for the award of Degree of **Master of Technology in Water Resources Development (Civil)** at the department of Water Resources Development and Management (WRD&M), Indian Institute of Technology, Roorkee is an authentic record of my own work carried out during the period of July, 2005 to June, 2006 under the supervision and guidance of **Dr. M.L. Kansal and Prof. G.C. Mishra**.

I have not submitted the matter embodied in this dissertation for the award of any other degree.

Place: Roorkee

Dated: June, 2006



.....  
**Vu Thai Long**

This is to certify that the above statement made by the candidature is correct to the best of our knowledge.



.....  
**M.L. Kansal**

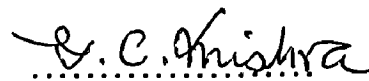
Associate Professor, WRD&M

IIT, Roorkee

Roorkee-247667

(India)

27/6/06



.....  
**G.C. Mishra**

Professor, WRD&M

IIT, Roorkee

Roorkee-247667

(India)

## ACKNOWLEDGEMENT

I take this opportunity to express my profound sense of gratitude and grateful regards to **Dr. M.L. Kansal and Prof. G.C. Mishra**, for their inspiring and constant encouragement during the period of preparing this dissertation work.

I am greatly thankful to Dr.S.K. Tripathi Professor & Head of WRD&M, IIT Roorkee for extending various facilities in completion of this dissertation.

I wish to express my thanks to Ministry of Water Resources of Viet Nam for giving me an opportunity to undergo M.Tech course at IIT Roorkee.

I am also grateful to the staff of WRD&M who extended all cooperation whenever required. I am thankful to all the staffs of computer lab and computer center for helping me in analyzing the data through computer. I am also thankful to the librarians for providing help on time.

I can not forget to express my profound gratitude and indebtedness to my parents. From the bottom of my heart, I thank my wife and my kid who extended their full moral support and encouraged me throughout the course of my study.

It would be unworthy, if I don't express my cordial thanks to all my friends who help in preparing this report.

Last but not the least, I would like to thank the Government of India for providing me this opportunity to study at IIT, Roorkee, India.

Place: Roorkee

**Vu Thai Long**

# **CONTENTS**

---

	<b>PAGE NO</b>
<b>CANDIDATE'S DECLARATION</b>	<b>(I)</b>
<b>ACKNOWLEDGEMENT</b>	<b>(II)</b>
<b>CONTENTS</b>	<b>(III)</b>
<b>LIST OF FIGURES</b>	<b>(VI)</b>
<b>LIST OF TABLES</b>	<b>(VIII)</b>
<b>LIST OF NOTATIONS</b>	<b>(IX)</b>
<b>ABSTRACT</b>	<b>(XI)</b>
<b>CHAPTERS</b>	
<b>1. INTRODUCTION</b>	<b>1-4</b>
<b>2. HYDROLOGIC DESIGN FOR UNGAUGED CATCHMENT</b>	<b>5-57</b>
2.1. General	
2.2 SCS-CN method	
2.3 Kinematics wave method	
2.3.1 General	
2.3.2 Statement of problem	
2.3.3 Analysis	
2.3.3.1 Continuity equation	
2.3.3.2 Characteristic equation	
2.3.3.3 Overland flow for uniform rainfall excess condition	
2.3.3.4 Velocity of flow of depth $y$	
2.3.3.5 Water surface profile and discharge hydrograph when $(t_c < t_r < \infty)$	
2.3.3.6 Water surface profile and discharge hydrograph when $(t_r < t_c)$	
2.3.3.7 Under varying rainfall intensity	
Appendix I – Computer programe	

## 2.4 Infiltration

### 2.4.1 General

### 2.4.2 Continuity

### 2.4.3 Momentum

### 2.4.4 Green-Ampt parameters

### 2.4.5 Ponding time

### Appendix II – Computer programe

## 2.5 Overland flow study for Wirpur Nulla watershed

### 2.5.1 General

### 2.5.2 Study SCS method for Wirpur Nulla Watershed

### 2.5.3 Study Kinematic wave method for Wirpur Nulla Watershed

### 2.5.4 Discussion of results

### Appendix III A – Result by using SCS-CN method

### Appendix III B- Result by using Kinematic wave method

## **3 HYDRAULIC DESIGN OF CULVERTS**

**58-72**

### 3.1 Flow controls in culverts

#### 3.1.1 Inlet control

#### 3.1.2 Outlet control

#### Example

#### Conclusion

## **4 HYDRAULIC DESIGN OF BRIDGES**

**73-140**

### 4.1 General

### 4.2 Hydraulics of Bridge waterway

#### 4.2.1 General

#### 4.2.2 Computation of Backwater

##### 4.2.2.1 Expression of Backwater

##### 4.2.2.2 Backwater coefficient

4.2.2.3	Difference in water level across approach embankment	
4.2.2.4	Distance to point of maximum Backwater	
4.3	Evaluating scour of bridge	
4.3.1	General	
4.3.2	Total scour	
4.3.3	Estimating scour at bridge	
	Example	
	Discussion of result and Conclusion	
<b>5</b>	<b>Conclusion and scope for future work</b>	<b>141-143</b>
	<b>REFERENCE</b>	<b>144-145</b>

## List of Figures

<i>Figure no.</i>	<i>Title</i>	<i>Page no.</i>
2.1a	Catchment pattern for overland flow analysis	9
2.1b	Section of the catchment	10
2.2	Rainfall excess pattern	10
2.3	Water surface profile	12
2.4	The elementary control volume in one dimensional flow Surface	13
2.5	The water surface profile	16
2.6	The shape of resulting hydrograph	17
2.7	Discharge hydrograph when $t_c < t_r$	21
2.8	The water surface profile when $t_c < t_r$	22
2.9	The water surface profile after cessation of rainfall	22
2.10	The water surface profile when $t_r < t_c$	24
2.11	Discharge hydrograph when $t_r < t_c$	26
2.12	Variables in the Green Ampt infiltration model	30
2.13	Infiltration into a column of soil of unit cross-sectional Area for the Green-Ampt model	31
2.14	Soil moisture before, during and after ponding occurs	34
2.15	Infiltration rate and cumulative infiltration for ponding Under constant intensity rainfall	36
2.16	Catchment plan for Wirpur Nulla watershed	41
2.17	0.5 hour unit hydrograph	42
2.18	Rainfall & Infiltration rate of three event	46
2.19	1 hour unit hydrograph	49
2.20	Hydrograph – Event 1	51
2.21	Hydrograph – Event 2	52
2.22	Hydrograph – Event 3	52
3.1	Different type of cross section of culvert	58
3.2	Four standard inlet type	59

3.3	Types of inlet control	60
3.4	Types of outlet control	65
3.5	Full-flow energy and hydraulic grade lines	67
4.1	Normal crossing	75
4.2	Type of water flow	76
4.3	Water profile	77
4.4	Aid for estimating $\alpha_2$	79
4.5	Backwater coefficient base curves	80
4.6	Incremental Backwater coefficient for piers	81
4.7	Incremental Backwater coefficient for eccentricity	82
4.8	Skewed crossings	83
4.9	Incremental Backwater coefficient for skew	84
4.10	Differential water level ratio base curves	85
4.11	Distance to maximum backwater	88
4.12	Schematic representation of scour at a cylindrical pier	99
4.13	Fall velocity of sand-sized particles	116
4.14	Common pier shapes	119
4.15	Abutment shapes	122
4.16	Abutments project into channel, no overbank flow	123
4.17	Bridge abutment in main channel and overbank flow	128
4.18	Bridge abutment set back from main channel bank and Relief bridge	129
4.19	Abutment set at edge of main channel	130
4.20	Scour estimate adjustment for skew	131



## List of Tables

<i>Table no</i>	<i>Title</i>	<i>Page no</i>
2.1	Model Geometry of the Wirpur Nulla	43
2.2	Parameter of clay soil	44
2.3	Observed and computed peak discharge	44
2.4	Percentage absolute error in peak discharge	45
2.5	Compute excess rainfall (event I)	47
2.6	Compute excess rainfall (event II)	47
2.7	Compute excess rainfall (event III)	48
2.8	Computation one hour unit hydrograph	48
2.9	Runoff hydrograph (event I)	49
2.10	Runoff hydrograph (event II)	50
2.11	Runoff hydrograph (event III)	51
3.1	Constants for inlet control design equations	63
3.2	Manning n values for culverts	68
3.3	Entrance loss coefficients for outlet control	68
3.4	Compare four type of culverts	69
4.1	Increase in equilibrium pier scour depth for bed Condition( $K_3$ )	118
4.2	Correction factor $K_1$ for pier nose shape	119
4.3	Correction factor $K_2$ for angle of attack of the flow	119
4.4	Abutment scour cases	122

## Notations/ Symbols

- $P$  = Total rainfall(mm)
- $I_a$  = Initial abstraction(mm)
- $F$  = Cumulative infiltration excluding  $I_a$ (mm)
- $Q$  = Direct runoff(mm)
- $S$  = Potential(mm)
- $CN$  = Curve number
- $q$  = flow rate( $m^3/s$ )
- $r$  = rainfall intensity(mm/min)
- $y$  = depth of flow(m)
- $n$  = roughness coefficient
- $S_o$  = bed slope
- $x$  = Distance from the boundary of catchment(m)
- $t$  = time(hr)
- $t_c$  = time of concentration(hr)
- $\theta_i$  = Initial moisture content
- $\eta$  = porosity
- $F$  = Cumulative infiltration(m)
- $h_o$  = ponded depth(m)
- $\psi$  = Suction head(m)
- $K$  = Hydraulic conductivity
- $S_e$  = Effective porosity
- $\theta_r$  = The residual moisture content
- $t_p$  = Ponding time(hr)
- $f$  = Infiltration rate(mm/min)
- $i$  = rainfall rate(mm/min)
- $H_w$  = headwater depth(m)ft
- $D$  = Interior height of the culvert barrel(m)ft.
- $A$  = Full cross-sectional area of the culvert barrel( $m^2$ ),ft<sup>2</sup>
- $C$  and  $Y$  = Constants

- $d_c$  = The critical depth(m)ft
- $V_c$  = The critical velocity(m/s)ft/s
- $H$  = Total head loss(m)ft
- $H_o$  = Exit loss(m)ft
- $H_e$  = entrance loss(m)ft
- $H_f$  = Friction loss(m)ft
- $h^*_1$  = Total backwater(m)
- $K^*$  = Total backwater coefficient
- $\alpha_1, \alpha_2$  = Kinetic energy coefficient
- $A_{n2}$  = Gross water area under bridge(m<sup>2</sup>)
- $V_{n2}$  = Average velocity in constriction(m/s)
- $\Delta h$  = difference in water surface elevation between the upstream and downstream side of bridge(m)
- $L^*$  = Distance to point of maximum backwater(m)
- $S_s$  = Specific gravity of bed material
- $W_1$  = Bottom width of the upstream main channel(m)
- $W_2$  = Bottom width of the main channel in the contracted section(m)
- $Q_1$  = Upstream flow (m<sup>3</sup>/s)
- $Q_2$  = Flow in the contracted channel(m<sup>3</sup>/s)
- $\tau$  = Shear stress on the bed(N/m<sup>2</sup>)
- $\rho$  = density of water(1Ton/m<sup>3</sup>)
- $w$  = fall velocity of bed material based on the  $D_{50}$ (m/s)
- $g$  = Acceleration of gravity (9.81m/s<sup>2</sup>)
- $S_1$  = Slope of energy grade line of main channel
- $y_s$  = Depth of scour(m)
- $K_1$  = Correction factor for pier nose
- $K_2$  = Correction factor for angle of attack of flow
- $K_3$  = Correction factor for bed condition
- $a$  = Pier width(m)
- $a'$  = Length of abutment (m)

## **ABSTRACT**

Bridges and culverts are important structures on highways. Hydrological and Hydraulic design of such structures is an important activity for the civil engineers. The aim of present study is to study in detail the hydrologic and hydraulic aspects of such design.

For designing the bridges or culverts, one of the most important hydrologic parameter is to estimate the design peak flood that is desired to pass off safely without harming the structure. To estimate peak runoff from adjoining areas in an ungauged catchment, there are several methods suggested in the literature. In the present study, the SCS method and Kinematic wave method are described in detail. SCS method compute the volume of surface runoff for a given rainfall event from small agricultural, forest, and urban watersheds. Once the volume of surface runoff is estimated. It is important to estimate peak runoff ,so synthetic unit hydrograph is used to compute peak runoff but also hydrograph of runoff. In Kinematic wave method, water surface profile and surface runoff hydrograph under varying rainfall excess, have been obtained using method of characteristics. The varying rainfall excesses are divided into small time interval and the average value of the rainfall excesses are considered to remain uniform in each respective time intervals. The time variant infiltration values are calculated by using Green and Ampts infiltration equation. From these time variant infiltration values, the varying rainfall excesses are found out and these values are used to find the water surface profile and surface runoff hydrographs.

In culverts, there are two basic types of flow control - inlet control and outlet control. In hydraulic design, depending on the type of flow control, the headwater elevation is estimated by assuming dimensions of culvert.

Bridges enable streams to maintain flow conveyance and to sustain aquatic life. In order to minimize the risk of failure, one must recognize and consider the hydraulic requirements of a stream crossing during the development. Following aspects of hydraulic design of a bridge are considered in the present work :

- Estimation of water surface profile (computation of backwater)
- Estimation of scour potential

In estimation of water surface profile, backwater depends on bridge constriction, piers, skew, and eccentricity. Depending on backwater, scour potential is estimated. After estimation of all components of scour, one has to consider the economic aspect, and decide if bridge should be expanded or constricted.

## INTRODUCTION

Culverts and bridges are important highway structures vulnerable to failure from flood. In order to minimize the risk of failure, we must recognize and consider the hydraulic requirements of a stream crossing the highway. A culvert is a hydraulically short closed conduit that conveys streamflow through a road embankment or some other type of flow obstruction. Usually, it is defined as a structure under roadway for drainage with a clear opening of 20 ft(6m) or less measured along the center of the roadway between inside of end wall. The flow in culverts may be full flow over all its length or partly full, resulting in pressurized flow and/or open channel flow. The characteristics of flow in culverts are very complicated because the flow is controlled by many variables, including inlet geometry, slope, size, flow rate, roughness, and approach and tail water conditions.

Bridges are usually defined as those structures which are more than 20 ft. (6 m) along the roadway centerline between the insides of the end walls. Bridges, as distinguished from culverts, are usually supported on piers or abutments. The bridge is integrated into both the stream and the roadway and must be fully compatible with both.

The objective of present study is to study the hydrologic and hydraulic aspects of culverts and bridge design.

In hydrologic design, the basic parameter required is to estimate the peak discharge which these structures are desired to pass off safely without causing any flooding. Since most of these structures pass the runoff from ungauged small catchments, the major part of the study deals with the estimation of peak runoff from ungauged catchments. Many methods are

reported in the literature for estimating the peak flood for ungauged catchment. In present study, SCS method and kinematic wave method are discussed to estimate the design flood.

SCS method is one of the most popular methods which is simple, easy to understand and apply, stable and useful for ungauged watersheds. This method rely on only one parameter, the curve number CN, which is a function of the major runoff-producing watershed characteristics: soil type, land use, surface condition, and antecedent moisture condition.

In Kinematics study, idealized overland flow is considered by assuming the catchment as two identical rectangular planes joined to form a V shape along the apex of which a line stream can flow. The surface roughness (n), slope (S) and flow regime will be assumed invariant in space and time.

The solution of the overland flow problem is derived using the following continuity and momentum equations:

$$\frac{\partial q}{\partial y} \frac{\partial y}{\partial x} + \frac{\partial y}{\partial t} = r$$

$$\text{and } q = \frac{1}{n} S_o^{1/2} y^{5/3}$$

where  $y$ = depth of flow

$q$ = discharge per unit width

$r$ = rainfall intensity

$n$ = roughness coefficient

$S_o$ = bed slope

$x$ = distance from the boundary of catchment

$t$ = time

In order to consider the infiltration, the actual infiltration rate at different periods of time is considered using Green and Ampts equation. The

varying rate of rainfall excess values are found out and utilized for the study of water surface profile and surface run off hydrograph. A Computer programmes has been written in C++ for the same.

In the hydraulic design of culverts, the flow characteristics are studied that involve many variables like inlet geometry, slope, size, flow rate, roughness, and approach and tail water conditions. Culverts have numerous cross-sectional shapes, material, and types of inlets. There are two basic types of flow control in culverts : inlet control and outlet control. In inlet control, flow is supercritical, shallow with high velocity, whereas, in outlet control, flow is sub-critical, deep with low velocity. So, it is desired to compare results of inlet control with outlet control to choose the best section.

Inlet design is important because the hydraulic capacity of a culvert may be improved by the appropriate inlet selection. Natural channels are usually much wider than the culvert barrel, so that the inlet is a flow contraction and can be the primary flow control.

Hydraulic analysis is required for designing all new bridges over waterways, bridge widening, bridge replacement, and roadway profile modifications that may adversely affect the floodplain, even if no structural modifications are necessary. Typically, this should include the following:

- i) Existing and proposed condition(s) of water surface profiles
- ii) Consideration for scour potential.

There can be three conditions of flow, which are : sub-critical, critical, and supercritical. Critical flow and supercritical flow don't make serious backwater. However, sub-critical flow creates the problem of back-water. Thus, in the present study, backwater computations have been considered for sub-critical flow.

Another most common effect of floods in bridges is the scouring of bridge foundation. Total scour at a highway crossing is comprised of three components, which are :



1. Long-term aggradation and degradation,
2. Contraction scour, and
3. Local scour.

In addition, lateral migration of the stream is considered while evaluating total scour at piers and abutments of highway crossings.

## **ORGANIZATION OF THE DISSERTATION**

Chapter – 1 introduces the culverts and bridges. It discusses the issues in the hydrologic and hydraulic design of culverts and bridges.

Chapter – 2 Discusses the hydrologic design of culverts and bridges. It discusses the methods of estimating the peak discharge and the runoff volume from an ungauged catchment. It describes the SCS and Kinematics methods.

Chapter – 3 discusses about the various parameters used in the hydraulic design of culverts. It discusses the types of control and the design procedure.

Chapter – 4 presents hydraulic design of bridges which comprises of the study of hydraulic bridge waterway and the evaluation of potential scour at piers and abutment of bridges.

Chapter – 5 discusses the results and summarize the conclusions.

---

## HYDROLOGIC DESIGN FOR UNGAUGED CATCHMENT

### 2.1 GENERAL

Many methods are used to estimate peak runoff for ungauged catchment; different methods developed for determining flood runoff may produce different results for a particular situation. In this thesis, SCS-CN method and Kinematic wave method are studied. SCS –CN method (Soil Conservation Service – Curve Number) developed the runoff curve number method as a means of estimating the amount of rainfall appearing as runoff, and a dimensionless unit hydrograph to provide estimation of peak discharges and runoff hydrographs from complex watersheds. Kinematic wave approach has been applied to describe flow over planes, as a model of the rainfall-runoff process. In this application the lateral flow is equal to the difference between the rates of rainfall and infiltration, and the channel flow is taken to be flow per unit width of plane. The characteristic equations can be solved analytically to simulate the outflow hydrograph in response to rainfall of a specified duration. By accumulating the flow from many such planes laid out over a watershed, an approximate model can be developed for the conversion of rainfall into streamflow at the watershed outlet.

### 2.2 SCS-CN Method

The SCS-CN method is based on the water balance equation and two fundamental hypotheses. The first hypothesis equates the ratio of the actual amount of direct surface runoff ( $Q$ ) to the total rainfall ( $P$ ) ( or maximum potential surface runoff) to the ratio of the amount of actual infiltration ( $F$ ) to the amount of the potential maximum retention ( $S$ ). The second hypothesis

relates the initial abstraction ( $I_a$ ) to the potential maximum retention. Thus, the SCS-CN method consists of

a) Water balance equation:

$$P = I_a + F + Q \quad (2.1)$$

b) Proportional equality hypothesis

$$\frac{Q}{P - I_a} = \frac{F}{S} \quad (2.2)$$

c)  $I_a$ -S hypothesis:

$$I_a = \lambda S \quad (2.3)$$

where  $P$  = total rainfall (cm),

$I_a$  = initial abstraction (cm),

$F$  = cumulative infiltration excluding  $I_a$  (cm),

$Q$  = direct runoff (cm), and

$S$  = potential maximum retention or infiltration.(cm)

Combining equation (2.1) and (2.2), the popular form of the SCS-CN method is obtained:

$$Q = \frac{(P - I_a)^2}{P - I_a + S} \quad (2.4)$$

Equation (2.4) is valid for  $P \geq I_a$ ;  $Q=0$  otherwise. For  $\lambda=0.2$ , equation (2.4) can be rewritten as

$$Q = \frac{(P - 0.2S)^2}{P + 0.8S} \quad (2.5)$$

Since parameter  $S$  can vary in the range of  $0 \leq S \leq \infty$ , it is mapped into a dimensionless curve number (CN), varying in a more appealing range

$0 \leq CN \leq 100$ , as follows:

$$S = \left( \frac{1000}{CN} - 10 \right) * 25.4 \quad (2.6)$$

The curve number 'CN' takes care of various factors influencing runoff. The 'CN' mainly depends upon the soil type, general hydrologic condition of watershed, land use and treatment practices and antecedent moisture conditions. Standard tables are available for 'CN' for different land uses, hydrologic Soil groups and antecedent moisture condition.

Soil conservation service (SCS) is one of the simple and commonly used technique for estimation of direct runoff depth from storm rainfall. In this approach the peak discharge and time to peak resulting from a particular storm falling over the watershed, are computed assuming the synthetic unit hydrograph shape as triangular one.

### **Synthetic Unit Hydrograph**

Time to peak: For a rainfall excess of 'D' hours duration the time to peak is given as

$$t_p = 0.5D + t_L$$

where  $t_p$  is time to peak in hours ;

D is duration of rainfall excess in hour ,  $D=0.133 T_c$  ;

$t_L$  is time lag, defined as the time difference between the mid of rainfall excess to peak of the hydrograph, in hours,  $t_L=0.6 T_c$  ;

$T_c$  is concentration time.

Recession Time: Recession time ( $t_R$ ) is given as

$$t_R = 1.67 t_p$$

### **Peak Discharge**

$$q_p = \frac{CA}{t_p}$$

where  $C=2.08$  and A is the drainage area in square kilometers, and

$q_p$  is the discharge ( $m^3/s.cm$ )

## Flood Hydrograph Computation

For a storm event having excess rainfall blocks of  $P_1, P_2, P_3, \dots$  etc., the flood hydrograph ordinates (DSRO) can be computed using the following convolution summation equation:

$$Q_j = \sum_{i=1}^j P_i U_{j-i+1}$$

where  $Q_j$  is the direct surface runoff

$P_i$  is the excess rainfall of  $i$ th block and

$U_j$  is the  $j$ th ordinate of  $D$ -hour unit hydrograph .

## **2.3 KINEMATIC WAVE METHOD**

### **2.3.1 General**

Study of Kinematics of overland flow includes the study of overland water surface profile and flow hydrograph. Many investigators have studied the Kinematics of overland flow for uniform rainfall excess. In reality , because of high rate of infiltration during the early hours of rainfall, the rainfall excess is not uniform. In the present study analysis of overland flow under time variant rainfall excess has been done.

Equation of continuity and momentum equation are utilized to find the characteristics equation. The characteristics equations are used to find water surface profile and the flow hydrograph.

When the rainfall intensity varies, there will not be any steady water surface profile. The profile will go on changing from the boundary of the catchment. When the rainfall intensity increases, the profile will continue to go higher up. It is difficult to find the profile under such circumstances.

In the present analysis the rainfall duration is divided into small time interval and the rainfall excess is assumed to be uniform in each interval of time.

### 2.3.2 Statement of problem

The catchment for which the overland flow analysis has been done is shown in figure 2.1 (a). The catchment consists of two identical rectangular planes of length  $L$  joined to form an open book. The whole system is slightly raised to cause a flow in the stream. The surface roughness ( $n$ ), slope ( $S$ ) and flow regime is assumed invariant in space and time.

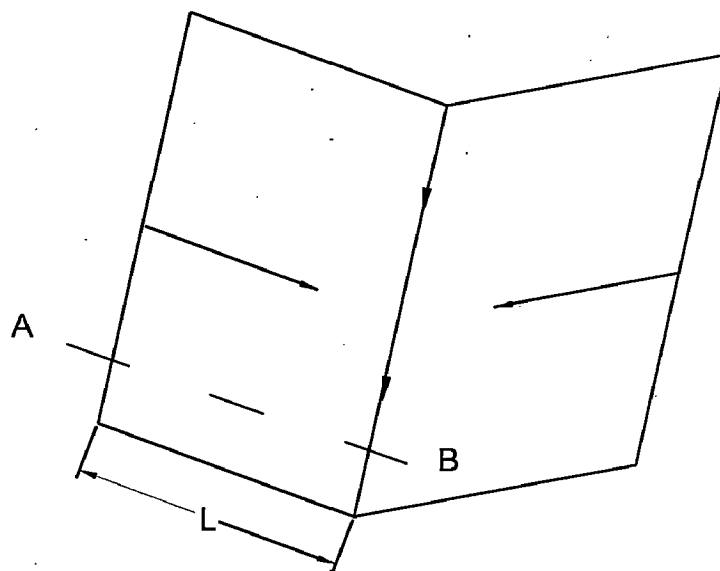


Fig. 2.1 (a)

Figure 2.1(b) shows a section of the catchment through AB. This is the elemental section considered for overland flow. It is assumed that point '0' is the water divide and the depth of flow at point '0' is zero for all time. Point D is the outfall. Before the onset of rainfall, the depth of water at every point between '0' and D zero.

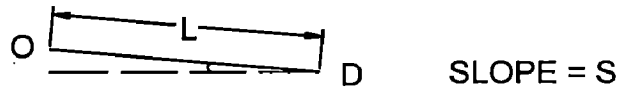


Fig. 2.1(b)

The rainfall excess under which the overland flow and water surface profile are intended to compute are shown in figure 2.2. As seen from the figure the rainfall excess is time variant. The rain continues upto time  $t_r$ . The determination of response of catchment to such an excitation is the aim of present analysis.

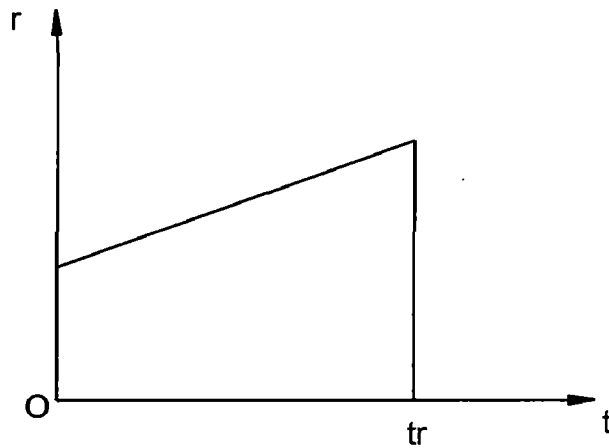


Fig. 2.2

### 2.3.3 Analysis

The time variant rainfall excess are discretized into small time step and average value of the rainfall excess for that time step are considered to continue uniformly for that period. So the solution of the varying rainfall excess is done starting from the uniform rainfall excess analysis.

#### 2.3.3.1 Continuity equation

For steady flow, the equation of continuity of flow through any channel states that the quantity of fluid passing through any transverse section in a given interval of time must be equal at all sections.

But when a flood wave approaches or when the input is also spatially distributed, then the continuity equation for a particular reach can be written as:

Input –output=Change in storage

$$I - Q = \frac{ds}{dt}$$

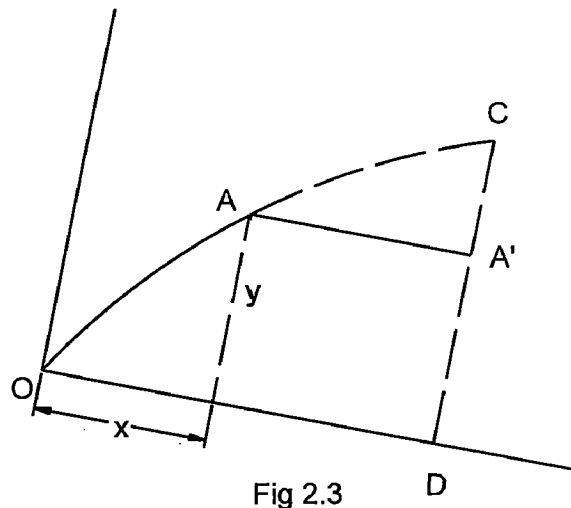
where I= Input

Q= Output

S= Storage

$\frac{ds}{dt}$  =change of storage

As the rainfall continues, the depth of overland flow increases and takes the shape like OAC ( as shown in the figure 2.3). The shape of profile changes with time.



Hence, y is a function of x and t.

$$y=f(x,t)$$



where  $y$  = depth at a distance  $x$  from boundary after time  $t$  from the start of rainfall.

The total derivative of  $y$  is given by:

$$dy = \frac{\partial y}{\partial x} .dx + \frac{\partial y}{\partial t} .dt \quad (2.7)$$

Mannings formula gives the stage discharge relationship as

$$q = \frac{1}{n} S_o^{1/2} y^{5/3} \quad (2.8)$$

where  $q$ = discharge per unit width .

$S_o$ = bed slope

$y$ = depth of flow

$n$ =roughness coefficient

A portion of flow profile, at a distance  $x$  from water divide, between two sections  $dx$  apart, is shown in fig.2.4

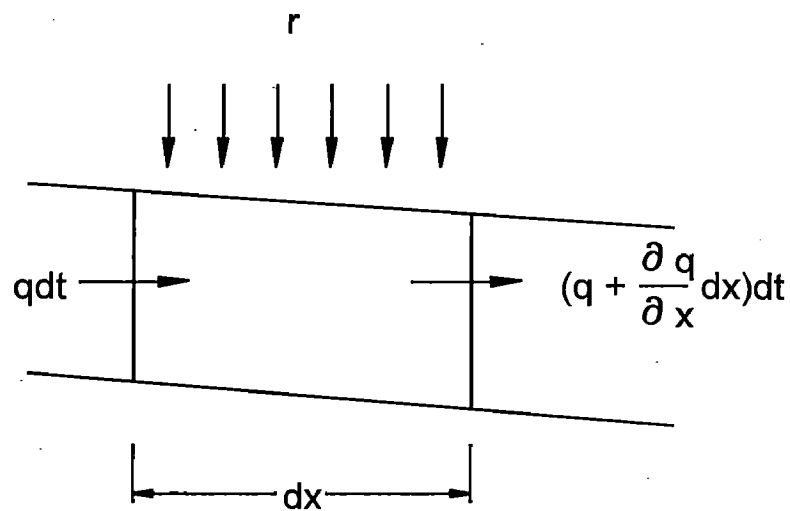


Fig 2.4

$r$  = rainfall intensity

$dx$  = length, i.e the distance between two sections of which the flow is considered

$dy$  = change in depth  $y$  in time  $dt$

$q$  = flow rate per unit width of catchment

Inflow =  $qdt + rdxdt$

Outflow =  $(q + \frac{\partial q}{\partial x} dx)dt$

Change of storage =  $dydx$

Inflow – outflow = change of storage

$$qdt + rdxdt - (q + \frac{\partial q}{\partial x} dx)dt = dydx \quad (2.9)$$

$$r - \frac{\partial q}{\partial x} = \frac{\partial y}{\partial t}$$

or 
$$\frac{\partial q}{\partial y} \frac{\partial y}{\partial x} + \frac{\partial y}{\partial t} = r \quad (2.10)$$

From Manning's Formula

$$q = \frac{1}{n} S_o^{1/2} y^{5/3}$$

$$\frac{\partial q}{\partial y} = \frac{1}{n} S_o^{1/2} \frac{5}{3} y^{2/3} \quad (2.11)$$

Substituting the value of  $\frac{\partial q}{\partial y}$  in equation (2.10)

$$\frac{1}{n} S_o^{1/2} \frac{5}{3} y^{2/3} \frac{\partial y}{\partial x} + \frac{\partial y}{\partial t} = r \quad (2.12)$$

### 2.3.3.2. Characteristic Equation

Comparing the equation (2.7) and (2.12) the characteristic equation are obtained and they are:

$$\frac{dx}{\frac{1}{n} S_o^{1/2} \frac{5}{3} y^{2/3}} = \frac{dt}{1} = \frac{dy}{r} \quad (2.13)$$

From this characteristic equation the following three equation are obtained

$$dx = \frac{1}{n} S_o^{1/2} \frac{5}{3} y^{2/3} dt \quad (2.14)$$

$$dx = \frac{1}{n} S_o^{1/2} \frac{5}{3} y^{2/3} \frac{dy}{r} \quad (2.15)$$

$$dy = r dt \quad (2.16)$$

### 2.3.3.3 Overland flow for uniform rainfall excess condition

It is assumed that there is no infiltration during and after the rainfall. The flow of water follows the characteristic equation as given in equation (2.13), (2.14), (2.15) and (2.16).

It follows

- (i) The initial condition that the depth is zero throughout the length of catchment

$$\text{i.e. } y=0 \quad \text{for } 0 \leq x < L$$

$$\text{at } t=0$$

- (ii) The boundary condition:

That the depth is zero at boundary of catchment for all time

$$\text{i.e. } y=0 \quad \text{at } x=0$$

$$\text{for } t > 0$$

As the rain falls on the catchment, it will start developing a depth profile. (Ref. Fig.2.5)  $Od$  is the length of catchment ( $L$ ). Point 'O' is the boundary of catchment and the depth of water is always zero here. If the rainfall is uniform it will give a steady profile like  $OABCD$ . Boundary excitation that starts from the point 'O' reaches the point A, B and C in time  $t_1, t_2$  and  $t_3$ . So after time  $t_1$  from the start of rain, the water surface profile is  $OAA'$ . Similarly at time  $t_2$  and  $t_3$  the profile becomes  $OBB'$  and  $OCC'$  respectively.

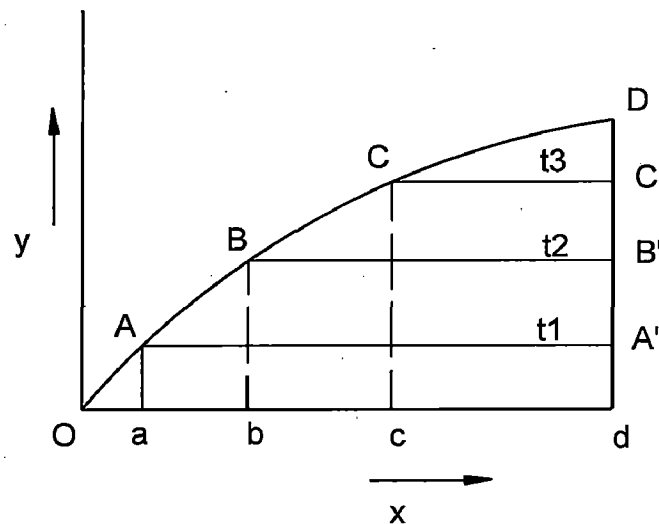


Fig 2.5

When the boundary excitation reaches the outfall point D, then the steady state profile is reached, and the time required to reach this state is called the time of concentration. Once the steady state condition is reached it will continue till the rainfall continues. When the rain stops, the depth will start decreasing and the outflow will be an exponentially decaying function of time.

The shape of resulting hydrograph under a rainfall case is shown in Fig.2.6, OE portion is the rising portion, EF is the steady state portion and FG is the recession portion. So the solution of the catchment outflow can conveniently be divided into three parts

- i) Rising portion
- ii) Steady state
- iii) Recession state

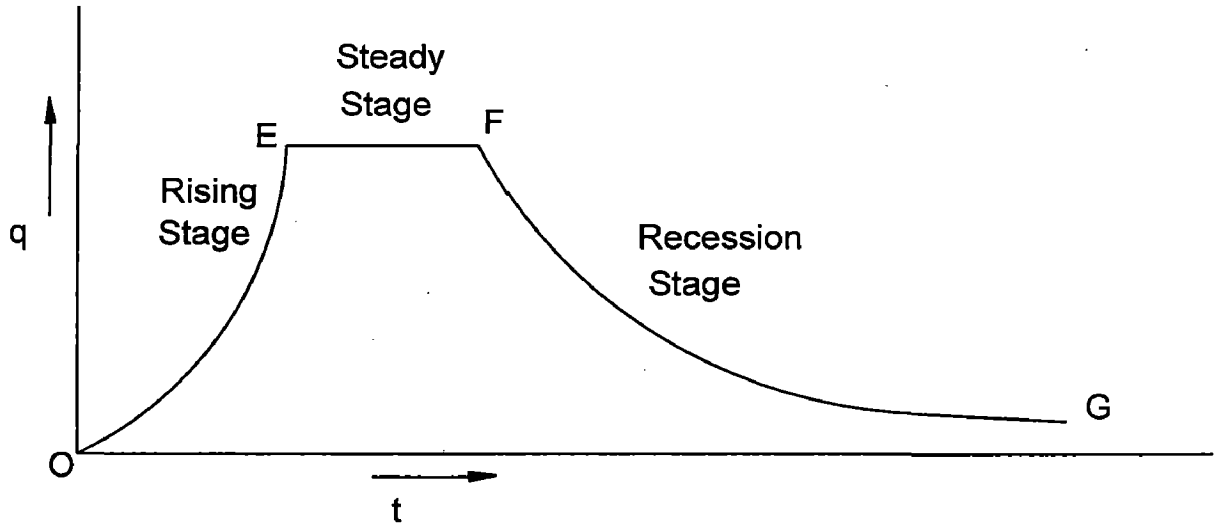


Fig 2.6

Time of concentration ( $t_c$ ) is the time taken by the runoff from farthest point of the catchment to reach the point of concentration.

### 2.3.3.4 Velocity of flow of depth y

The stage-discharge relation is given as

$$q = \frac{1}{n} S_o^{1/2} y^{5/3}$$

The characteristic equations are

$$\frac{dx}{\frac{1}{n} S_o^{1/2} \frac{5}{3} y^{2/3}} = \frac{dt}{1} = \frac{dy}{r}$$

The depth is a function of x & t i.e.,

$$y=f(x,t)$$

Total derivative of y

$$dy = \frac{\partial y}{\partial x} .dx + \frac{\partial y}{\partial t} .dt$$

To find the travel of equal depth of flow i.e., y remain constant  $dy=0$

So

$$\frac{\partial y}{\partial x} .dx + \frac{\partial y}{\partial t} .dt = 0$$

$$\frac{\partial y}{\partial x} .dx = -\frac{\partial y}{\partial t} .dt$$

$$\frac{dx}{dt} = -\left(\frac{\partial y / \partial t}{\partial y / \partial x}\right)$$

Let  $\left(\frac{dx}{dt}\right)_y$  = velocity of flow of depth y

The continuity equation is

$$\frac{\partial q}{\partial y} \frac{\partial y}{\partial x} + \frac{\partial y}{\partial t} = r$$

When the rainfall has stopped

$$\frac{\partial q}{\partial y} \frac{\partial y}{\partial x} + \frac{\partial y}{\partial t} = 0$$

Now 
$$\frac{\partial q}{\partial y} = \frac{1}{n} S_o^{1/2} \frac{5}{3} y^{2/3}$$

Hence

$$\frac{1}{n} S_o^{1/2} \frac{5}{3} y^{2/3} \frac{\partial y}{\partial x} + \frac{\partial y}{\partial t} = 0$$

or 
$$\frac{\partial y}{\partial t} = -\frac{1}{n} S_o^{1/2} \frac{5}{3} y^{2/3} \frac{\partial y}{\partial x}$$

or 
$$-\left(\frac{\partial y / \partial t}{\partial y / \partial x}\right) = \frac{1}{n} S_o^{1/2} \frac{5}{3} y^{2/3}$$

Thus, velocity of flow of depth y

$$(v)_y = \left(\frac{\partial x}{\partial t}\right)_y = \frac{1}{n} S_o^{1/2} \frac{5}{3} y^{2/3} \quad (2.17)$$

### Response to The Initial Condition

Rainfall intensity is invariant in time and space.

$T_c$  = time of concentration

$t_r$  = duration of rainfall.

The initial condition is

$$y(x,0)=0$$

and the boundary condition is

$$y(0,t)=0$$

As the rain begins to fall at  $t=t_o=0$ , the local depth will increase everywhere at the rate

$$\frac{dy}{dt} = r$$

$r$  = constant rate of rainfall

$$dy = r dt$$

After lapse of time t, the depth is obtained by integrating between zero to any time t.

$$\int_{t_o}^t dy = \int_{t_o}^t r dt$$

$$y - y_o = r(t - t_o)$$

As  $y_o=0$  at  $t_o=0$

$$y = rt \quad (2.18)$$

This expression gives the depth of build up with respect to time. From the characteristic equation (2.14)

$$dx = \frac{1}{n} S_o^{1/2} \frac{5}{3} y^{2/3} dt$$

Integrating for  $t_0$  to  $t$

$$x(t) - x(0) = \frac{1}{n} S_o^{1/2} \frac{5}{3} \int_{t_0}^t (rt)^{2/3} dt = \frac{1}{n} S_o^{1/2} \frac{1}{r} (y^{5/3} - y_0^{5/3}) \quad (2.19)$$

As  $x(0)=0$ , and  $y_0=0$ ;

$$x = \frac{1}{n} S_o^{1/2} \frac{1}{r} y^{5/3}$$

### 2.3.3.5 Water surface profile and discharge hydrograph when time of rainfall is more than time of concentration ( $t_c \leq t_r < \infty$ )

During build up stage, the discharge increases as the depth of flow increases with time and the discharge can be found by the Manning's equation. The discharge will go on increasing till the first boundary response reaches the outfall and the corresponding time is the time of concentration  $t_c$ .

When the boundary response reaches the outfall

$$x=L$$

$$t=t_c$$

The depth  $y=rt_c$

$$L = \frac{1}{n} S_o^{1/2} \frac{1}{r} y^{5/3} = \frac{1}{n} S_o^{1/2} \frac{1}{r} (rt_c)^{5/3}$$

$$t_c = \left( \frac{Ln}{\sqrt{S_o}} \right)^{3/5} \frac{1}{r^{2/5}}$$

And the discharge at  $t=t_c$  is  $q_c$ .

Hence,



$$q_c = \frac{1}{n} S_o^{1/2} (rt_c)^{5/3}$$

$$q_c = \frac{1}{n} S_o^{1/2} r^{5/3} \left[ \left( \frac{Ln}{\sqrt{S_o}} \right)^{3/5} \frac{1}{r^{2/5}} \right]^{5/3} = Lr$$

This is the peak discharge rate.

This discharge rate is equal to the rate of total amount of water falling on the whole length of catchment and this is the total amount of inflow coming to the reach  $x=L$  from upstream portion i.e, at the outfall. So after the time  $t=t_c$  the discharge rate will continue at  $q=q_c$  till the uniform rainfall intensity  $r$  continues i.e, for the time  $(t_r-t_c)$ . The shape of discharge hydrograph during the steady stage discharge is shown by horizontal straight line EF in fig.2.7.

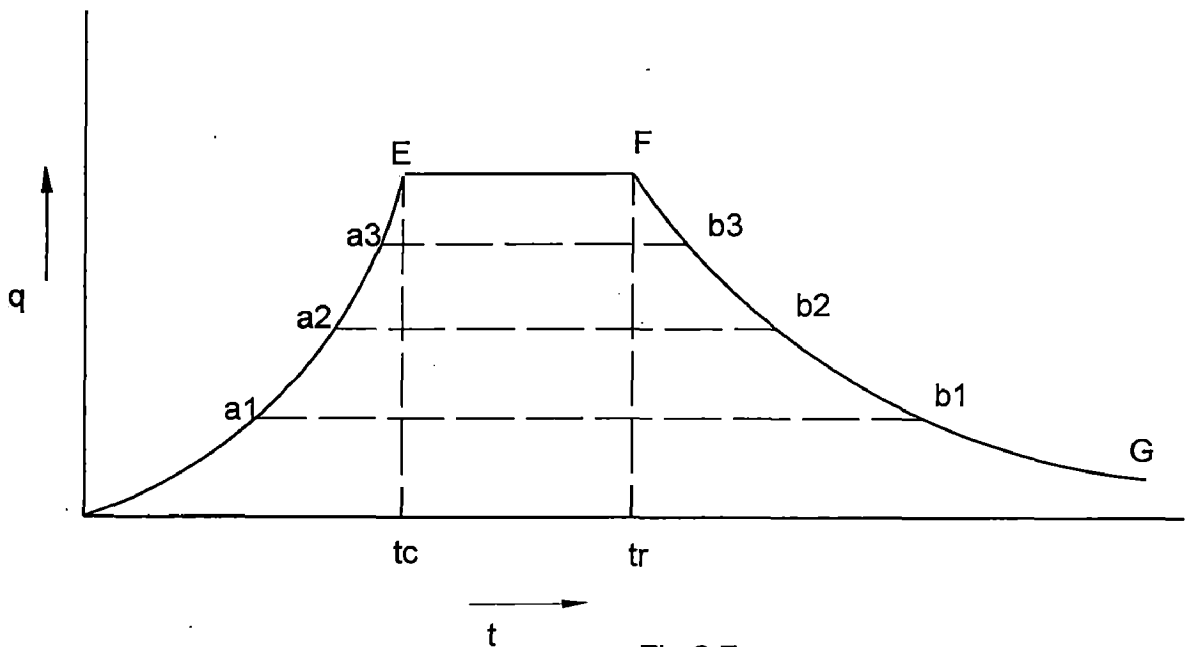


Fig 2.7

Water surface profile during the build up stage can be found out from the equation (2.12) and (2.13) and the type of water surface profile that will build up is shown in fig.2.8.

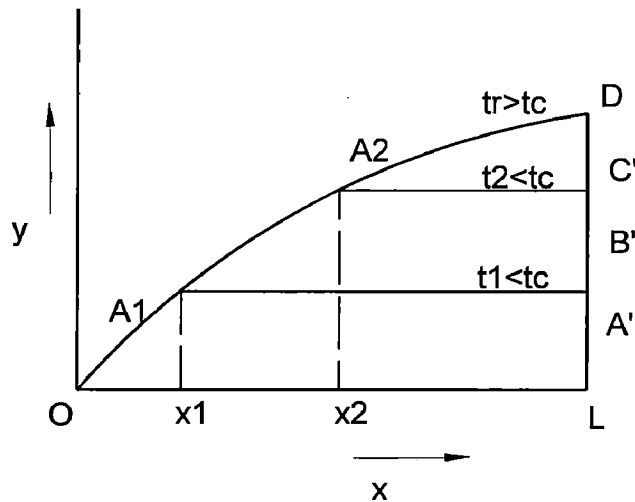


Fig 2.8

The profile will continue to remain in that state till the rainfall continues i.e., for the period  $(t_r - t_c)$ .

**Water surface profile after the cessation of rainfall**

How the water surface configuration changes after cessation of rainfall is shown in figure 2.9. OBC is the limiting profile for long storm and the curve  $OB_1C_1$  is a subsequent profile for a time following cessation of rainfall.

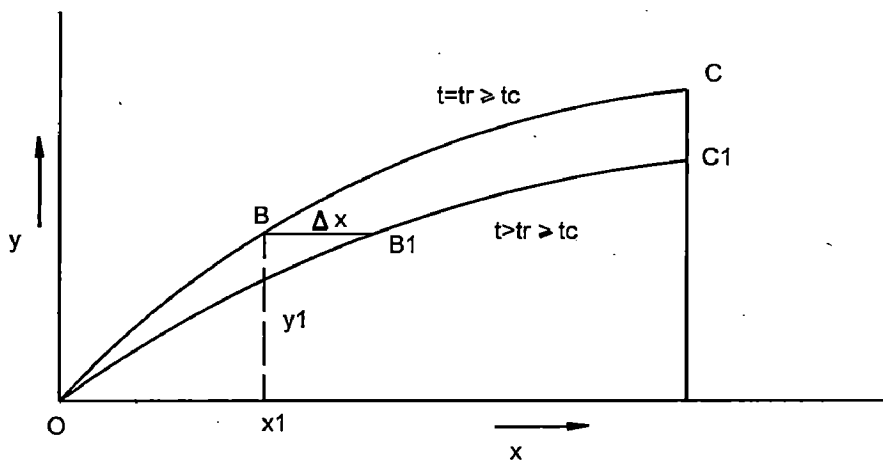


Fig 2.9

B was a point on the limiting profile at  $t = t_r$ . So after the cessation of rainfall in time  $(t - t_r)$  the point B say travels a distance  $\Delta X$  and comes to  $B_1$  (a point on the flow profile of that time)

Distance traveled in  $(t-t_r)$  time by point B

$$=\Delta x=(v)_{y_1} \cdot \Delta t = \frac{1}{n} S_o^{1/2} \frac{5}{3} y_1^{2/3} (t-t_r)$$

where  $(v)_{y_1}$  is velocity of flow of depth  $y_1$ .

The x coordinate of the section of the profile having depth y at any time  $t, t > t_r$

$$= \frac{1}{n} S_o^{1/2} \frac{1}{r} y^{(5/3)} + \frac{1}{n} S_o^{1/2} \frac{5}{3} y^{2/3} (t-t_r) = \frac{1}{n} S_o^{1/2} \frac{1}{r} y^{(2/3)} \left[ \frac{y}{r} + \frac{5}{3} (t-t_r) \right]$$

So from this the water surface profile for any time t greater than  $t_r$  can be found out.

### Flow Hydrograph After Cessation of Rainfall (i.e for $t > t_r \geq t_c$ )

When  $t=t_r$ , there will be a limiting water surface profile. Every point on that profile will flow with the velocity corresponding to its depth. Let for any particular point on the limiting profile, the depth is y, distance from boundary is x and the velocity of flow corresponding discharge is  $(q)_y$ . Time required to travel the remaining  $(L-x)$  portion of the catchment

= Travel time

$$\stackrel{y}{=} t_{tv}$$

$$= \frac{L-x}{V_y}$$

$$= \frac{L-x}{\frac{1}{n} S_o^{1/2} \frac{5}{3} y^{2/3}}$$

The discharge rate will start declining in exponential decay form after cessation of rainfall and will be equal to that of the corresponding depth reaching the outfall.

Total time taken by the discharge  $q_y$  corresponding to depth y after cessation of rainfall

$$=T$$

$$= \text{Rainfall duration} + \text{travel time}$$

Hence

$$T = t_r + t_{tr}$$

$$= t_r + \frac{L-x}{\frac{1}{n} S_o^{1/2} \frac{5}{3} y^{2/3}}$$

From this relation the recession portion of discharge can be found and the type of curve is shown by the curve FG in figure 2.7.

### 2.3.3.6 Water surface Profile and Flow Hydrograph when $t_r < t_c$

Here the rainfall ceases before the boundary excitation reaches the outfall of the catchment.

At time  $t_r$  the boundary excitation has reached the point A and the water surface profile at this stage is OAB. This is shown in the figure 2.10.

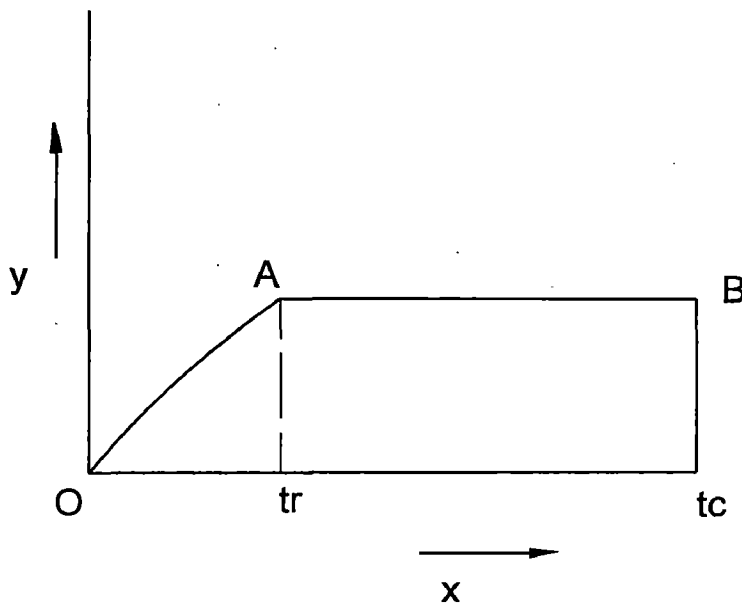


Fig 2.10

End depth at time  $t_r$  at B will be equal to that of A and is

$$y_{tr} = r \cdot t_r$$

The end depth  $y_{tr}$  is the maximum depth reached during build up phase and remains constant until point A reaches to B and this will occur at time  $t$  and is given by equation (2.12). The depth  $y=rt$  for  $0 < t \leq t_r < t_c$ , and discharge

$$q = \frac{1}{n} S_o^{1/2} y^{5/3}$$

Maximum depth

$$y_L = r \cdot t_r$$

and discharge

$$q_L = \frac{1}{n} S_o^{1/2} y_L^{5/3}$$

For time  $t > t_r$

the end depth is given by the expression

$$x + v_y(t - t_r) = L$$

$$\text{or } \frac{1}{n} S_o^{1/2} \frac{1}{r} y^{(5/3)} + \frac{1}{n} S_o^{1/2} \frac{5}{3} y^{2/3} (t - t_r) = L$$

$$\frac{1}{n} S_o^{1/2} y^{2/3} \left[ \frac{y}{r} + \frac{5}{3} (t - t_r) \right] = L$$

In the above expression  $t$  is the time at which the wave of depth  $y$  will reach the outfall.

Fig 2.11 show flow hydrograph when  $t_r < t_c$

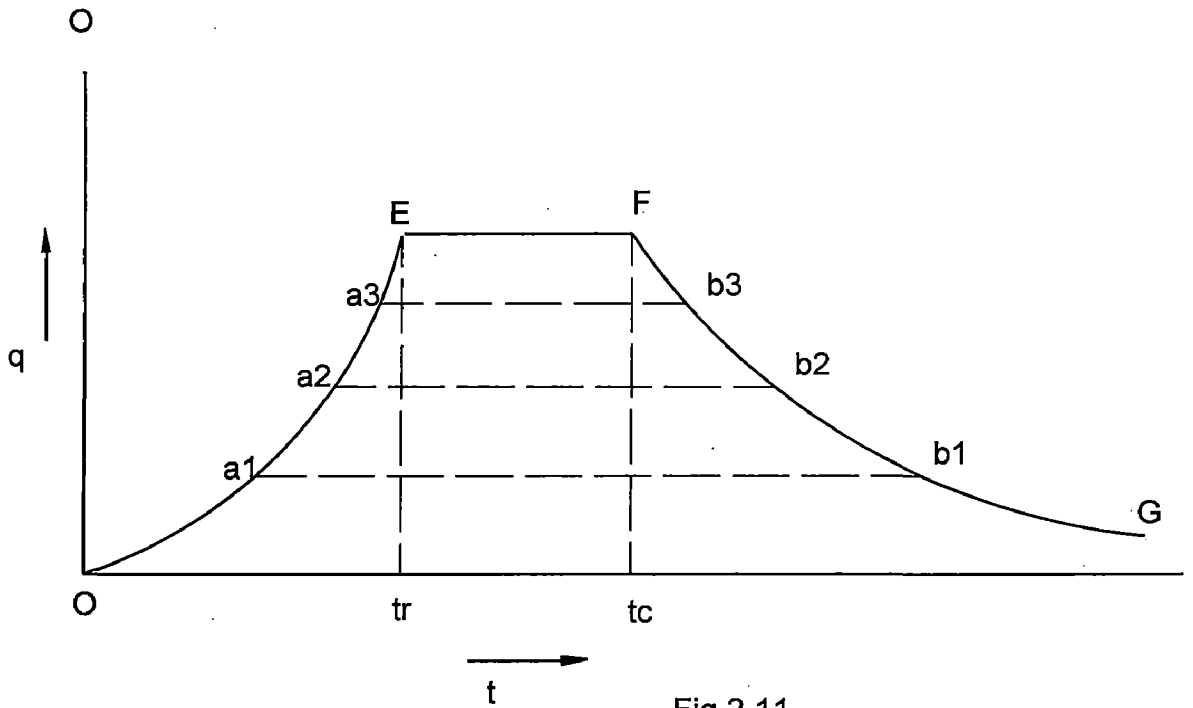


Fig 2.11

### 2.3.3.7. Under varying rainfall intensity

Rainfall intensity is considered as varying and infiltration is not taken into consideration.

The rainfall excesses at  $\Delta t$  interval of time are found out and say they are  $r_e(0), r_e(1), r_e(2), \dots$

Then the average value of rainfall excesses are calculated out as

$$R_1 = \frac{r_e(0) + r_e(1)}{2}$$

$$R_2 = \frac{r_e(1) + r_e(2)}{2} \text{ and so on}$$

These  $R_1, R_2, \dots$  values are considered to continue uniformly for the respective  $\Delta t$  duration.

Relationship of  $x$  and  $y$  of the water surface profile in terms of time  $t$ :

Now the small time interval is taken as  $\Delta t$  initially at time  $t=t_0=0$

$$x=x_0=0$$

$$y=y_0=0$$

From the characteristic equations

$$\frac{dy}{dt} = \bar{r} \quad \text{where } \bar{r} = \text{average value of rainfall excess}$$

$$dy = \bar{r} dt$$

$$y - y_0 = \bar{r} (t - t_0) = \bar{r} \Delta t$$

Again from characteristic equation

$$dx = \frac{1}{n} S_o^{1/2} \frac{5}{3} y^{2/3} dt$$

Integrating,

$$x - x_0 = \frac{1}{n} S_o^{1/2} \frac{5}{3} \int_{t_0}^t y^{2/3} dt = \frac{1}{n} S_o^{1/2} \frac{5}{3} \int_{t_0}^t [y_0 + \bar{r}(t - t_0)]^{2/3} dt$$

$$x - x_0 = \frac{1}{n} S_o^{1/2} \frac{5}{3} \frac{[y_0 + \bar{r}(t - t_0)]^{5/3} - y_0^{5/3}}{\frac{5}{3} \bar{r}}$$

$$= \frac{1}{n} S_o^{1/2} \frac{1}{\bar{r}} [y^{5/3} - y_0^{5/3}]$$

$$x = x_0 + \frac{1}{n} S_o^{1/2} \frac{1}{\bar{r}} [y^{5/3} - y_0^{5/3}]$$

Now this set of x and y value are considered as initial values to find the x and y values for next  $\Delta t$  duration and by doing so the water surface profile can be found.

( Computer programme to find the coordinates of water surface profiles at different time and flow hydrograph in case infiltration is considered upto the time of rainfall is given in Appendix I).

## APPENDIX I

(SURFACE RUNOFF HYDROGRAPH AND PROFILE FOR VARYING RAINFALL)

```
#include <iostream.h>
#include <math.h>
#include <conio.h>
#include <fstream.h>
#include <iomanip.h>
void main()
{ float r[20],t[20],x[20],y[20],Q[20],V[20],T[20],Tr[20];
int i,m;float n,S,W,L;float Tc;ifstream f1; ofstream f2;
f1.open ("order.dat");
f2.open ("order.res");
f1>>n>>S>>W>>L;f1>>m;
for (i=0;i<m;i++)
{f1>>r[i];}
for (i=0;i<m;i++)
{f1>>t[i];}
float a;y[0]=r[0]*t[0];
x[0]=(1/n)*sqrt(S)*pow(r[0],0.66667)*pow(t[0],1.66667);
if (x[0]>=W)
{x[0]=W;t[0]=pow(x[0]*n/sqrt(S)/pow(r[0],0.66667),0.6);
y[0]=r[0]*t[0];Q[0]=(1/n)*pow(y[0],1.66667)*sqrt(S)*L;
V[0]=(1/n)*sqrt(S)*1.66667*pow(y[0],0.66667);m=1;Tc=t[0];}
if (x[0]<W)
{Q[0]=(1/n)*pow(y[0],1.66667)*sqrt(S)*L;
V[0]=(1/n)*sqrt(S)*1.66667*pow(y[0],0.66667);
Tr[0]=(W-x[0])/V[0];}T[0]=t[0];
for (i=1;i<m;i++)
{y[i]=y[i-1]+r[i]*t[i];T[i]=T[i-1]+t[i];
x[i]=x[i-1]+sqrt(S)/n/r[i]*(pow(y[i],1.66667)-pow(y[i-1],1.66667));
if (x[i]<W)
{Q[i]=1/n*pow(y[i],1.66667)*sqrt(S)*L;
V[i]=(1/n)*sqrt(S)*1.66667*pow(y[i],0.66667);
Tc=(T[i]+(W-x[i])/V[i])/3600;Tr[i]=(W-x[i])/V[i];}
```



```

if (x[i]>=W)
{x[i]=W;
y[i]=pow((x[i]-x[i-1])*n*r[i]/sqrt(S)+pow(y[i-1],1.66667),0.6);
Q[i]=1/n*pow(y[i],1.66667)*sqrt(S)*L; m=i+1;
V[i]=(1/n)*sqrt(S)*1.66667*pow(y[i],0.66667);Tr[i]=(W-x[i])/V[i];
Tc=((W-x[i-1])/V[i]+T[i-1])/3600;break;}}
f2<<"t"<<setw(10)<<"y"<<setw(15)<<"x"<<setw(10)<<"Q"<<setw(15)<<"Tr"<<setw(15)
)<<"V"<<endl;
for (i=0;i<m;i++)
{ f2<<t[i]<<setw(10)<<y[i]<<setw(15)<<x[i]<<setw(10)<<Q[i]<<setw(15)<<Tr[i]<<setw(15)
)<<V[i]<<endl;}
f2<<"Time concentration:"<<Tc;}

```

## 2.4 INFILTRATION

### 2.4.1 General

Watershed models simulating runoff, must have a means of estimating rainfall excess i.e. rainfall minus infiltration. Several methods are used to simulate infiltration which broadly fall into the group of empirical methods. Horton's equation (1933,1939), Phillip's equation (1957,1969), Green and Ampt(1911)equation are popular because of simplicity and basing on actual amount of cumulative infiltration that is taking place up to the time under consideration. The rate of infiltration is high at the beginning of rainfall and it gradually decreases.

Green and Ampt proposed the simplified picture of infiltration shown in Fig.2.12. The wetting front is a sharp boundary dividing soil of moisture content  $\theta_i$  below from saturated soil with moisture content  $\eta$  above. The wetting front has penetrated to a depth  $L$  in time  $t$  since infiltration began. Water is ponded to a small depth  $h_o$  on the soil surface.

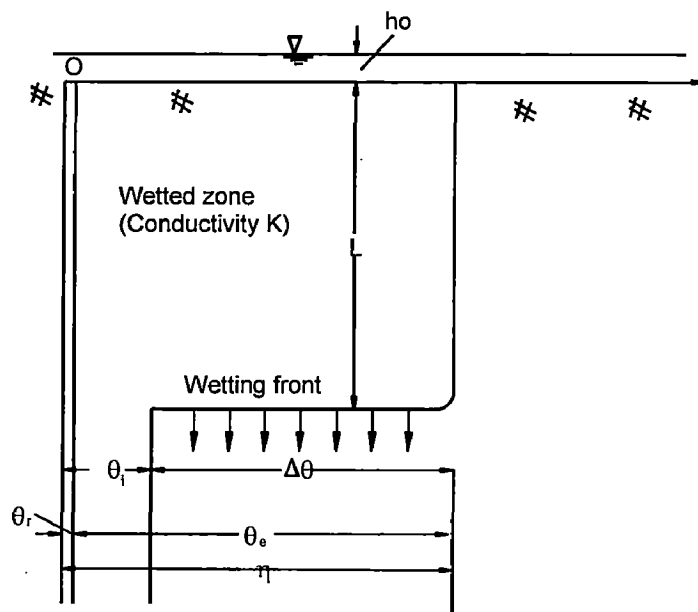


Fig 2.12. Variables in Green Ampt infiltration model

### 2.4.2 Conservation of mass

Consider a vertical column of soil of unit horizontal cross-sectional area (Fig.2.13) and let a control volume be defined around the wet soil between the surface and depth  $L$ . If the soil was initially of moisture content  $\theta_i$  throughout its entire depth, the moisture content will increase from  $\theta_i$  to  $\eta$  (the porosity) as the wetting front passes, so the increase in the water stored within the control volume as a result of infiltration is  $L(\eta - \theta_i)$  for a unit cross section. By definition this quantity is equal to  $F$ , the cumulative depth of water infiltrated into the soil. Hence,

$$F(t) = L(\eta - \theta_i) = L\Delta\theta \quad (2.20)$$

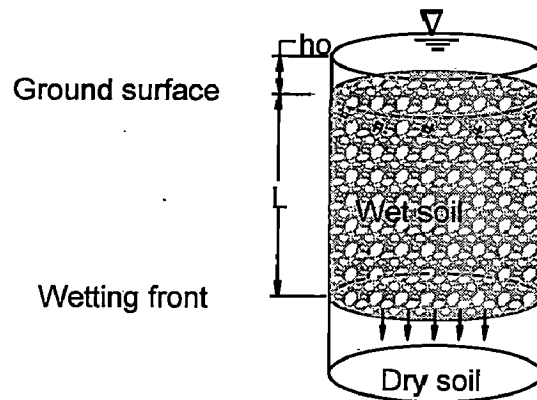


Fig 2.13. Infiltration into a column of soil of unit cross-sectional area for the Green-Ampt model

### 2.4.3. Conservation of Momentum

Darcy's law may be expressed

$$q = -K \frac{\partial h}{\partial z} \quad (2.21)$$

In this case the Darcy flux  $q$  is constant throughout the depth  $L$  and is equal to  $-f$ , because  $q$  is positive upward while  $f$  is positive downward. If

points 1 and 2 are located respectively at the ground surface and just on the dry side of the wetting front, (2.21) can be approximated by

$$f = K \left[ \frac{h_1 - h_2}{z_1 - z_2} \right] \quad (2.22)$$

The head  $h_1$  at the surface is equal to the ponded depth  $h_0$ . The head  $h_2$ , in the dry soil below the wetting front, equal  $-\psi-L$ . Darcy's law for this system is written

$$f = K \left[ \frac{h_0 - (-\psi - L)}{L} \right] \approx K \left[ \frac{\psi + L}{L} \right] \quad (2.23)$$

if the ponded depth  $h_0$  is negligible compared to  $\psi$  and  $L$ . This assumption is usually appropriate for surface water hydrology problems because it is assumed that ponded water becomes surface runoff.

From (2.20) the wetting front depth is  $L=F/\Delta\theta$ , and assuming  $h_0=0$ , substitution into (2.23) gives

$$f = K \left[ \frac{\psi\Delta\theta + F}{F} \right] \quad (2.24)$$

Since  $f=dF/dt$ , (2.24) can be expressed as a differential equation in the one unknown  $F$ :

$$\frac{dF}{dt} = K \left[ \frac{\psi\Delta\theta + F}{F} \right]$$

or 
$$\left[ \frac{F}{\psi\Delta\theta + F} \right] dF = K dt$$

splitting the left-hand side into two parts

$$\left[ \frac{F + \psi\Delta\theta}{F + \psi\Delta\theta} - \frac{\psi\Delta\theta}{F + \psi\Delta\theta} \right] dF = K dt$$

and integrate

$$\int_0^{F(t)} \left[ 1 - \frac{\psi\Delta\theta}{F + \psi\Delta\theta} \right] dF = \int_0^t K dt$$

one obtains

$$F(t) - \psi\Delta\theta \{ \ln[F(t) + \psi\Delta\theta ] - \ln(\psi\Delta\theta) \} = Kt$$

or

$$F(t) - \psi\Delta\theta \ln\left(1 + \frac{F(t)}{\psi\Delta\theta}\right) = Kt \quad (2.25)$$

This is the Green-Ampt equation for cumulative infiltration, and the infiltration rate  $f$  can be obtained from (2.23) or

$$f = K \left[ \frac{\psi\Delta\theta}{F(t)} + 1 \right] \quad (2.26)$$

#### 2.4.4. Green\_Ampt parameters

Application of the Green-Ampt model requires estimates of the hydraulic conductivity  $K$ , the porosity  $\eta$ , and the wetting front soil suction head  $\psi$ . The change in the moisture content when the wetting front passes is

$$\Delta\theta = \eta - \theta_i = \eta - (s_e \theta_e + \theta_r) = (1 - s_e) \theta_e$$

where  $s_e$  is effective saturation

$$s_e = \frac{\theta_i - \theta_r}{\eta - \theta_r}$$

$\theta_i$  is initial moisture content

$\theta_e$  is effective porosity  $\theta_e = \eta - \theta_r$

$\theta_r$  is the residual moisture content of the soil after it has been thoroughly drained

#### 2.4.5. Ponding time

In the preceding sections Green and Ampt method for computing the rate of infiltration into the soil was presented. This methods used the assumption that water is ponded to a small depth on the soil surface so all the water the soil can infiltrate is available at the surface. However, during a rainfall, water will pond on the surface only if the rainfall intensity is greater than the infiltration capacity of the soil. The ponding time  $t_p$  is the elapsed

time between the time rainfall begins and the time water begins to pond on the soil surface.

If rainfall begins on dry soil, the vertical moisture profile in the soil may appear as in Fig.2.14. Prior to the ponding time ( $t < t_p$ ), the rainfall intensity is less than the potential infiltration rate and the soil surface is unsaturated. Ponding begins when the rainfall intensity exceeds the potential infiltration rate. At this time ( $t = t_p$ ), the soil surface is saturated. As rainfall continues ( $t > t_p$ ), the saturated zone extends deeper into the soil and overland flow occurs from the ponded water.

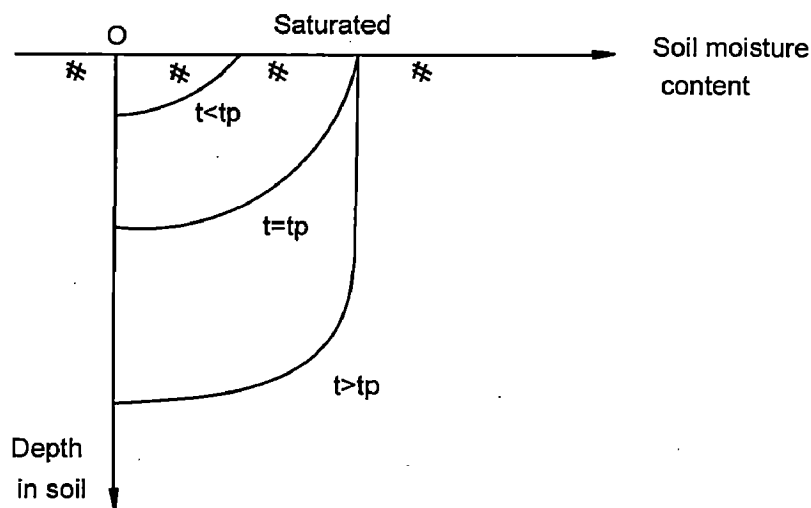


Fig 2.14. Soil moisture before, during and after ponding occurs

Mein and Larson (1973) presented a method for determining the ponding time with infiltration into the soil described by the Green-Ampt equation for rainfall of intensity  $i$  starting instantaneously and continuing indefinitely. There are three principles involved: (1) prior to the time ponding occurs, all the rainfall is infiltrated; (2) the potential infiltration rate  $f$  is a function of the cumulative infiltration  $F$ ; and (3) ponding occurs when the potential infiltration rate is less than or equal to the rainfall intensity.

In the Green-Ampt equation, the infiltration rate  $f$  and cumulative infiltration  $F$  are related by

$$f = K \left[ \frac{\psi \Delta \theta}{F(t)} + 1 \right] \quad (2.26)$$

The cumulative infiltration at the ponding time  $t_p$  is given by  $F_p = it_p$  and the infiltration rate  $f=i$ ; substituting into Eq.(2.26)

$$i = K \left[ \frac{\psi \Delta \theta}{it_p} + 1 \right]$$

solving.

$$t_p = \frac{K\psi\Delta\theta}{i(i-K)}$$

To obtain the actual infiltration rate after ponding, a curve of potential infiltration is constructed beginning at a time  $t_0$  such that the cumulative infiltration and the infiltration rate at  $t_p$  are equal to those observed under rainfall beginning at time 0 (see dashed line in Fig. 2.15). Substituting  $t=t_p - t_0$  and  $F=F_p$  into Eq (2.19)

$$F_p - \psi \Delta \theta \ln \left( 1 + \frac{F_p}{\psi \Delta \theta} \right) = K(t_p - t_0) \quad (2.27)$$

For  $t > t_p$

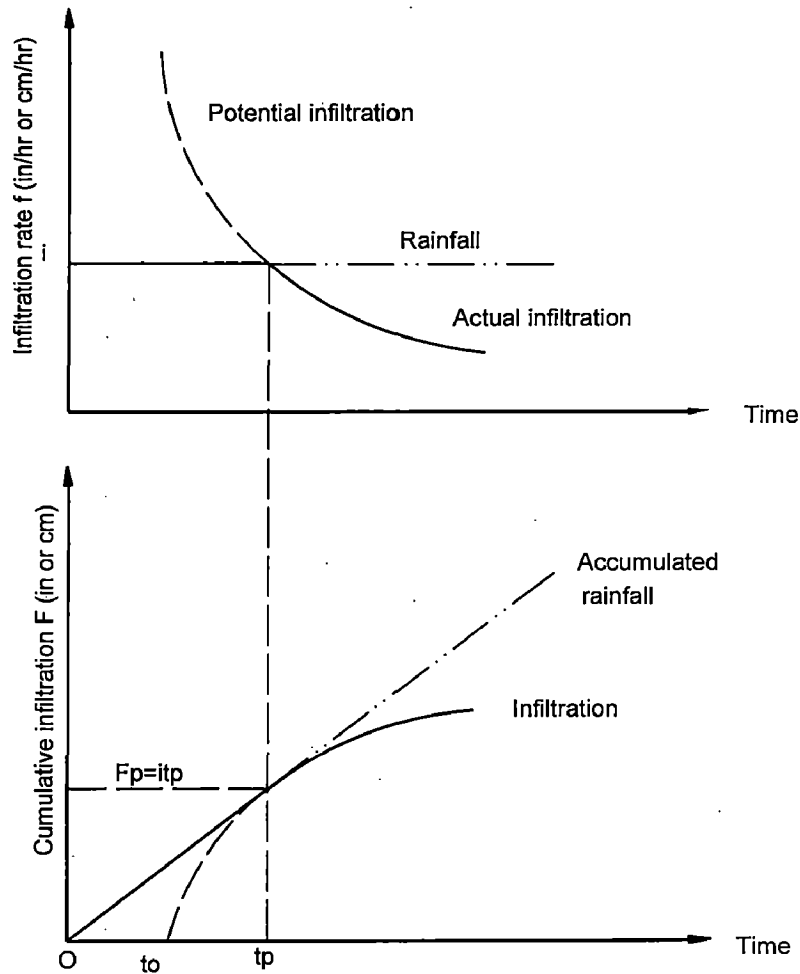
$$F - \psi \Delta \theta \ln \left( 1 + \frac{F_p}{\psi \Delta \theta} \right) = K(t - t_0) \quad (2.28)$$

And subtracting (2.28) from (2.27).

$$F - F_p - \psi \Delta \theta \left[ \ln \left( 1 + \frac{F}{\psi \Delta \theta} \right) - \ln \left( 1 + \frac{F_p}{\psi \Delta \theta} \right) \right] = K(t - t_p)$$

or

$$F - F_p - \psi \Delta \theta \ln \left( \frac{\psi \Delta \theta + F}{\psi \Delta \theta + F_p} \right) = K(t - t_p)$$



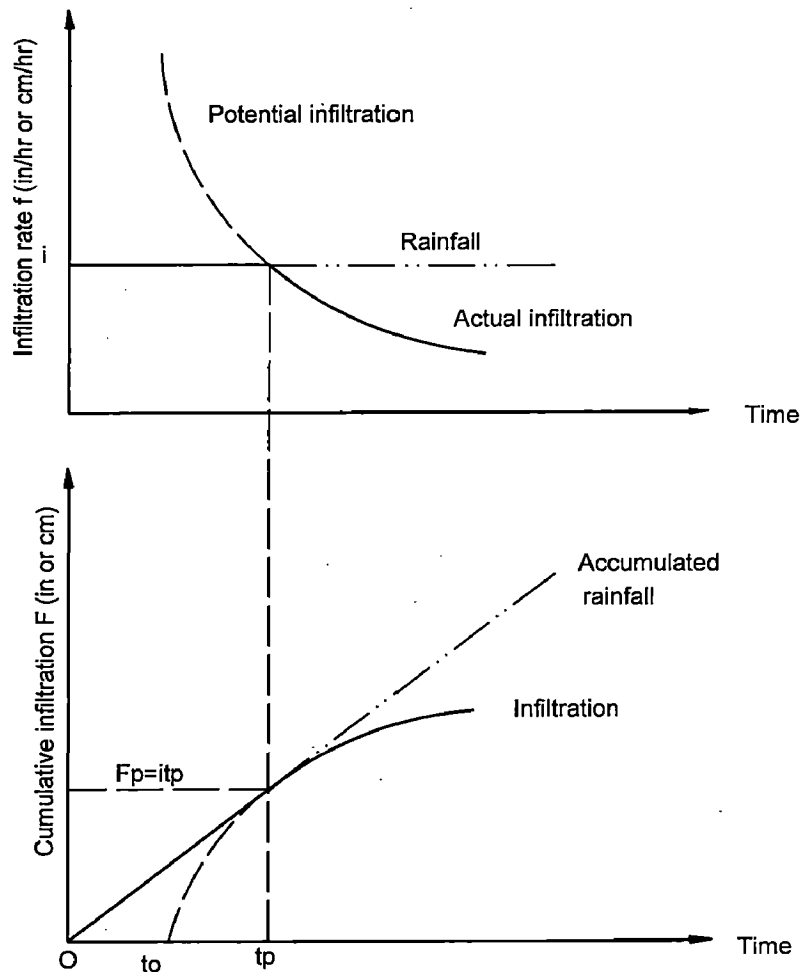
1

Fig 2.15. Infiltration rate and cumulative infiltration for ponding under constant intensity rainfall.

Consider a time interval from  $t$  to  $t + \Delta t$ . The rainfall intensity during this interval is denoted  $i_t$  and is constant throughout the interval. The potential infiltration rate and cumulative infiltration at the beginning of the interval are  $f_t$  and  $F_t$ , respectively, and the corresponding values at the end of the interval are  $f_{t+\Delta t}$  and  $F_{t+\Delta t}$ . It is assumed that  $F_t$  is known from given initial condition or previous computation.

$$f_t = K \left[ \frac{\psi \Delta \theta}{F_t} + 1 \right] \quad (2.26)$$





1

Fig 2.15. Infiltration rate and cumulative infiltration for ponding under constant intensity rainfall.

Consider a time interval from  $t$  to  $t + \Delta t$ . The rainfall intensity during this interval is denoted  $i_t$  and is constant throughout the interval. The potential infiltration rate and cumulative infiltration at the beginning of the interval are  $f_t$  and  $F_t$ , respectively, and the corresponding values at the end of the interval are  $f_{t+\Delta t}$  and  $F_{t+\Delta t}$ . It is assumed that  $F_t$  is known from given initial condition or previous computation.

$$f_t = K \left[ \frac{\psi \Delta \theta}{F_t} + 1 \right] \quad (2.26)$$

The result  $f_t < i_t$ , the cumulative infiltration at the end of the interval,  $F_{t+\Delta t}$  is calculated from

$$F_{t+\Delta t} - F_t - \psi\Delta\theta \ln\left(\frac{\psi\Delta\theta + F_{t+\Delta t}}{\psi\Delta\theta + F_t}\right) = K\Delta t$$

In case  $f_t > i_t$  and no ponding at the beginning of the interval, assume that this remains so throughout the interval. Then cumulative infiltration at the end of the time interval is

$$F_{t+\Delta t} = F_t + i_t\Delta t$$

If  $f_{t+\Delta t} < i_t$ , ponding occurs during the interval. The cumulative infiltration  $F_p$  at ponding time is found by setting  $f_t = i_t$  and  $F_t = F_p$  in (2.26) and solving for  $F_p$  to give, for the Green-Ampt equation,

$$F_p = \frac{K\psi\Delta\theta}{i_t - K}$$

The ponding time is then  $t + \Delta t'$ , where

$$\Delta t' = \frac{F_p - F_t}{i_t}$$

And the cumulative infiltration  $F_{t+\Delta t}$  is found by substituting  $F_t = F_p$  and  $\Delta t = \Delta t - \Delta t'$ .

( A computer programme has been made to find the rate of infiltration from the Green-Ampt equations. The programme is given in Appendix II)

## APPENDIX II

(COMPUTATION INFILTRATION RATE USING GREEN AND AMPT EQN)

```
#include <iostream.h>
#include <math.h>
#include <fstream.h>
#include <iomanip.h>
void main()
{ float r[20],t[20],f[20],F[20],R[20];
int i,m;float K,Se,Oe,Y,DelO,Fp,delt,tp,fp;
ifstream f1; ofstream f2;f1.open ("infil.dat");f2.open ("infil.res");
f2<<"Value of K,Se,Oe,Y"<<"\n";f1>>K>>Se>>Oe>>Y;
f2<<K<<setw(10)<<Se<<setw(10)<<Oe<<setw(15)<<Y<<endl;f1>>m;DelO=(1-
Se)*Oe;
for (i=0;i<m;i++)
{f1>>r[i];}tp=K*Y*DelO/r[0]/(r[0]-K);
for (i=0;i<m;i++)
{f1>>t[i];}if (tp<t[0])
{ Fp=K*Y*DelO/(r[0]-K);delt=Fp/r[0];fp=K*(Y*DelO/Fp+1);R[0]=Fp;
do
{R[0]=R[0]+0.00001;
F[0]=Fp+K*(t[0]-tp)+Y*DelO*log((R[0]+Y*DelO)/(Fp+Y*DelO));}
while ((R[0]-F[0]<0.0001)||((R[0]-F[0]>0.0002)));
f[0]=K*(Y*DelO/F[0]+1);
for (i=0;i<m;i++)
{R[i+1]=R[i];
do
{ R[i+1]=R[i+1]+0.00001;
F[i+1]=F[i]+K*t[i+1]+Y*DelO*log((R[i+1]+Y*DelO)/(F[i]+Y*DelO));}
while ((R[i+1]-F[i+1]<0.0001)||((R[i+1]-F[i+1]>0.0002)));
f[i+1]=K*(Y*DelO/F[i+1]+1);}}if (tp>t[0])
{F[0]=t[0]*r[0]; f[0]=K*(Y*DelO/F[0]+1);
for (i=0;i<m;i++)
{F[i+1]=F[i]+r[i+1]*t[i+1];f[i+1]=K*(Y*DelO/F[i+1]+1);
if (f[i+1]<=r[i+2])
```

```

{Fp=K*Y*DelO/(r[i+1]-K);delt=(Fp-F[0])/r[i+1];tp=t[i]+delt;
fp=K*(Y*DelO/Fp+1);R[i+1]=Fp;
do
{R[i+1]=R[i+1]+0.00001;
F[i+1]=Fp+K*(t[i+1]-delt)+Y*DelO*log((R[i+1]+Y*DelO)/(Fp+Y*DelO));}
While
((R[i+1]-F[i+1]<0.0001)||R[i+1]-F[i+1]>0.0002));f[i+1]=K*(Y*DelO/F[i+1]+1);}
for (i=0;i<=m;i++)
{ R[i+2]=R[i+1];
do
{R[i+2]=R[i+2]+0.00001;
F[i+2]=F[i+1]+K*t[i+2]+Y*DelO*log((R[i+2]+Y*DelO)/(F[i+1]+Y*DelO));}
while ((R[i+2]-F[i+2]<0.0001)||R[i+2]-
F[i+2]>0.0002));f[i+2]=K*(Y*DelO/F[i+2]+1);}}
f2<<"Cumulative infiltration at ponding time:"<<Fp<<endl;
f2<<" infiltration rate at ponding time:"<<fp<<endl;
f2<<"ponding time tp:"<<tp<<endl;
f2<<"t"<<setw(15)<<"r"<<setw(15)<<"f"<<setw(15)<<"F"<<endl<<endl;
t[m]=0;r[m]=0;
for (i=0;i<=m;i++)
{ f2<<t[i]<<setw(15)<<r[i]<<setw(15)<<f[i]<<setw(15)<<F[i]<<endl;}}

```

## **2.5 STUDY FOR WIRPUR NULLA WATERSHED**

### **2.5.1 General**

The approaches presented in the earlier section has been applied to the three flood events of Wirpur Nulla watershed. The details of the basin and availability of data are presented in following sections.

#### General Description of the Basin

The Wirpur Nulla is a tributary of Wardha river in the Godavari basin having a catchment area of 137 Sq.km. The catchment is geographically located between 78°15' and 78°26' East longitudes, and 21°40' North and 21°51' North Latitudes. The study area lies in the southern part of Madhya Pradesh in India

#### Soils:

From the soil classification map, the basin soils are identified and classified as black soil. The black soils are clayey in texture (group D)

#### Land Use :

From the irrigation atlas of India, nearly 95% of the basin area is identified as arable land. About 5% of the basin area is covered by dense forests

#### Rainfall Data

Hourly rainfall runoff data and rainfall intensity of two flood events for the year 1961-64 have been used for the study.

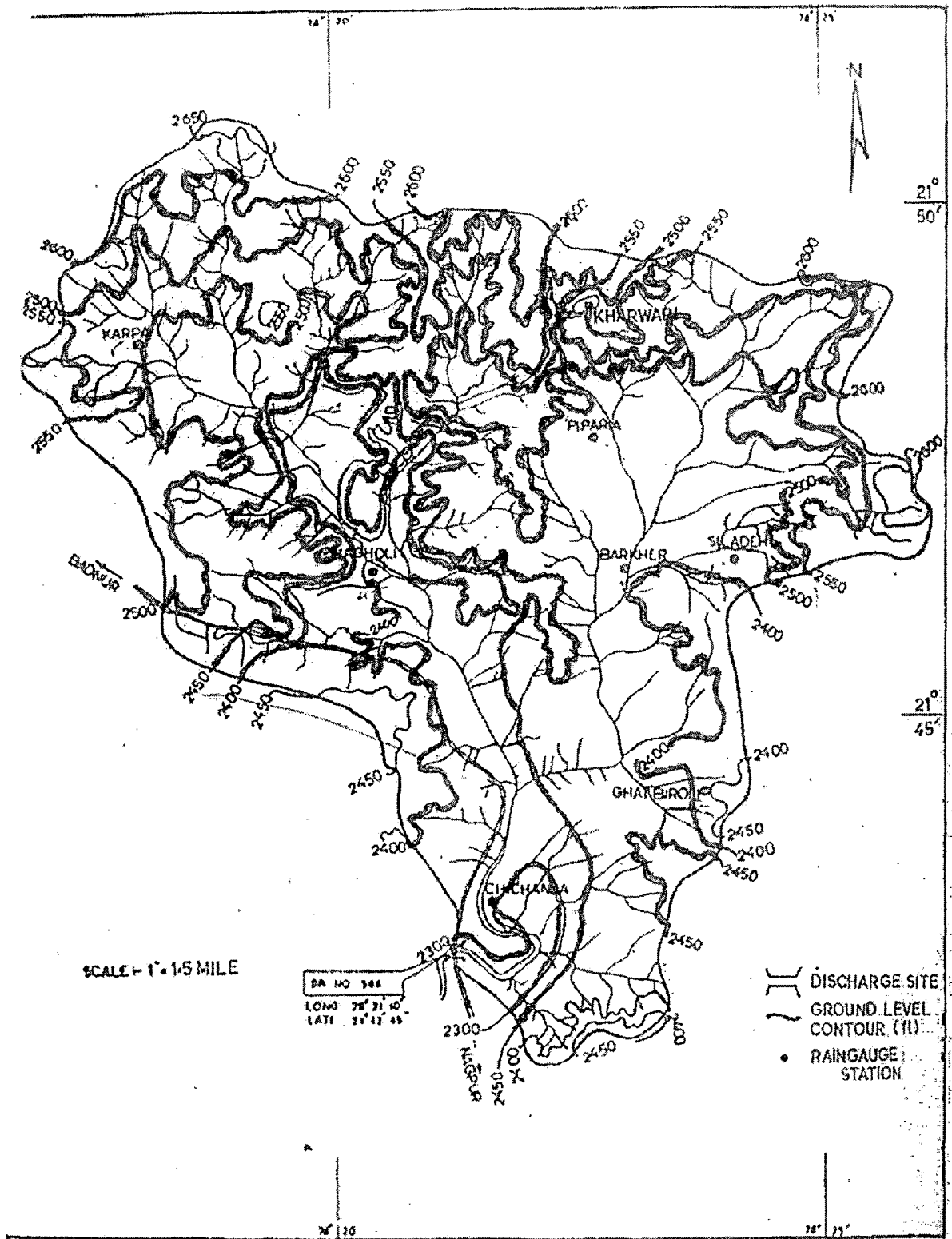


Fig 2.16 . CATCHMENT PLAN FOR WIRPUR NULLA WATERSHED

## 2.5.2 Study SCS method for Wirpur Nulla watershed

### Estimation of Curve number for the basin

The curve numbers for Wirpur Nulla watershed under AMC III for different land use practices and soil type, were obtained from standard tables and the weighted CN was computed as 96.

### Time of Concentration

The time of concentration for Wirpur Nulla watershed was computed by Kirpitch (1940)

$$T_c = 3.81 \text{ hr}$$

### UH Shape by SCS Approach

For  $T_c = 3.81 \text{ hr}$ , duration of rainfall excess  $D = 0.5 \text{ hr}$ , the time to peak is estimated as 2.5 hr, time recession  $t_r = 4.175 \text{ hr}$ , the  $q_p = 113.98 \text{ m}^3/\text{s}/\text{cm}$ . For triangular shape of UH, the ordinates are plotted in Fig.2.17

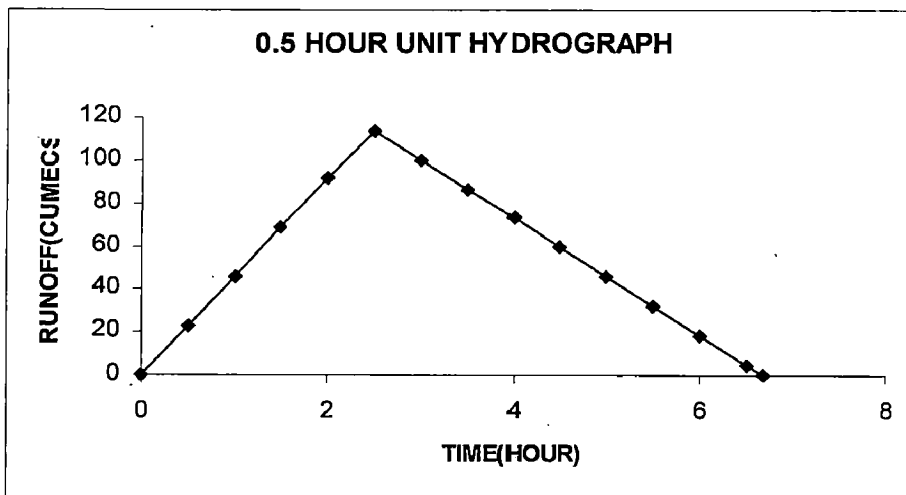


Figure.2.17 0.5 Hour Unit Hydrograph

(Result by SCS-CN method in APPENDIX IIIA)

### 2.5.3 Study Kinematic wave for Wirpur Nulla watershed

The Wirpur Nulla watershed has been divided into 8 elements consisting of planes. The size of the plane element is fixed according to its uniformity in slope. The dimensions of the planes are measured from the map and the average slopes of planes are estimated from the contour lines. The slope, length, width and sequence of flow have been shown in Table 2.1(Jeyselan-1984)

TABLE 2.1: Model Geometry of the Wirpur Nulla Watershed Segment

Seg.No	Type	Length in m	Width in m	Slope
1	Plane 1	4350	5402	0.02
2	Plane 2	1597	5402	0.019
3	Plane 3	4053	4750	0.0014
4	Plane 4	2047	10750	0.014
5	Plane 5	2850	10750	0.015
6	Plane 6	3875	4000	0.0074
7	Plane 7	2344	5848	0.01
8	Plane 8	1000	3750	0.028

The roughness coefficient varies for the different surfaces and flow condition. On the basis of the information available regarding the cropped area, nature of soil surface, the corresponding Manning's 'n' for turbulent flow condition is 0.03.

#### Infiltration Parameter

Follow table 4.3.1 (Green-Ampt infiltration parameters for various soil classes-Applied Hydrology-Ven Te Chow). The corresponding clay soil, parameters are listed in following table



**TABLE 2.2: Parameters Of Clay Soil**

Effective $\theta_e$	Suction head $\psi$ (cm)	Hydraulic conductivity K (cm/h)	Effective saturation $s_e$
0.385	31.63	0.03	0.85

The runoff hydrographs have been obtained using method of characteristics (Kinematic wave approach) and have been computed on Appendix IIIB

**Discussion of results**

Two methods namely Kinematics wave approach and SCS approach were used to estimate runoff from the data related to Wirpur Nulla . It is located near Wardha district of Maharashtra. The catchment area of this nulla is 137 square kilometer. The soils of the watershed are clayey in texture while land use is mostly arable. The three rainfall events and runoff observed due to these events were used for analysis as depicted in Figure 2.18. Criteria of percentage absolute difference in peak discharge between observed and computed discharges by different approaches are used for comparison. The magnitude of the observed and computed peak discharges are shown in Table 2.3 for different storms for the above explained two approaches. The percentages absolute error in peak discharges are shown in Table 2.4.

**Table 2.3 Observed and Computed Peak Discharges**

Event	Date	Peak discharge (cumecs)		
		Observed	Kinematics wave approach	SCS approach
1	25.7.61	87.15	82.97	74.27
2	10.8.62	320	287.42	298.36
3	26.7.64	193.1	213.91	204.3

Table 2.4 Percentage Absolute Error in Peak Discharge

Event	Date	Percentage Absolute Error in Peak	
		Kinematics wave approach	SCS - CN approach
1	25.7.61	4.8	14.78
2	10.8.62	10.18	6.76
3	26.7.64	10.78	5.8

Peak Runoff have been simulated for three rainfall events recorded in the basin. The magnitude of the peak flow of first event for the observed, Kinematic wave study and SCS-CN method are 87.15 m<sup>3</sup>/s, 82.97 m<sup>3</sup>/s and 74.27 respectively. The percentage absolute error in peak for Kinematic wave study and SCS-CN method are 4.8% and 14.78 % respectively.

Prediction of peak runoff for the second event shows that the magnitude of peak flow of the observed, Kinematic wave study and SCS-CN method are 320 m<sup>3</sup>/s, 287.42m<sup>3</sup>/s and 298.36 m<sup>3</sup>/s respectively, and percentage absolute error in peak of Kinematic wave study and SCS-CN method are 10.18 and 6.76 respectively.

Simulation of the third event reveals that the magnitude of peak flow of the observed, Kinematic wave study and SCS-CN method are 193.1m<sup>3</sup>/s, 213.91 m<sup>3</sup>/s and 204.3 m<sup>3</sup>/s respectively. Corresponding value for The percentage absolute error in peak for Kinematic wave study and SCS-CN method are 10.78 and 5.8 respectively.

The data revealed that there was a narrow difference in peak rate of runoff as computed by two approaches in all the three events. But there was a marked difference in peak rate of runoff computed by both approaches when compared with observed value. It may be attributed to inherent characteristics of individual method.

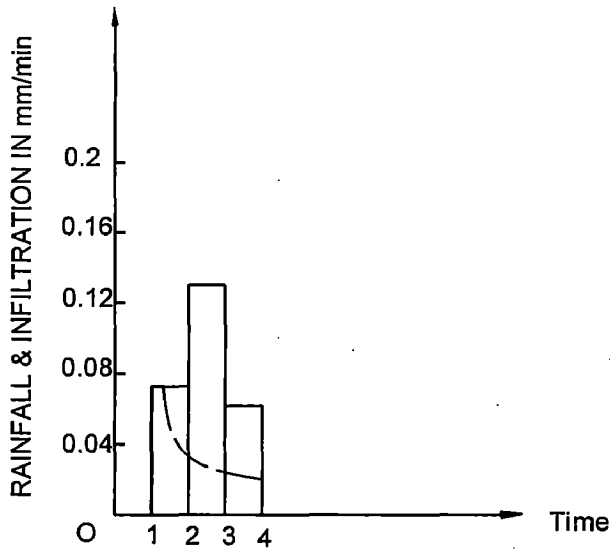


Figure 2.18a. Rainfall & Infiltration rate (event 1)

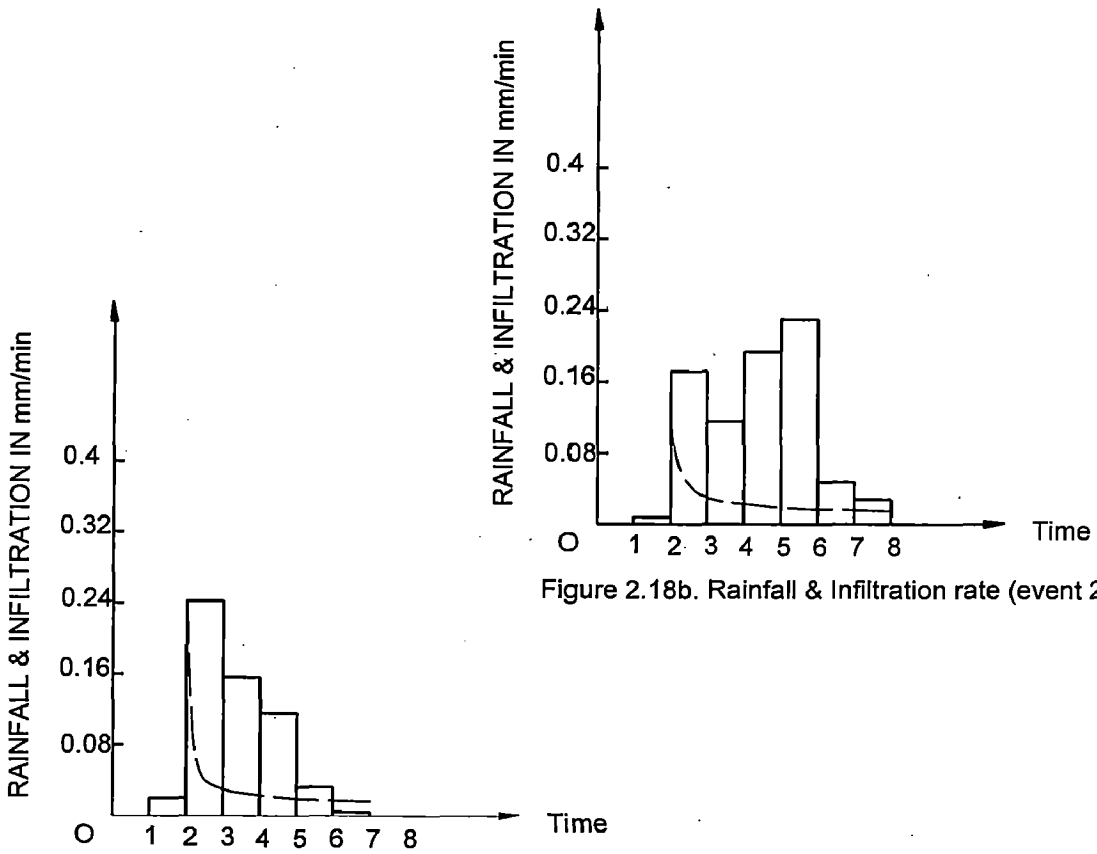


Figure 2.18b. Rainfall & Infiltration rate (event 2)

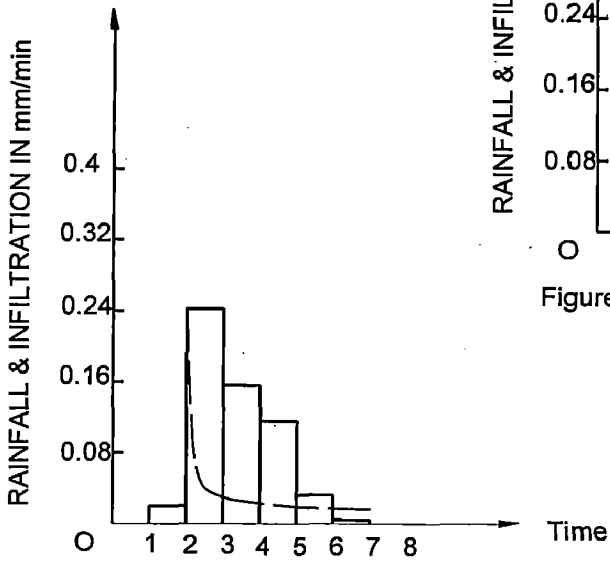


Figure 2.18c. Rainfall & Infiltration rate (event 3)

Fig 2.18. Rainfall & Infiltration rate of three event

**APPENDIX IIIA**  
**(RESULT BY USING SCS-CN APPROACH)**

**Table 2.5 Compute excess rainfall (event I)**

Time	Rainfall		Ia	Intensity	Excess rainfall	
	incremental	Cumulative			Cumulative	Incremental
	mm	mm			mm	mm
0						
1	0	0	2.12	0.073	0.00	0.00
2	4.38	4.38	2.12	0.13	0.40	0.40
3	7.8	12.18	2.12	0.062	4.90	4.50
4	3.72	15.9	2.12		7.79	2.89

**Table 2.6 Compute excess rainfall (event II)**

Time	Rainfall		Ia	Intensity	Excess rainfall	
	incremental	Cumulative			Cumulative	Incremental
	mm	mm			mm	mm
0						
1	0	0	2.12	0.008	0.00	0.00
2	0.48	0.48	2.12	0.172	0.00	0.00
3	10.32	10.8	2.12	0.116	3.91	3.91
4	6.96	17.76	2.12	0.194	9.32	5.41
5	11.64	29.4	2.12	0.23	19.65	10.32
6	13.8	43.2	2.12	0.048	32.65	13.01
7	2.88	46.08	2.12	0.028	35.42	2.77
8	1.68	47.76	2.12		37.04	1.62

Table 2.7 Compute excess rainfall (event III)

Time		Rainfall	Ia		Excess rainfall	
	incremental	Cumulative		Intensity	Cumulative	Incremental
	mm	mm	Mm	mm/min	mm	mm
0						
1	0	0	2.12	0.02	0.00	0.00
2	1.2	1.2	2.12	0.242	0.00	0.00
3	14.52	15.72	2.12	0.156	7.64	7.64
4	9.36	25.08	2.12	0.116	15.71	8.07
5	6.96	32.04	2.12	0.032	22.09	6.38
6	1.92	33.96	2.12	0.004	23.89	1.79
7	0.24	34.2	2.12		24.11	0.23

Table 2.8 Computation one hour Unit Hydrograph

Time	0.5h.U.H m3/s	Scurve addition	Scurve	Standard S hydrograph	Scurve lagged 1 hr	Difference	1h.UH m3/s
0	0.00	0.00	0.00	0.00	0.00	0.00	0.00
0.5	22.80	0.00	22.80	11.40	0.00	11.40	11.40
1	45.59	22.80	68.39	34.19	0.00	34.19	34.19
1.5	68.39	68.39	136.78	68.39	11.40	56.99	56.99
2	91.18	136.78	227.96	113.98	34.19	79.79	79.79
2.5	113.98	227.96	341.94	170.97	68.39	102.58	102.58
3	100.15	341.94	442.09	221.05	113.98	107.07	107.07
3.5	86.53	442.09	528.62	264.31	170.97	93.34	93.34
4	72.90	528.62	601.52	300.76	221.05	79.71	79.71
4.5	59.27	601.52	660.80	330.40	264.31	66.09	66.09
5	45.65	660.80	706.44	353.22	300.76	52.46	52.46
5.5	32.02	706.44	738.47	369.23	330.40	38.84	38.84
6	18.40	738.47	756.86	378.43	353.22	25.21	25.21
6.5	4.77	756.86	761.63	380.82	369.23	11.58	11.58
7	0.00	761.63	761.63	380.82	378.43	2.38	2.38
7.5		761.63	761.63	380.82	380.82	0.00	0.00

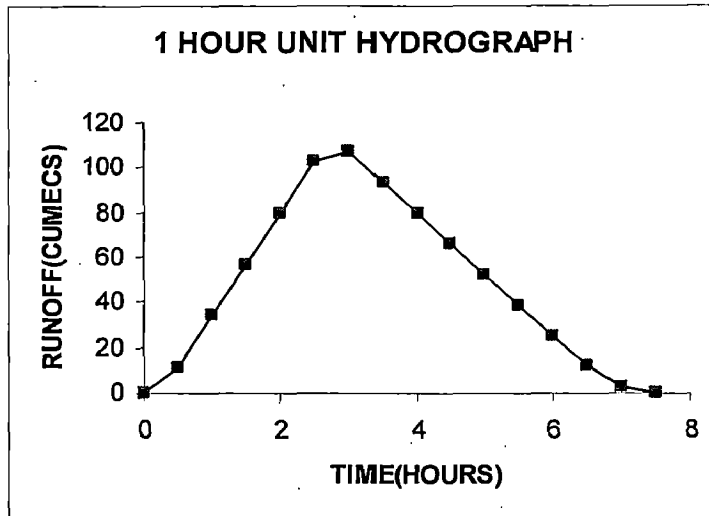


Figure .2.19. 1 Hour Unit Hydrograph

Table 2.9 Runoff Hydrograph (event I)

Time	U-H	DRH due to	DRH due to	DRH due to	DRH
	1hr	0.04cm	0.45cm	0.289 cm	
0	0.00	0.00			0
0.5	11.40	0.43			0.43
1	34.19	1.30	0.00		1.30
1.5	56.99	2.17	5.13		7.29
2	79.79	3.03	15.39	0.00	18.42
2.5	102.58	3.90	25.65	3.29	32.84
3	107.07	4.07	35.90	9.88	49.85
3.5	93.34	3.55	46.16	16.47	66.18
4	79.71	3.03	48.18	23.06	74.27
4.5	66.09	2.51	42.00	29.65	74.16
5	52.46	1.99	35.87	30.94	68.81
5.5	38.84	1.48	29.74	26.98	58.19
6	25.21	0.96	23.61	23.04	47.60
6.5	11.58	0.44	17.48	19.10	37.02
7	2.38	0.09	11.34	15.16	26.60
7.5	0	0	5.21	11.22	16.44
8			1.07	7.29	8.36
8.5			0.00	3.35	3.35
9				0.69	0.69
9.5					0.00

Table 2.10 Runoff Hydrograph (event II)

Time	U-H	DRH due to	DRH due to	DRH due to	DRH due to	DRH due to	DRH due to	DRH
	1hr	0.391cm	0.541 cm	1.032 cm	1.301 cm	0.277 cm	0.162 cm	
0	0.00	0.00						0.00
0.5	11.40	4.46						4.46
1	34.19	13.37	0.00					13.37
1.5	56.99	22.28	6.17					28.45
2	79.79	31.20	18.50	0.00				49.70
2.5	102.58	40.11	30.83	11.76				82.70
3	107.07	41.86	43.16	35.29	0.00			120.32
3.5	93.34	36.50	55.50	58.81	14.83			165.64
4	79.71	31.17	57.92	82.34	44.49	0.00		215.92
4.5	66.09	25.84	50.50	105.86	74.14	3.16		259.50
5	52.46	20.51	43.13	110.49	103.80	9.47	0.00	287.40
5.5	38.84	15.18	35.75	96.33	133.46	15.79	1.85	298.36
6	25.21	9.86	28.38	82.26	139.29	22.10	5.54	287.44
6.5	11.58	4.53	21.01	68.20	121.44	28.42	9.23	252.82
7	2.38	0.93	13.64	54.14	103.71	29.66	12.93	215.00
7.5	0.00	0.00	3.41	40.08	85.98	25.86	16.62	171.94
8		0.00	0.70	26.02	68.25	22.08	17.34	134.39
8.5			0.00	11.95	50.52	18.31	15.12	95.90
9				2.46	32.80	14.53	12.91	62.70
9.5				0.00	15.07	10.76	10.71	36.53
10					3.10	6.98	8.50	18.58
10.5					0.00	3.21	6.29	9.50
11						0.66	4.08	4.74
11.5						0.00	1.88	1.88
12							0.39	0.39
12.5							0.00	0.00

Table 2.11 Runoff Hydrograph (event III)

Time	U-H	DRH due to	DRH due to	DRH due to	DRH due to	DRH due to	DRH
	1hr	0.764cm	0.807 cm	0.638 cm	0.179 cm	0.023 cm	
0	0.00	0.00					0.00
0.5	11.40	8.71					8.71
1	34.19	26.12	0.00				26.12
1.5	56.99	43.54	9.20				52.74
2	79.79	60.96	27.59	0.00			88.55
2.5	102.58	78.37	45.99	7.27			131.64
3	107.07	81.80	64.39	21.82	0.00		168.00
3.5	93.34	71.31	82.78	36.36	2.04		192.50
4	79.71	60.90	86.40	50.90	6.12	0.00	204.33
4.5	66.09	50.49	75.33	65.45	10.20	0.26	201.73
5	52.46	40.08	64.33	68.31	14.28	0.79	187.79
5.5	38.84	29.67	53.33	59.55	18.36	1.31	162.23
6	25.21	19.26	42.34	50.86	19.16	1.84	133.45
6.5	11.58	8.85	31.34	42.16	16.71	2.36	101.42
7	2.38	1.82	20.34	33.47	14.27	2.46	72.37
7.5	0.00	0.00	9.35	24.78	11.83	2.15	48.10
8			1.92	16.08	9.39	1.83	29.23
8.5			0.00	7.39	6.95	1.52	15.86
9				1.52	4.51	1.21	7.24
9.5				0.00	2.07	0.89	2.97
10					0.43	0.58	1.01
10.5					0.00	0.27	0.27
11						0.05	0.05
11.5						0.00	0.00

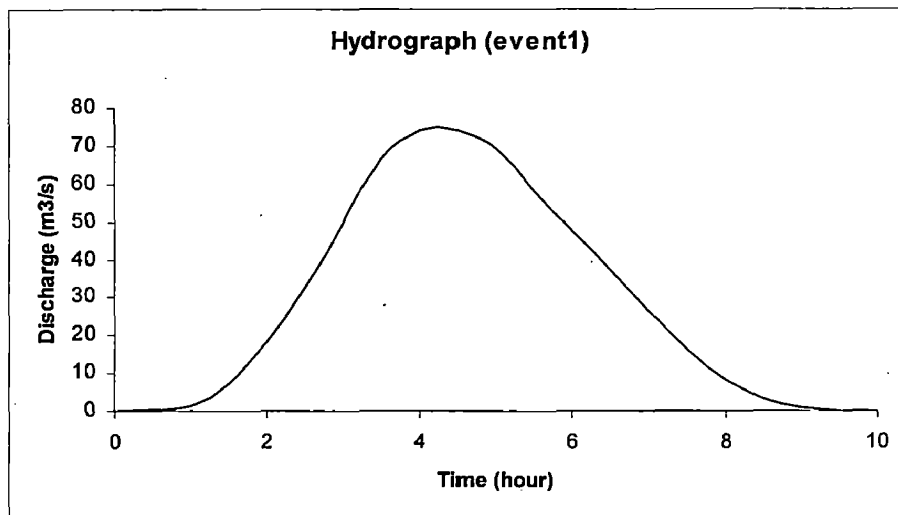
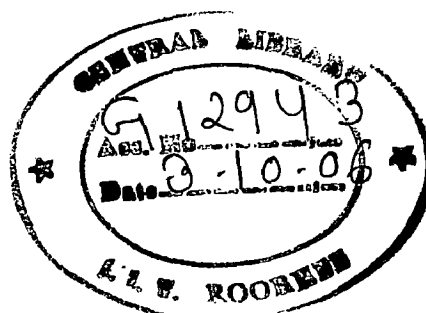


Figure .2.20. Hydrograph – Event 1





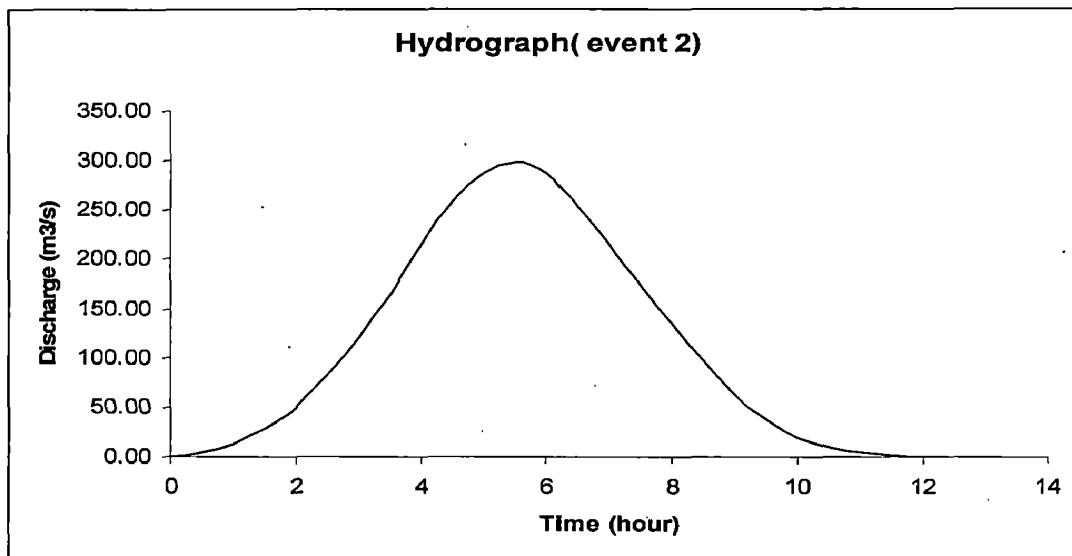


Figure .2.21. Hydrograph – Event 2

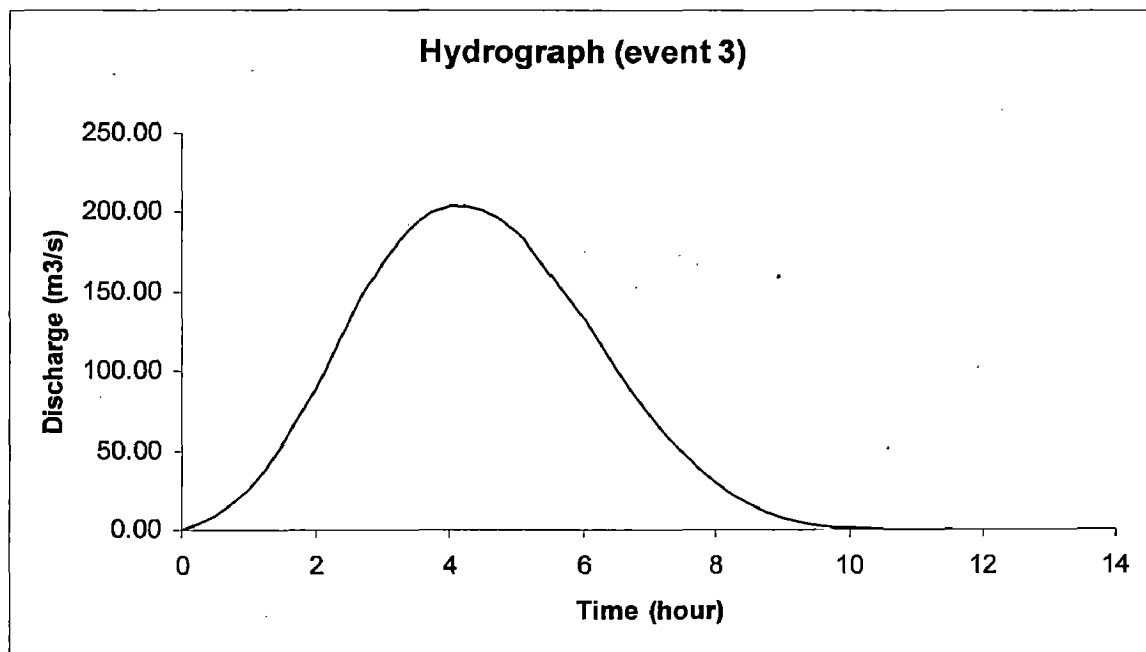


Figure .2.22. Hydrograph – Event 3

## APPENDIX IIIB

### (RESULT BY USING KINEMATICS APPROACH)

Computation infiltration for first event

Value of K,Se,Oe,Y

0.005 0.85 0.385 316.299988

Cumulative infiltration at ponding time:1.363158

infiltration rate at ponding time:0.072

ponding time tp:18.932755

t	r	f	F
60	0.072	0.033389	3.217091
60	0.13	0.023733	4.87531
60	0.063	0.019805	6.169035
0	0	0.019805	6.169035

Computation overland flow for first event

P1

t	y	x	Q	Tr	V
2464	0.001257	135.258743	0.372641	46067.710937	0.09149
3600	0.007413	871.783081	7.176225	11644.972656	0.298688
3600	0.009871	2061.991943	11.567579	6328.496094	0.361541

Time concentration:4.44236

P2

t	y	x	Q	Tr	V
2464	0.001257	131.833923	0.363205	16430.5	0.089174
3600	0.007413	849.709045	6.994519	2566.904541	0.291125
3600	0.009048	1597	9.751545	0	0.332464

Time concentration:2.308815

P3

t	y	x	Q	Tr	V
2464	0.001257	35.786102	0.086692	165959.3125	0.024206
3600	0.007413	230.65213	1.669491	48368.542969	0.079025
3600	0.009871	545.551819	2.691104	36667.832031	0.095655

Time concentration:12.869953

P4

t	y	x	Q	Tr	V
2464	0.001257	113.165596	0.62043	25263.640625	0.076546
3600	0.007413	729.386108	11.948104	5272.552734	0.249901
3600	0.009871	1725.186279	19.259518	1063.894409	0.302487

Time concentration:2.979971

P5

t	y	x	Q	Tr	V
2464	0.001257	117.137512	0.642206	34491.558594	0.079233
3600	0.007413	754.986328	12.367462	8099.124023	0.258672
3600	0.009871	1785.737427	19.935493	3399.077881	0.313103

Time concentration:3.628633

P6

t	y	x	Q	Tr	V
2464	0.001257	82.274689	0.16784	68151.625	0.055651
3600	0.007413	530.284973	3.232231	18409.417969	0.181685
3600	0.009871	1254.260742	5.210133	11916.972656	0.219917

Time concentration:5.994714

P7

t	y	x	Q	Tr	V
2464	0.001257	95.64238	0.285251	34754.101563	0.064693
3600	0.007413	616.443726	5.493307	8179.54248	0.211205
3600	0.009871	1458.048462	8.854831	3465.516357	0.255648

Time concentration:3.647088

P8

t	y	x	Q	Tr	V
2464	0.001257	160.040314	0.306077	7759.256348	0.108253
3600	0.007259	1000	5.692225	0	0.348463

Time concentration:1.35402

Computation infiltration for second event

Value of K,Se,Oe,Y

0.005 0.85 0.385 316.299988

Cumulative infiltration at ponding time:0.546896

infiltration rate at ponding time:0.172

ponding time tp:60.388927

t	r	f	F
60	0.008	0.195274	0.48
60	0.172	0.030716	3.55156
60	0.116	0.022843	5.118686
60	0.194	0.01933	6.373576
60	0.23	0.017233	7.466197
60	0.048	0.015802	8.45507
60	0.028	0.014747	9.370294

0 0 0.014747 9.370493

P1

t	y	x	Q	Tr	V
3577	0.007673	655.948608	7.600667	12086.552734	0.305633
3600	0.013109	1999.293335	18.558355	5381.735352	0.436793
3600	0.023477	3957.000488	49.015892	610.093628	0.644163
3600	0.025569	4350	56.509335	0	0.681807

Time concentration:3.153725

P2

t	y	x	Q	Tr	V
3577	0.007673	639.3396	7.408214	3214.765137	0.297894
3600	0.011818	1597	15.219643	0	0.397266

Time concentration:1.66323

P3

t	y	x	Q	Tr	V
3577	0.007673	173.547684	1.768234	47975.65625	0.080863
3600	0.013109	528.963257	4.317452	30494.066406	0.115565
3600	0.023477	1046.923828	11.403153	17638.246094	0.170429
3600	0.036185	1765.483398	23.451601	10059.126953	0.227407
3600	0.038093	2598.455566	25.548609	6180.805664	0.235332
3600	0.038849	3451.244141	26.399265	2523.763184	0.238436

Time concentration:6.694656

P4

t	y	x	Q	Tr	V
3577	0.007673	548.805969	12.65478	5858.933594	0.255711
3600	0.013109	1672.728882	30.898857	1024.144409	0.365448
3600	0.015869	2047	42.485703	0	0.415041

Time concentration:2.244102

P5

t	y	x	Q	Tr	V
3577	0.007673	568.068115	13.098942	8621.276367	0.264686
3600	0.013109	1731.438721	31.983355	2957.011963	0.378274
3600	0.020358	2850	66.613144	0	0.507237

Time concentration:2.606168

P6

t	y	x	Q	Tr	V
3577	0.007673	398.997955	3.423403	18697.289063	0.185909
3600	0.013109	1216.122681	8.358835	10007.401367	0.265691
3600	0.023477	2406.949463	22.07716	3746.662598	0.391829
3600	0.034928	3875	42.805553	0	0.510594

Time concentration:3.792273

P7

t	y	x	Q	Tr	V
3577	0.007673	463.825684	5.818211	8699.867187	0.216115
3600	0.013109	1413.713867	14.20618	3012.003418	0.30886
3600	0.020476	2344	29.873896	0	0.415754

Time concentration:2.615163

P8

t	y	x	Q	Tr	V
3577	0.007673	776.128845	6.242987	619.061279	0.36163
3600	0.008573	1000	7.510537	0	0.389327

Time concentration:1.153339

Computation infiltration for third event

Value of K,Se,Oe,Y

0.005 0.85 0.385 316.299988

Cumulative infiltration at ponding time:0.385365

infiltration rate at ponding time:0.242

ponding time tp:56.633743

t	r	f	F
60	0.02	0.08111	1.2
60	0.242	0.030082	3.64127
60	0.156	0.022612	5.185764
60	0.116	0.019203	6.430441
60	0.032	0.01715	7.516936
60	0.004	0.015743	8.501619
0	0	0.015743	8.501838

P1

t	y	x	Q	Tr	V
3600	0.006372	583.274231	5.577	13949.032227	0.270035
3600	0.014148	1911.484619	21.074984	5305.890137	0.459586
3600	0.019836	3778.939453	37.014008	991.916382	0.575714
3600	0.020063	4350	37.723042	0	0.580033

Time concentration:3.273481

P2

t	y	x	Q	Tr	V
3600	0.006372	568.505371	5.435787	3907.692139	0.263197

3600 0.012823 1597 17.436337 0 0.419472

Time concentration:1.681078

P3

t	y	x	Q	Tr	V
3600	0.006372	154.319855	1.297444	54569.339844	0.071445
3600	0.014148	505.731293	4.902925	29172.78125	0.121595
3600	0.019836	999.813416	8.611012	20044.591797	0.15232
3600	0.020664	1555.759155	9.218382	15953.796875	0.15653

Time concentration:8.43161

P4

t	y	x	Q	Tr	V
3600	0.006372	488.002228	9.285462	6900.436523	0.225927
3600	0.014148	1599.262817	35.088932	1164.412598	0.384518
3600	0.015915	2047	42.693161	0	0.415851

Time concentration:2.299077

P5

t	y	x	Q	Tr	V
3600	0.006372	505.13028	9.611366	10026.93457	0.233857
3600	0.014148	1655.394165	36.320496	3001.419922	0.398014
3600	0.018465	2850	56.610123	0	0.475273

Time concentration:2.698199

P6

t	y	x	Q	Tr	V
3600	0.006372	354.79187	2.511926	21431.253906	0.164256
3600	0.014148	1162.710693	9.492345	9702.148437	0.279556
3600	0.019836	2298.63916	16.671413	4501.400879	0.350193
3600	0.020664	3576.796387	17.847317	828.637756	0.359872

Time concentration:4.230177

P7

t	y	x	Q	Tr	V
3600	0.006372	412.437164	4.269121	10115.886719	0.190944
3600	0.014148	1351.623779	16.132624	3053.684082	0.324977
3600	0.018534	2344	25.301683	0	0.389026

Time concentration:2.708591

P8

t	y	x	Q	Tr	V
3600	0.006372	690.139404	4.5808	969.800598	0.31951
3600	0.008282	1000	7.090558	0	0.380467

Time concentration:1.226228

**HYDRAULIC DESIGN OF CULVERTS**

A culvert conveys surface water through a roadway embankment or away from the highway right – of way. In addition to this hydraulic function, it must also carry construction and highway traffic and earth loads, therefore culvert design involves both hydraulic and structural design. The hydraulic and structural design must be such that minimal risk to traffic, property damage, and failure from floods prove the result of good engineering practice and economics. Culvert is considered minor structure, but they are of great importance to adequate drainage and the integrity of the facility.

Culverts have numerous cross – sectional shapes. The most commonly used shape are open bottom, box, pipe – arch, Multiple and Cylindrical culvert and are shown below :

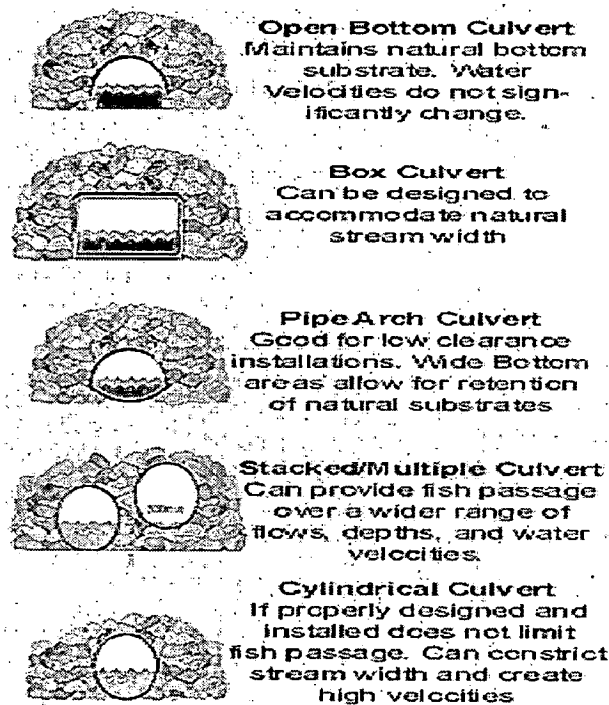


Fig 3.1. Different cross sections of culvert

Besides the shape, there are different types of inlet to the culvert barrels which are both prefabricated and constructed-in-place installation. Commonly used inlet configuration include the following:

- Projecting culvert barrels
- Cast-in-place concrete headwalls
- Precast or prefabricated end section
- Culvert end mitered to conform to the fill slope

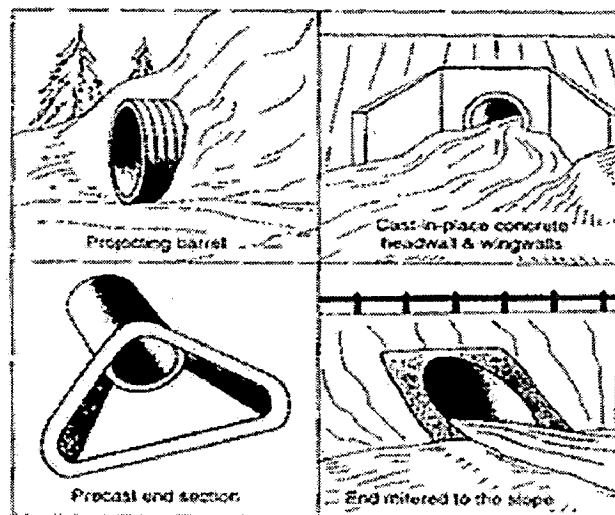


Fig 3.2. Four standard inlet type

Inlet design is important because the hydraulic capacity of a culvert may be improved by the appropriate inlet selection. Natural channels are usually much wider than the culvert barrel, so that the inlet is a flow contraction and can be the primary flow control.

The hydraulic design of culvert depends upon the type of flow control. This chapter discusses the various types of flow control and the design equations corresponding to these flow controls.



### 3.1 FLOW CONTROLS IN CULVERTS

There are two basic types of flow control: inlet control and outlet control. These are explained as follows :

#### 3.1.1 INLET CONTROL

Culvert with inlet control have high-velocity shallow flow that is supercritical, as shown in Figure 3.3. The control section is at the upstream end (inlet). The figure illustrates four different examples of inlet control that depend on the submergence of the inlet and outlet ends of the culvert.

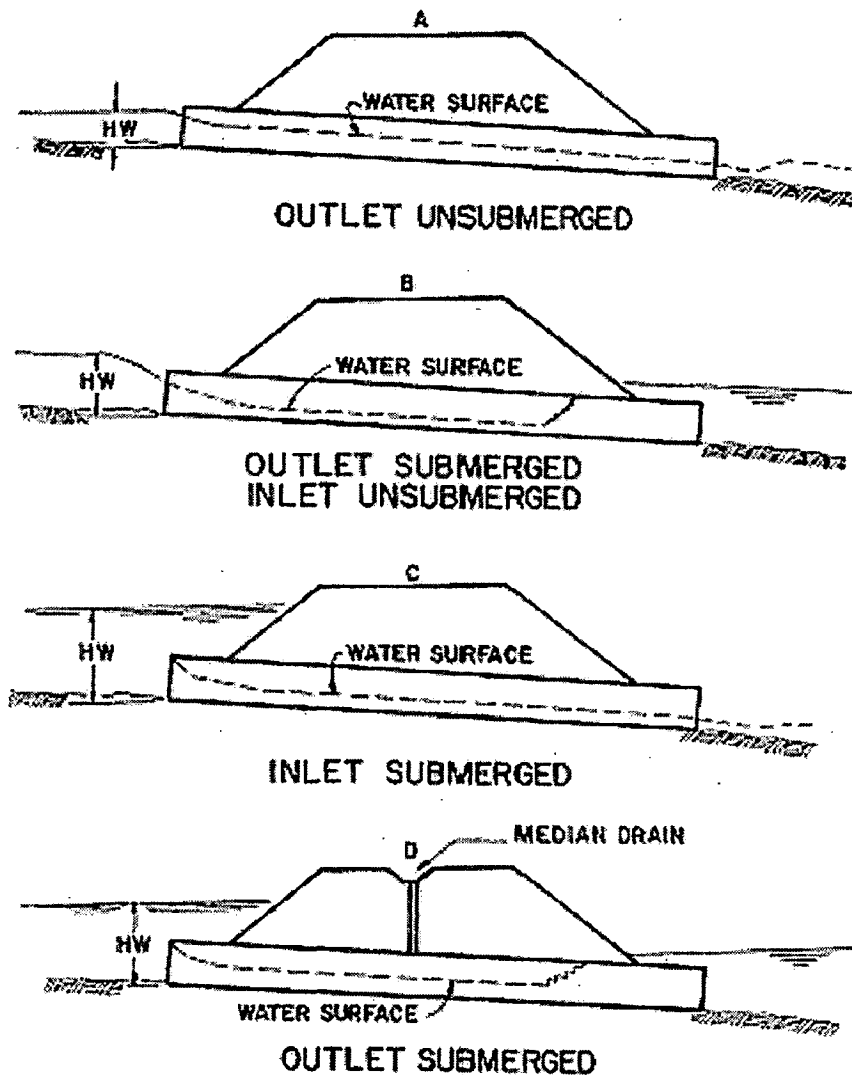


Figure 3.3. Types of inlet control

In Figure 3.3a, neither end of the culvert is submerged. Flow passes through critical depth just downstream of the culvert entrance with supercritical flow in the culvert barrel. Partly full flow occurs throughout the length of the culvert, approaching normal depth at the outlet.

In Figure 3.3b, the outlet is submerged and the inlet is unsubmerged. The flow just downstream of the inlet is supercritical and a hydraulic jump occurs in the culvert barrel.

In Figure 3.3c, the inlet is submerged and the outlet is unsubmerged. Supercritical flow occurs throughout the length of the culvert barrel, with critical depth occurring just downstream of the culvert entrance. Flow approaches normal depth at the downstream end. This flow condition is typical of design condition.

In Figure 3.3d shows an unusual condition in which submergence occurs at both ends of the culvert with a hydraulic jump occurring in the culvert barrel. Note the median inlet, which provides ventilation of the culvert barrel.

### **Inlet-control design equation**

A culvert under inlet-control conditions performs as an orifice when the inlet is submerged and as a weir when it is unsubmerged.

The (submerged) orifice discharge equation is computed using:

$$\frac{Hw}{D} = C \left( \frac{K_u Q}{AD^{0.5}} \right)^2 + Y + Z \qquad \text{For} \left( \frac{K_u Q}{AD^{0.5}} \right)^2 \geq 4 \qquad (a)$$

where:  $K_u$  is 1.811 SI (1.0 English)

$Hw$  is the headwater depth above the inlet control section invert m(ft)

$D$  is the interior height of the culvert barrel m(ft)

Q is the discharge  $m^3/s(ft^3/s)$

A is the full cross-sectionnal area of the culvert barrel in  $m^2(ft^2)$

C and Y are constants from table 3.1 and

Z is the slope correction factor, where  $Z=-0.5 S_o$  in general and  $Z=+ 0.7 S_o$  for mitered inlet.

The (unsubmerged) weir discharge equation is (Form 1):

$$\frac{H_w}{D} = \frac{H_c}{D} + K \left( \frac{K_u Q}{AD^{0.5}} \right)^M + Z \quad \text{For} \left( \frac{K_u Q}{AD^{0.5}} \right)^2 \leq 3.5 \quad (b)$$

where:

$H_c$  is the specific head at critical depth ( $H_c = d_c + V_c^2/2g$ ) m(ft)

$d_c$  is the critical depth m(ft)

$V_c$  is the critical velocity m/s(ft/s), and K and M are constants in Table 3.1

A simpler equation to use for the unsubmerged condition is (form 2):

$$\frac{H_w}{D} = K \left( \frac{K_u Q}{AD^{0.5}} \right)^M + Z \quad \text{For} \left( \frac{K_u Q}{AD^{0.5}} \right)^2 \leq 3.5 \quad (c)$$

Equations (a) to (c) are implemented by assuming a culvert diameter D and using it on the right- hand side of these equations and solving for (Hw/D). The headwater depth is then obtained by multiplying D(Hw/D). We can use nomographs to design culverts.

Table 3.1. Constants for Inlet Control Design Equations

Chart No	Shape And Material	Monograph Scale	Inlet Edge Description	Unsubmerged			Submerged		
				Equation					
				Form	K	M	C	Y	
1	Circular	1	Square edge w/headwall	1	0.0098	2	0.0398	0.67	
	Concrete	2	Groove and w/headwall		0.0078	2	0.0292	0.74	
		3	Groove and projecting		0.0045	2	0.0317	0.69	
2	Circular	1	Headwall	1	0.0078	2	0.0379	0.69	
	CMP	2	Mitered to slope		0.021	1.33	0.0463	0.75	
		3	Projecting		0.034	1.5	0.0553	0.54	
3	Circular	A	Beveled ring, 45° bevel	1	0.0018	2.5	0.03	0.74	
		B	Beveled ring, 33.7° bevel		0.0018	2.5	0.0243	0.83	
8	Rectangular	1	30° to 75° wingwall flares		0.026	1	0.0385	0.81	
	Box	2	90° to 15° wingwall flares	1	0.061	0.75	0.04	0.8	
		3	0° wingwall flares		0.061	0.75	0.0423	0.82	
9	Rectangular	1	45° wingwall flare d=0.043	2	0.51	0.667	0.0309	0.8	
	Box	2	18° to 33.7° wingwall flare d=0.083		0.486	0.667	0.0249	0.83	
10	Rectangular	1	90° headwall w/3/4" chamfers	2	0.515	0.667	0.0375	0.79	
		Box	2	90° headwall w/45° chamfers		0.495	0.667	0.0314	0.82
			3	90° headwall w/33.7° bevels		0.486	0.667	0.0252	0.865
11	Rectangular	1	3/4" chamfers; 45° skewed headwall	2	0.522	0.667	0.0402	0.73	
		Box	2	3/4" chamfers; 30° skewed headwall		0.533	0.667	0.0425	0.705
			3	3/4" chamfers; 15° skewed headwall		0.545	0.667	0.04505	0.68
				45° bevels; 10°-45° skewed headwall		0.498	0.667	0.0327	0.75
12	Rectangular	1	45° non offset wingwall flares	2	0.497	0.667	0.0339	0.805	
		Box	2	18.4° non offset wingwall flares		0.493	0.667	0.0361	0.806
		3/4" chamfers	3	18.4° non offset wingwall flares		0.495	0.667	0.386	0.71
				30° skewed barrel					
13	Rectangular	1	45° wingwall flares - offset	2	0.495	0.667	0.0302	0.835	
		Box	2	33.7° wingwall flares - offset		0.493	0.667	0.0252	0.881
		Top bevels	3	18.4° wingwall flares - offset		0.497	0.667	0.0227	0.887
16-19	CM boxes	1	90° headwall	1	0.0083	2	0.0379	0.69	
			2	Thick wall projecting		0.0145	1.75	0.0419	0.64
			3	Thin wall projecting		0.034	1.5	0.0496	0.57
29	Horizontal	1	Square edge with headwall	1	0.01	2	0.0398	0.67	
	Ellipse	2	Groove end with headwall		0.0018	2.5	0.0292	0.74	
	Concrete	3	Groove end projecting		0.0045	2	0.0317	0.69	
30	Vertical	1	Square edge with headwall	1	0.01	2	0.0398	0.67	
	Ellipse	2	Groove end with headwall		0.018	2.5	0.0292	0.74	
	Concrete	3	Groove end projecting		0.0095	2	0.0317	0.69	
34	Pipe arch	1	90° headwall	1	0.0083	2	0.0379	0.69	
	18" corner	2	Mitered to slope		0.03	1	0.0463	0.75	
	Radius CM	3	Projecting		0.034	1.5	0.0496	0.57	
35	Pipe arch	1	90° headwall	1	0.0296	1.5	0.0487	0.55	
	18" corner	2	No. bevels		0.0087	2	0.0361	0.66	

Table 3.1. Constants for Inlet Control Design Equations(continue)

Chart No	Shape And Material	Monograph Scale	Inlet Edge Description	Unsubmerged			Submerged	
				Equation				
				Form	K	M	C	Y
	Radius CM	3	33.7° bevels		0.003	2	0.0264	0.75
36	Pipe arch	1	Projecting	1	0.0296	1.5	0.0487	0.55
	31" corner		No.bevels		0.0087	2	0.0361	0.66
	Radius CM		33.7° bevels		0.003	2	0.0264	0.75
40-42	Arch CM	1	90° headwall	1	0.0083	2	0.0379	0.69
		2	Mitered to slope		0.03	1	0.0463	0.75
		3	Thin wall projecting		0.034	1.5	0.0496	0.57
55	Circular	1	Smooth tapered inlet throat	2	0.534	0.555	0.0196	0.89
		2	Rough tapered inlet throat		0.519	0.64	0.0289	0.9
56	Elliptical	1	Tapered inlet-beveled edges	2	0.536	0.622	0.0368	0.83
	Inlet face	2	Tapered inlet-square edges		0.5035	0.719	0.0478	0.8
		3	Tapered inlet-thin edge projecting		0.547	0.8	0.0598	0.75
57	Rectangular	1	Tapered inlet throat	2	0.475	0.667	0.0179	0.97
58	Rectangular	1	Side tapered-less favorable edges	2	0.56	0.667	0.0466	0.85
	Concrete	2	Side tapered-more favorable edges		0.56	0.667	0.3978	0.87
59	Rectangular	1	Slope tapered-less favorable edges	2	0.5	0.667	0.0466	0.65
	Concrete		Slope tapered-more favorable edges		0.5	0.667	0.0378	0.71

### **3.1.2 OUTLET CONTROL**

Culvert with outlet control have lower velocity, deeper flow that is subcritical as shown in Figure 3.4 The control section is at the downstream and( outlet) of the culvert. Tailwater depths are either critical depth or higher. The Figure illustrates five flow condition for outlet control. Subcritical flow occurs for the partly full flow conditions.

In Figure 3.4.a is the classic condition with both the inlet and the outlet submerged, with pressurized flow throughout the culvert.

In Figure 3.4.b, the outlet is submerged and the inlet is unsubmerged

In Figure 3.4.c ,the entrance is submerged enough that full flow occurs throughout the culvert length but the exit is unsubmerged

In Figure 3.4.d is a typical condition in which the entrance is submerged by the headwater and the outlet end flows freely with a low tailwater. The

culvert barrel flows partly full part of the length with subcritical flow and passes through critical just upstream of the outlet.

In Figure 3.4.e is another typical condition in which neither the inlet nor the outlet is submerged. The flow is subcritical and partly full throughout the length of the culvert barrel.

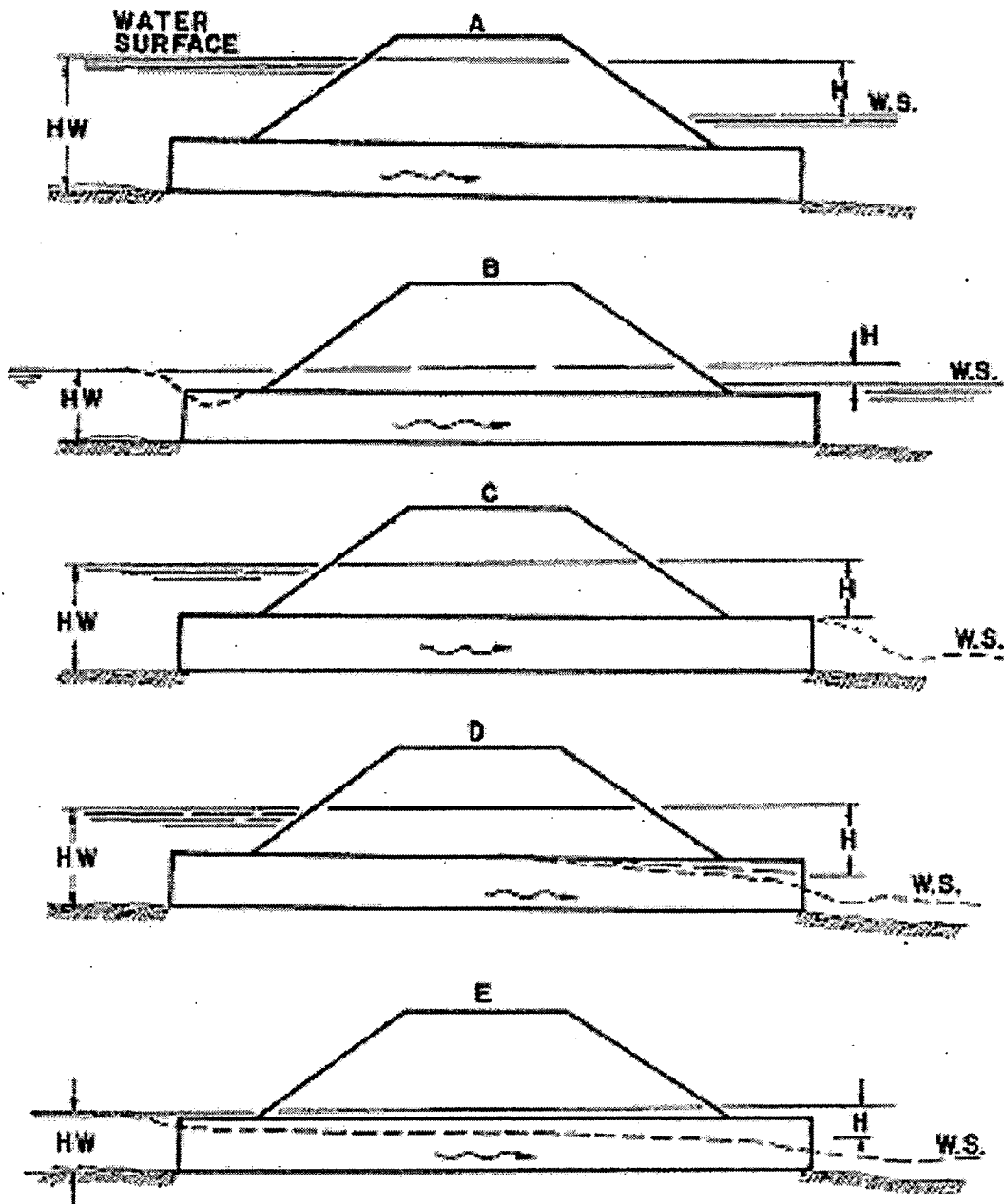


Figure 3.4. Types of outlet control

## Outlet-control design equation

A culvert under outlet control condition has either subcritical flow or full culvert flow, so that outlet control flow condition can be calculated using an energy balance. For the condition of full culvert flow, considering entrance loss  $H_e$ , friction loss (using Manning's equation)  $H_f$  and exit loss  $H_o$ , the total headloss  $H$  is

$$H = H_o + H_e + H_f$$

And in U.S. customary units is:

$$H = \left[ 1 + K_e + \left( \frac{K_u n^2 L}{R^{1.33}} \right) \right] \frac{V^2}{2g}$$

Where

$K_u = 19.63$  (29 in English units)

$K_e$  is the entrance loss coefficient,  $n$  is Manning's roughness coefficient,

$R$  is the hydraulic radius of the full-culvert barrel in ft (m),

$V$  is the velocity in ft/s (m/s), and

$L$  is the culvert length in ft(m).

Table 3.2 lists common values of Manning's  $n$  values for culverts and table 3.3 lists entrance loss coefficient for outlet control, full or part full flow.

Figure 3.5 illustrates the energy and hydraulic grade lines for full flow in a culvert. Equating the total energy at section 1 (upstream) and section 2 (downstream) gives

$$HW_o + \frac{V_u^2}{2g} = TW + \frac{V_d^2}{2g} + H_f + H_e + H_o$$

where

$HW_o$  is the headwater depth above the outlet invert

TW is the tail water depth above the outlet invert.

Neglecting the approach velocity head and the downstream velocity head we get:

$$HW_o = TW + H_f + H_e + H_o$$

For full flow  $TW \geq D$ ; however, for partly full flow, the head loss should be computed from a back-water analysis. An empirical equation for the head loss  $H$  for this condition is

$$H = HW_o - h_o$$

Where  $h_o = \max [TW, (D+d_c)/2]$

$$\text{and } HW = H + h_o - LS_o$$

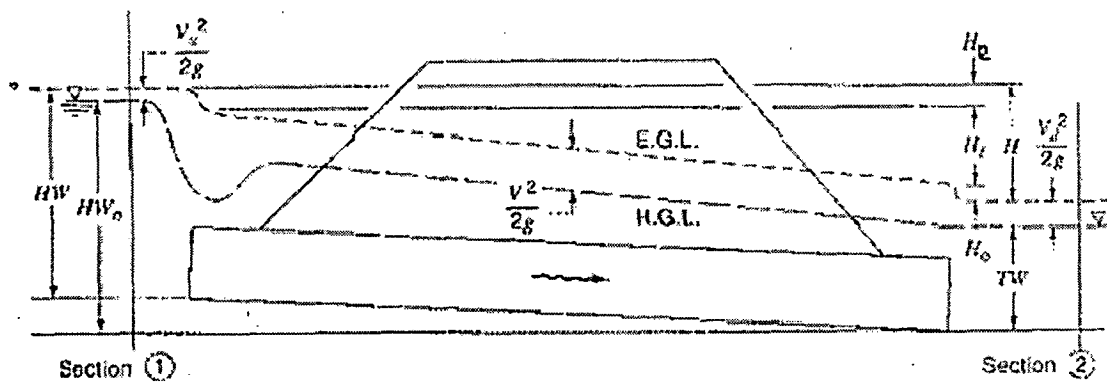


Figure 3.5. Full-flow energy and hydraulic grade lines



Table 3.2 Manning n Values for Culverts

Type of conduit	Wall Description	Manning n
Concrete pipe	Smooth walls	0.01-0.013
Concrete boxes	Smooth walls	0.012-0.015
Corrugated metal pipes and boxes	68 mm by 13mm corrugations	0.022-0.027
, annular or helical pipe (manning n varies with barrel size)	6" by 1" corrugations	0.022-0.025
	5" by 1" corrugation	0.025-0.026
	3" by 1" corrugation	0.027-0.028
	6" by 2" structural plate corrugations	0.033-0.035
	9" by 2 1/2" structural plate corrugations	0.033 -0.037
Corrugated metal pipes, helical corrugations, full circular flow	2 2/3" by 1/2" corrugations	0.012-0.024
Spiral rib metal pipe	Smooth walls	0.012-0.013

Table 3.3. Entrance loss Coefficients for Outlet Control, Full or Partly Full  $H_e = k_e [ V^2/2g ]$

Type of structure and Design of Entrance	Coefficient K
<b>Pipe, concrete</b>	
Mitered to conform to fill slope	0.7
End section conform to fill slope	0.5
Projecting from fill, sq. cut end	0.5
Headwall or headwall and wing walls	
Square-edge	0.5
rounded (radius = 1/12D)	0.2
Socket end of pipe ( groove – end)	0.2
Projecting from fill, socket end(groove-end)	0.2
Beveled edges, 33.7° or 45° bevels	0.2
Side- or slope-tapered inlet	0.2
<b>Pipe or pipe- arch, corrugated metal</b>	
Projecting from fill (no headwall)	0.9
Mitered to conform to fill slope, paved or unpaved slope	0.7
Headwall or headwall and wing walls square-edge	0.5
End section conform to fill slope	0.5
Beveled edges, 33.7° or 45° bevels	0.2
Side- or slope-tapered inlet	0.2
<b>Box, reinforced concrete</b>	
Wingwalls parallel( extension of sides)	
Square-edged at crown	0.7
Wingwalls at 10° to 25° or 30° to 75° to barrel	

Table 3.3. Entrance loss Coefficients for Outlet Control, Full or Partly Full  
 $H_e = k_e [V^2/2g]$  (continue)

Type of structure and Design of Entrance	Coefficient K
Square-edged on 3 edges	0.5
Rounded on 3 edges to radius of 1/12 barrel dimension, or beveled edges on 3 sides	0.2
Wingwalls at 30° to 75° to barrel	
Crown edge rounded to radius of 1/12 barrel dimension, or beveled top edge	0.2
Side- or slope-tapered inlet	0.2

**Example**

A culvert at a new roadway crossing must be designed to pass the 25-year flood. Hydrologic analysis indicates a peak flow rate of 5.663 m<sup>3</sup>/s. Use the following site information:

Elevation at Culvert Face: 30.480 m

Natural Stream Bed Slope: 1 percent = 0.01 m/m

Tailwater for 25-Year Flood: 1.067 m

Approximate Culvert Length: 60.960 m

Shoulder Elevation: 33.528m

Design a circular pipe culvert for this site. Consider the use of a corrugated metal pipe with standard 68 x 13 mm in corrugations and beveled edges and concrete pipe with a groove end. Base the design headwater on the shoulder elevation with a 0.61 m freeboard (elevation 32.918 m). Set the inlet invert at the natural streambed elevation (no FALL).

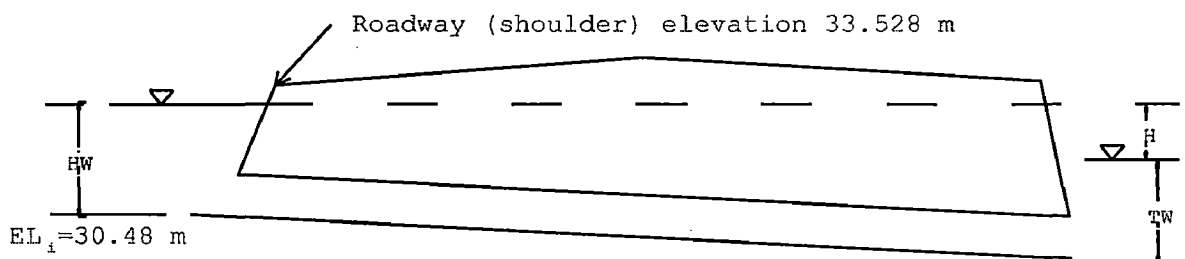


Table 3.4. Compare four type of culverts

Culvert Description Material-Shape-Size- Entrance	Flow Q (m <sup>3</sup> /s)	Headwater Calculations														Control Headwater Elevation
		Inlet Control						Outlet Control								
		HW <sub>i</sub> /D	HW <sub>i</sub> (m)	EL <sub>hi</sub> (m)	TW (m)	d <sub>c</sub> (m)	(d <sub>c</sub> +D)/2 (m)	h <sub>o</sub> (m)	k <sub>c</sub>	n	H (m)	EL <sub>ho</sub> (m)				
1800 mm CMP 45° Beveled Ring	5.663	0.97	1.75	32.23	1.07	1	1.4	1.4	0.2	0.024	0.8	32.07	32.23			
1500 mm CMP 45° Beveled Ring	5.663	1.41	2.12	32.6	1.07	1.1	1.3	1.3	0.2	0.024	1.95	33.12	33.12			
1500 mm Conc Grooved end in head wall	5.663	1.38	2.07	32.55	1.07	1.1	1.3	1.3	0.2	0.012	0.95	32.12	32.55			
1350mm Conc Grooved end in head wall	5.663	1.82	2.46	32.94	1.07	1.2	1.28	1.28	0.2	0.012	1.5	32.65	32.94			

### **Discussion of results**

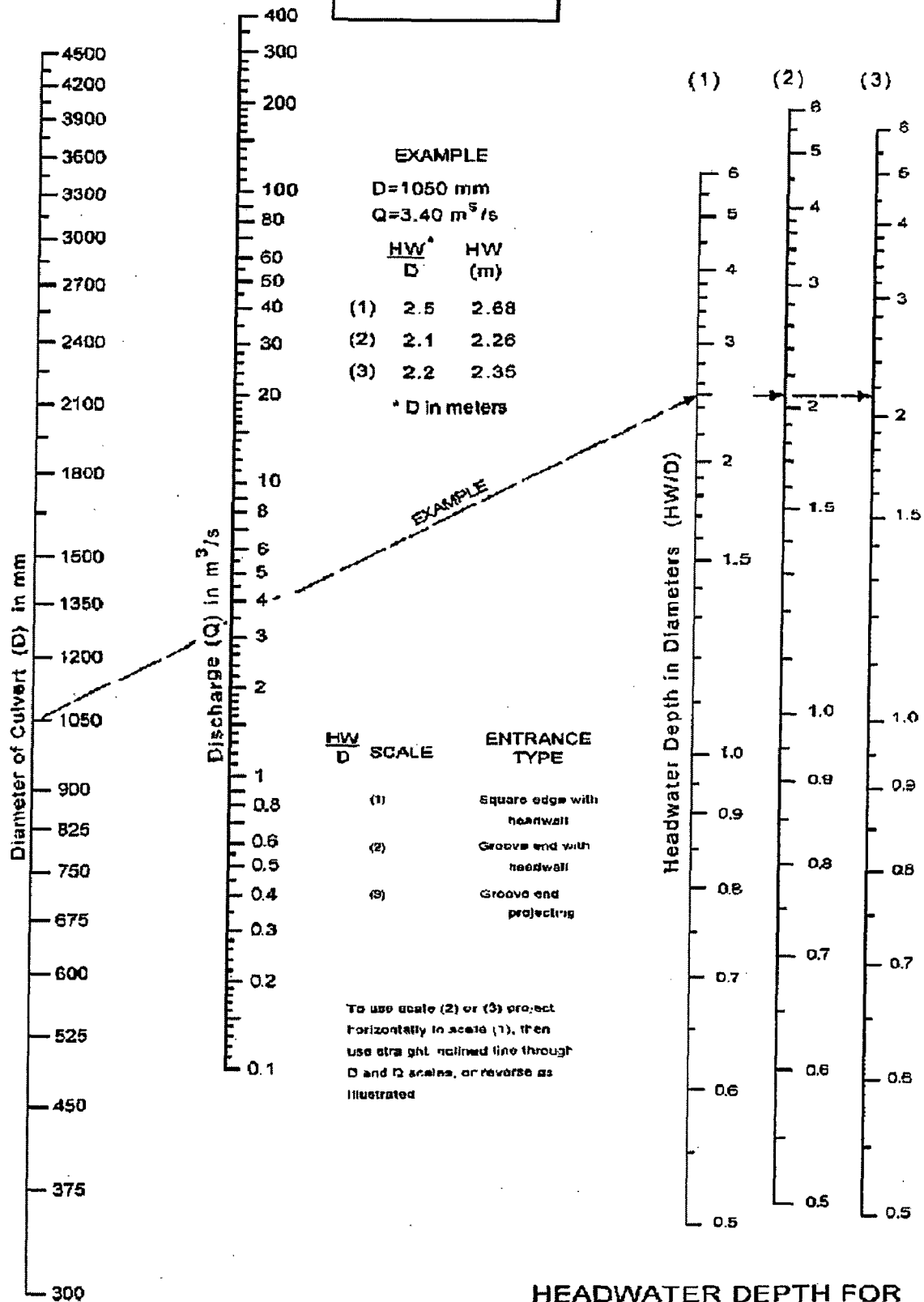
Hydraulic design of culverts depend on condition flow through culverts which is inlet control or outlet control.

From table 3.4 the culvert with 1800 mm in diameter, corrugated 45° Beveled Ring and 1500 mm in diameter, concrete grooved end in head wall have control headwater elevation are 32.23 m and 32.55 m respectively is lower than shoulder elevation –free board (32.918 m ). So ok

### **Conclusion**

In this chapter, the hydraulic design of culverts has been discussed. The hydraulics of flow in the culvert depend on many variables including inlet geometry, slope, size, flow rate, roughness and approach and tailwater conditions. While, designing the culverts, one should consider these parameters and the flow control conditions.

# CHART 1A

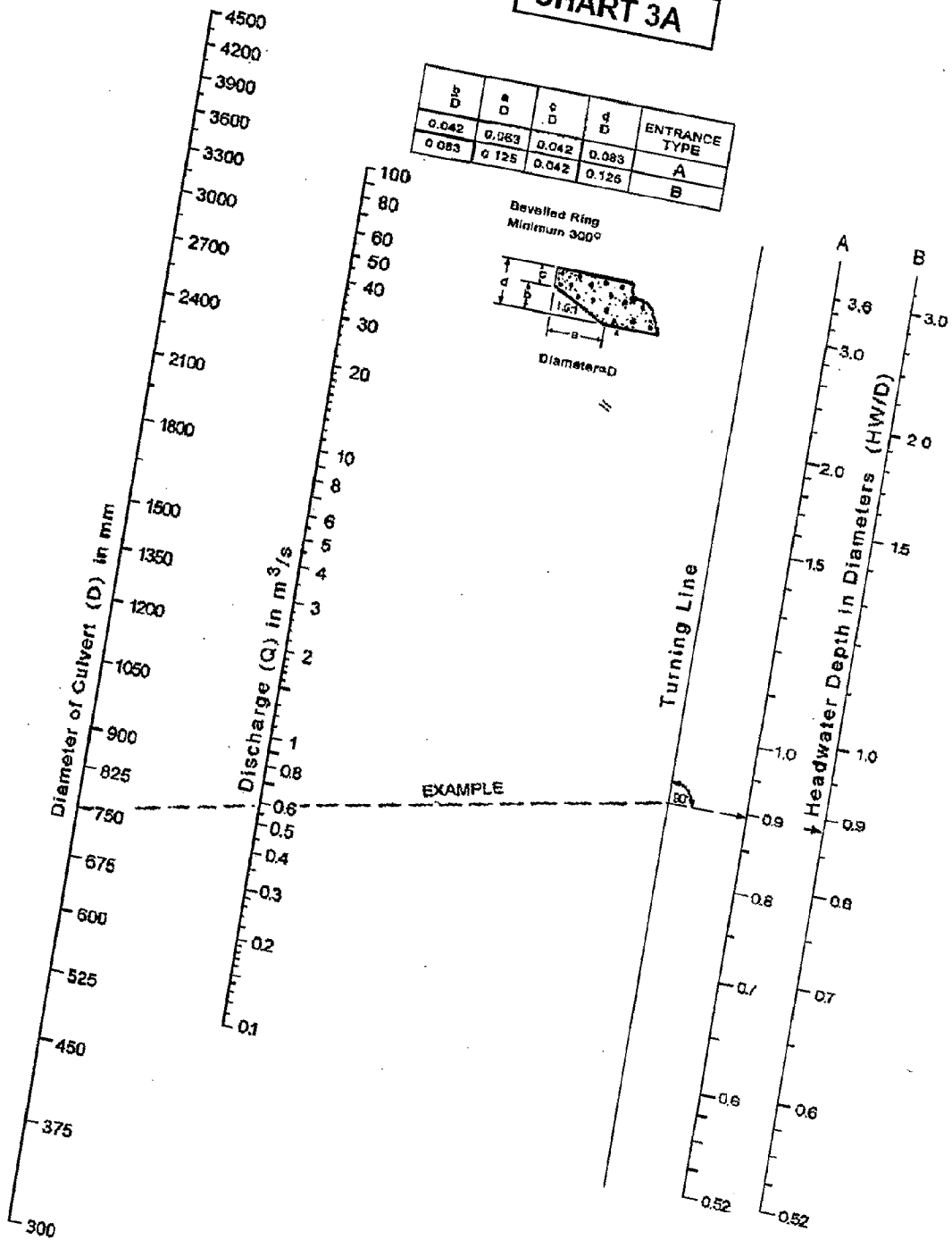


## HEADWATER DEPTH FOR CONCRETE PIPE CULVERTS WITH INLET CONTROL

Adapted from  
 Hureau & Public Roads Jan. 1963

# CHART 3A

b/D	a/D	c/D	d/D	ENTRANCE TYPE
0.042	0.063	0.042	0.083	A
0.083	0.125	0.042	0.126	B



Adapted from  
Federal Highway Administration May 1973

HEADWATER DEPTH FOR  
CIRCULAR PIPE CULVERTS  
WITH BEVELED RING  
INLET CONTROL

---

---

**HYDRAULIC DESIGN OF BRIDGES****4.1. GENERAL**

Bridges enable streams to maintain flow conveyance and to sustain aquatic life. They are important and expensive highway hydraulic structures vulnerable to failure from flood related causes. Thus, hydraulic design of bridges is an important activity for highway engineers. An important hydraulic feature at bridge crossing is the backwater effect produced by constricting the flow of a stream with the highway or railway crossings. In addition, the increased velocity of the stream through the bridge opening and the turbulence produced by over-bank flow returning to the channel can produce scour sufficient to endanger the bridge structure. Confining flood waters unduly by bridge can cause excessive backwater resulting in flooding of upstream property, overtopping of roadways, excessive scour under the bridge, costly maintenance or even loss of a bridge

The estimation of scour in braided rivers due to constriction by the construction of bridge approaches is a considerable problem of river morphology. To predict constriction scour at the bridge, many equations are used such as Laursen's equation, Liu.et.al's equation and Froehlich's equations. In this chapter, the main two aspects – backwater effects, and the scour are considered while designing the bridges.

## **4.2. HYDRAULICS OF BRIDGE WATERWAY**

### **4.2.1. General**

There was a time, now past, when backwater caused by the presence of bridges during flood periods was considered a necessary nuisance . With the spread of urbanization; with indefinite, unenforceable restrictions on the construction of housing and business establishments on flood plains of rivers and streams throughout the country, with new highway bridges being constructed at an ever-increasing rate. It is now imperative that the backwater produced by new bridges be kept within very knowledgeable and reasonable limits.

Confining flood waters unduly by bridges can cause excessive backwater resulting in flooding of upstream property, backwater damage suits, overtopping of roadways, excessive scour under the bridge, costly maintenance, or even loss of a bridge.

It is seldom economically feasible or necessary to bridge the entire width of a stream as it occurs at flood flow. Where conditions permit, approach embankments are extended out onto the flood plain to reduce costs, recognizing that, in so doing, the embankments will constrict the flow of the stream during flood stages.

Constriction of the flow causes a loss of energy, the greater portion occurring in the re-expansion downstream. This loss of energy is reflected in a rise in the water surface and in the energy line upstream from the bridge. This is best illustrated by a profile along the center of the stream, as shown in Figure 4.1.

There are three types of flow which may be encountered in bridge waterway design. These are labeled types I through III on Figure 4.2.



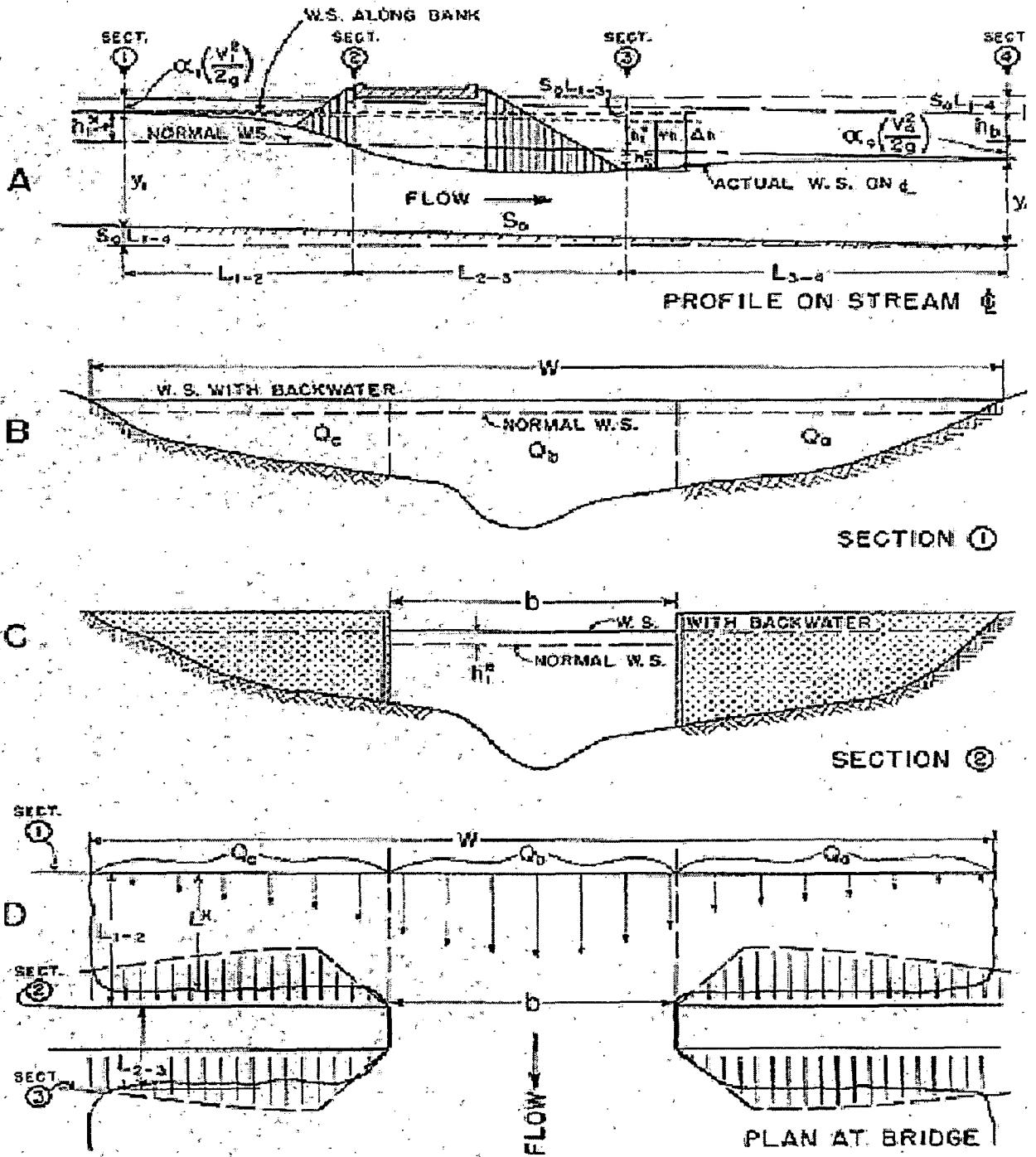


Figure 4.1. Normal crossing

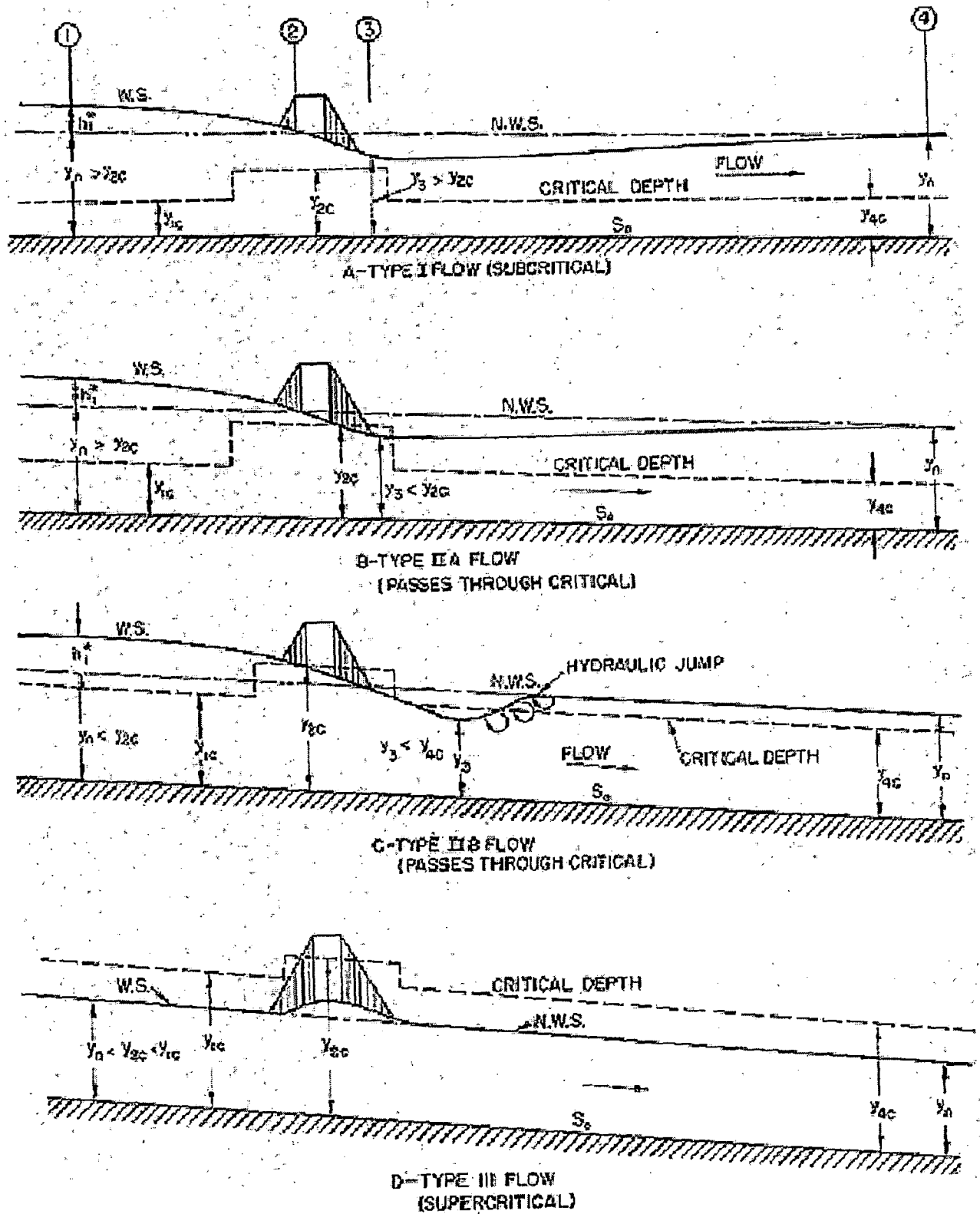


Figure 4.2. Type of water flow

## 4.2.2. Computation of Backwater

### 4.2.2.1. Expression of Backwater

An expression for backwater has been formulated by applying the principle of conservation of energy between the point of maximum backwater upstream from the bridge, section 1, and a point downstream from the bridge at which the normal stage has been reestablished, section 4 (Figure 4.3). The method was developed on the basis that the channel in the vicinity of the bridge is essentially straight, the cross sectional area of the stream is reasonably uniform and the gradient of the bottom is constant between sections 1 and 4.

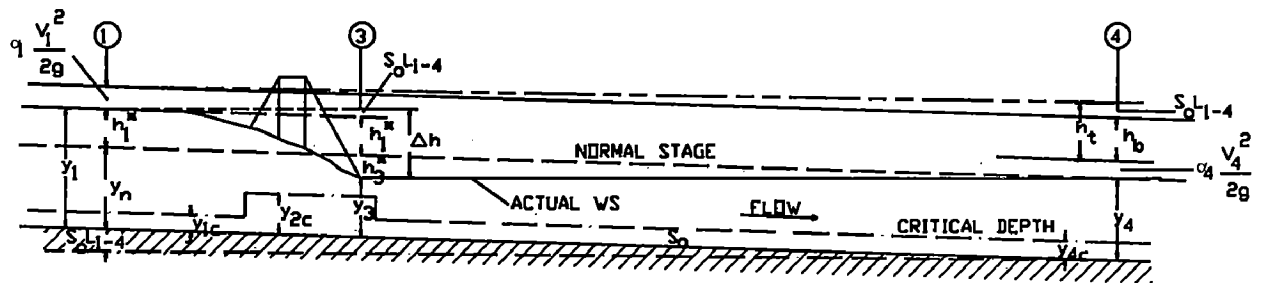


Figure 4.3. Water profile

Equating the energy between sections 1 and 4

$$S_0 L_{1-4} + y_1 + \frac{\alpha_1 V_1^2}{2g} = y_4 + \frac{\alpha_4 V_4^2}{2g} + h_t \quad (4.1)$$

where  $h_t$  is the total energy loss between sections 1 and 4.

$$\text{or } y_1 - y_4 = \frac{\alpha_4 V_4^2}{2g} - \frac{\alpha_1 V_1^2}{2g} + h_b \quad (4.2)$$

The additional loss,  $h_b$ , can be expressed as the product of a loss coefficient,  $K^*$ , and a velocity head.

$$h_b = K^* \frac{\alpha_2 V_{n2}^2}{2g}$$

where  $V_{n2}$  is average velocity in the contracted section based on the flow area below normal water surface.

Replacing  $y_1 - y_4$  with  $h_1^*$ , and  $h_b = K^* \frac{\alpha_2 V_{n2}^2}{2g}$ , equation becomes

$$h_1^* = K^* \alpha_2 \frac{V_{n2}^2}{2g} + \left[ \frac{\alpha_4 V_4^2}{2g} - \frac{\alpha_1 V_1^2}{2g} \right] \quad (4.3)$$

Since the analysis is based on the assumption that the cross sectional areas at sections 1 and 4 are essentially the same,  $\alpha_4$  can be replaced by  $\alpha_1$ . Also from the equation of continuity  $A_1 V_1 = A_4 V_4 = A_{n2} V_{n2}$ , velocities can be expressed as areas. So the expression for backwater becomes:

$$h_1^* = K^* \alpha_2 \frac{V_{n2}^2}{2g} + \alpha_1 \left[ \left( \frac{A_{n2}}{A_4} \right)^2 - \left( \frac{A_{n2}}{A_1} \right)^2 \right] \frac{V_{n2}^2}{2g} \quad (4.4)$$

where:  $h_1^*$  = total backwater (ft.).

$K^*$  = total backwater coefficient.

$\alpha_1$  &  $\alpha_2$  = Kinetic Energy Coefficient

$A_{n2}$  = gross water area in constriction measured below normal stage (sq. m.).

$V_{n2}$  = average velocity in constriction or  $Q/A_{n2}$  (m/s.). The velocity,  $V_{n2}$ , is not an actual measurable velocity, but represents a reference velocity readily computed for both model and field structures.

$A_4$  = water area at section 4 where normal stage is reestablished (sq. m.).

$A_1$  = total water area at section 1, including that produced by the backwater (sq. m.).

To compute backwater, it is necessary to obtain the approximate value of  $h_1^*$  by using the first part of the expression (4.4): (4.4a)

The value of  $A_1$  is the second part of expression (4.4), which depends on  $h_1^*$ , can then be determined and the second term of the expression evaluated: (4.4b)

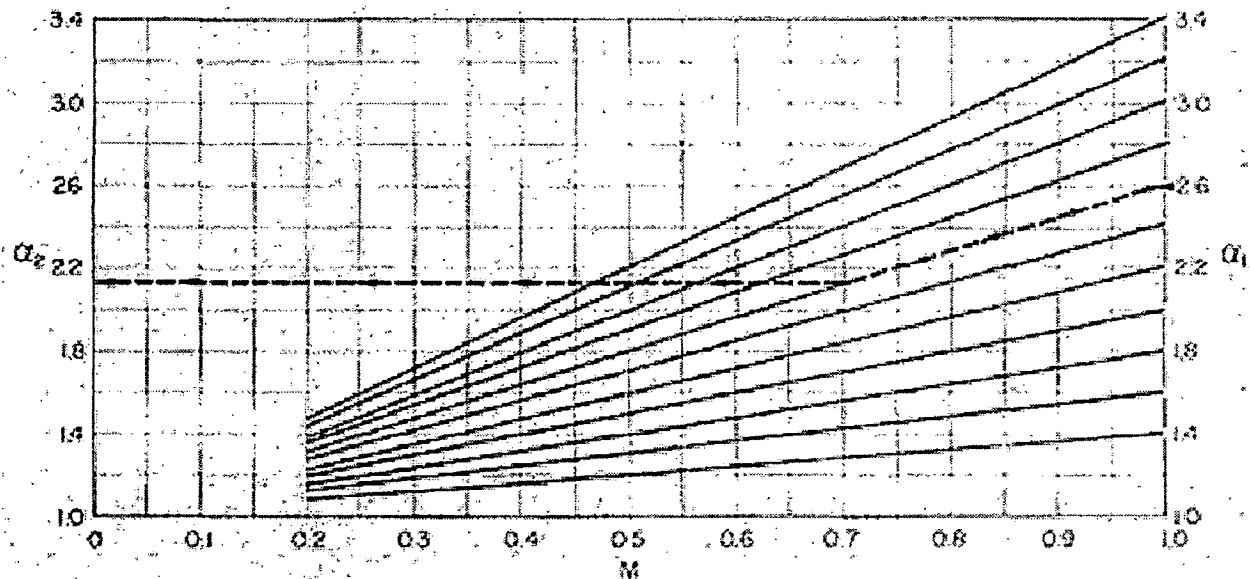


Figure 4.4 .Aid for Estimating  $\alpha_2$

#### 4.2.2.2 Backwater Coefficient

Total backwater coefficients  $K^*$  dependent on the degree of constriction of flow at a bridge but also affected by: Number, size, shape, and orientation of piers in the constriction, eccentricity or asymmetric position of bridge with

respect to the valley cross section, and skew (bridge crosses stream at other than 90° angle).

$$K^* = K_b + \Delta K_p + \Delta K_e + \Delta K_s \quad (4.5)$$

where

$K_b$  is known as a base coefficient and the curves on Figure 4.5 are called base curves.  $K_b$  depend on the opening ratio,  $M$  and abutment shape, length

$$M = \frac{Q_b}{Q_a + Q_b + Q_c} = \frac{Q_b}{Q} \quad (\text{from figure 4.1})$$

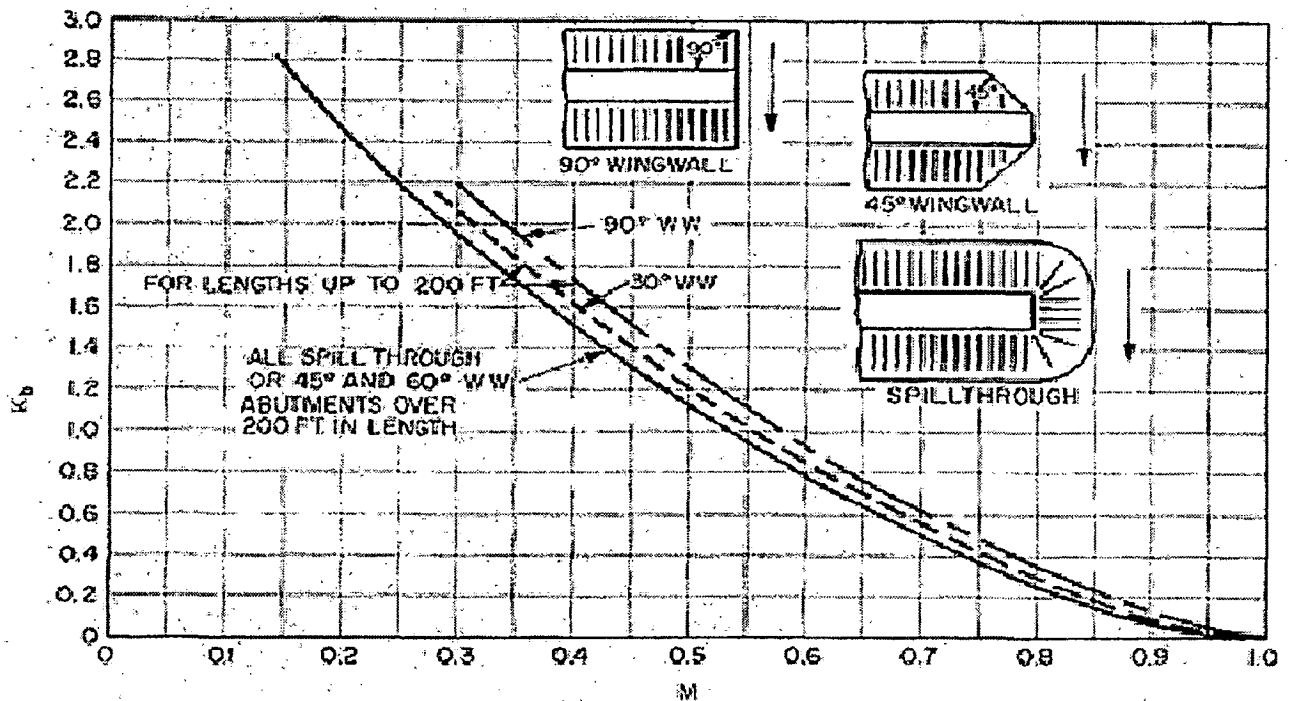


Figure 4.5. Backwater coefficient base curves (subcritical flow).

$\Delta K_p$ , is dependent on the ratio that the area of the piers bears to the gross area of the bridge opening, the type of piers (or piling in the case of pile bents), the value of the bridge opening ratio,  $M$ , and the angularity of the piers with the direction of flood flow. The ratio of the water area occupied by piers,  $A_p$ , to the gross water area of the

constriction,  $A_{n2}$ , both based on the normal water surface, has been assigned the letter  $J$ . In computing the gross water area,  $A_{n2}$ , the presence of piers in the constriction is ignored. Obtain the correction factor,  $\sigma$ , from chart B for opening ratios other than unity. The incremental backwater coefficient is then:

$$\Delta K_p = \sigma \Delta K \text{ (Figure 4.6)}$$

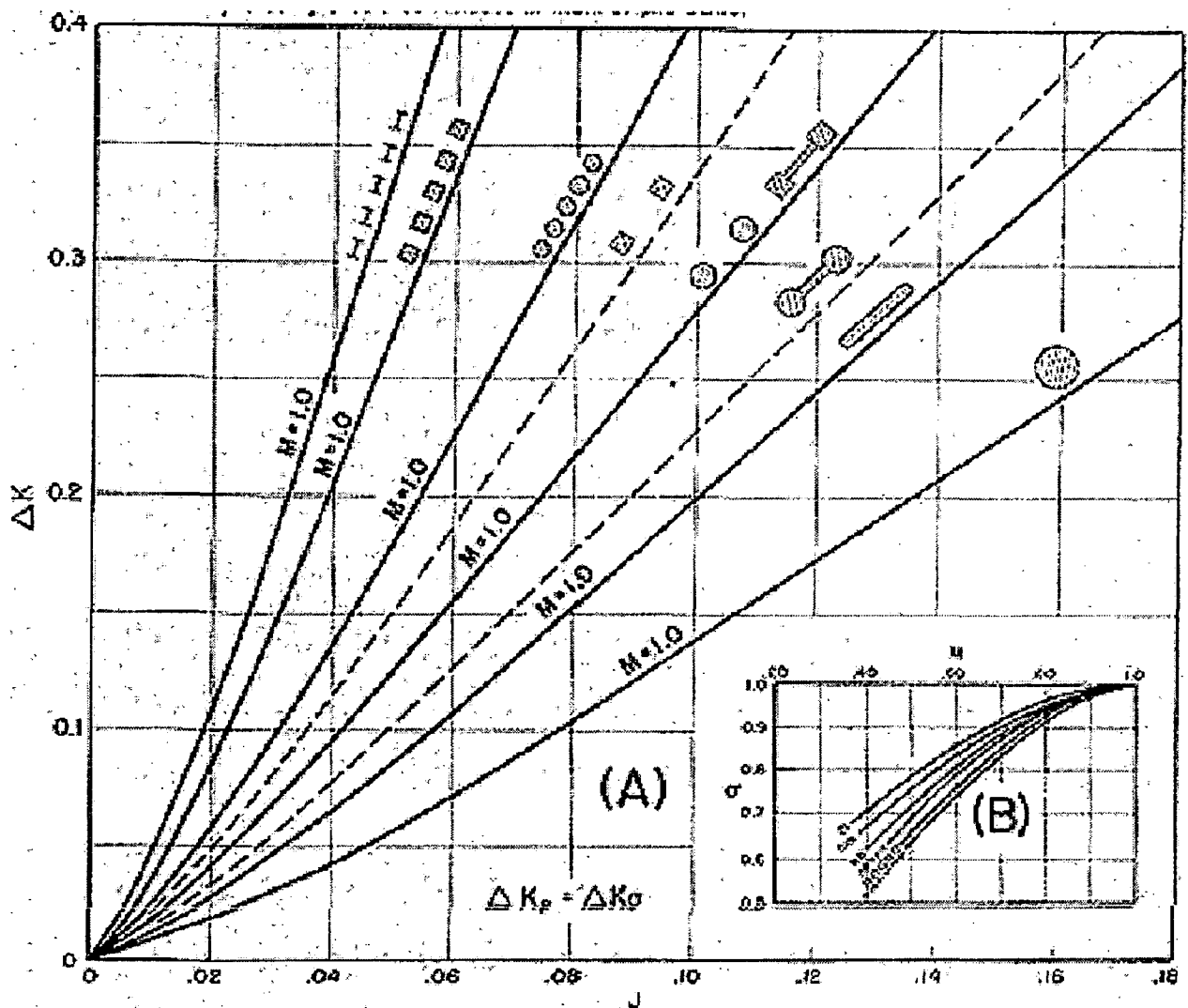


Figure 4.6. Incremental backwater coefficient for piers.

$\Delta K_e$  accounting for the effect of eccentricity (Figure 4.7)

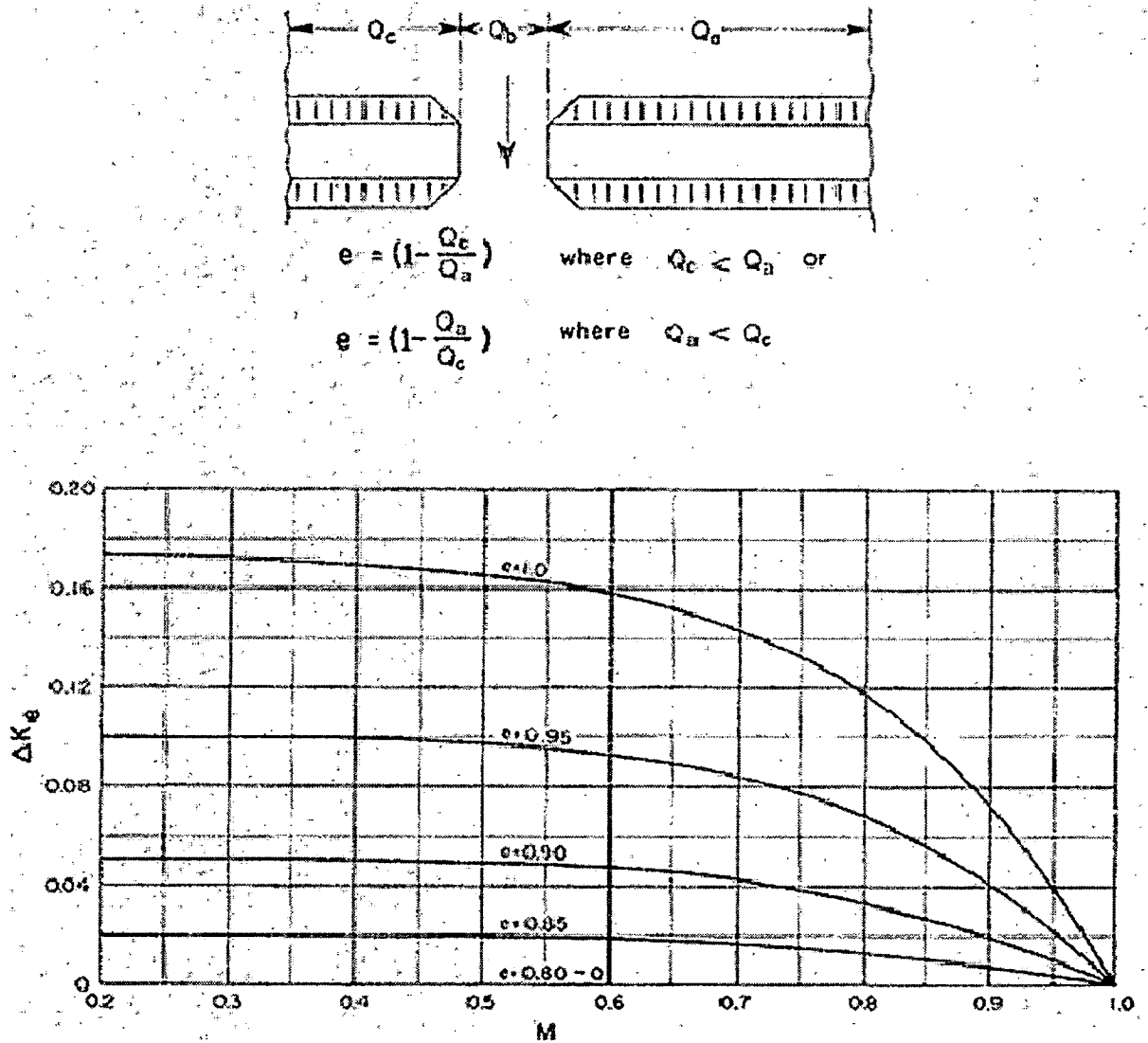


Figure 4.7. Incremental backwater coefficient for eccentricity.

$\Delta K_s$  for the effect of skew, for wingwall and spillthrough type abutments. The incremental coefficient varies with the opening ratio,  $M$ , the angle of skew of the bridge  $\phi$ , with the general direction of flood flow, and the alignment of the abutment faces, as indicated by the sketches in Figure 4.9. The length of the constricted opening is  $b \cos \phi$ , and the area  $A_{n2}$  is based on this length in Figure 4.8.



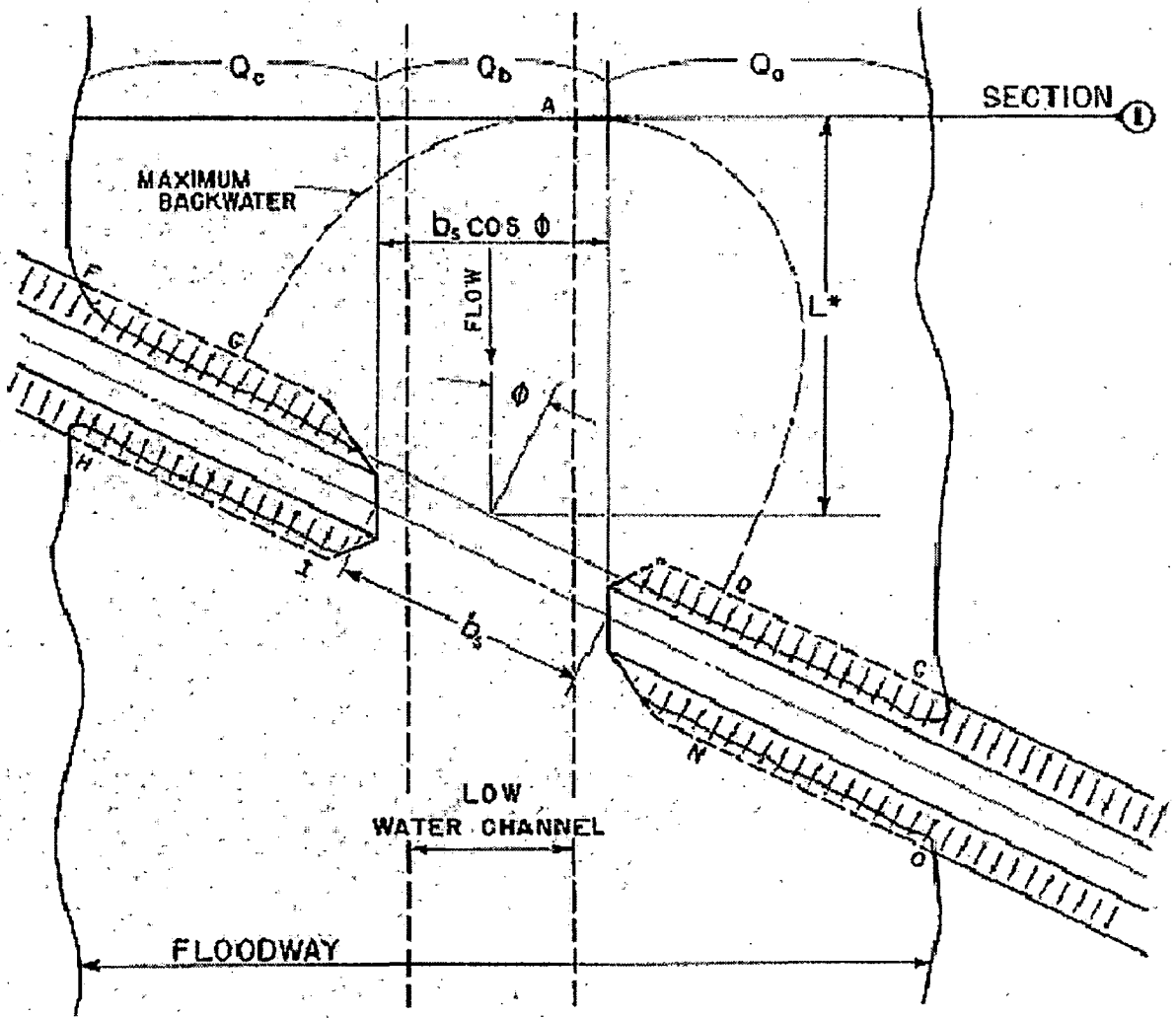


Figure 4.8. Skewed crossings

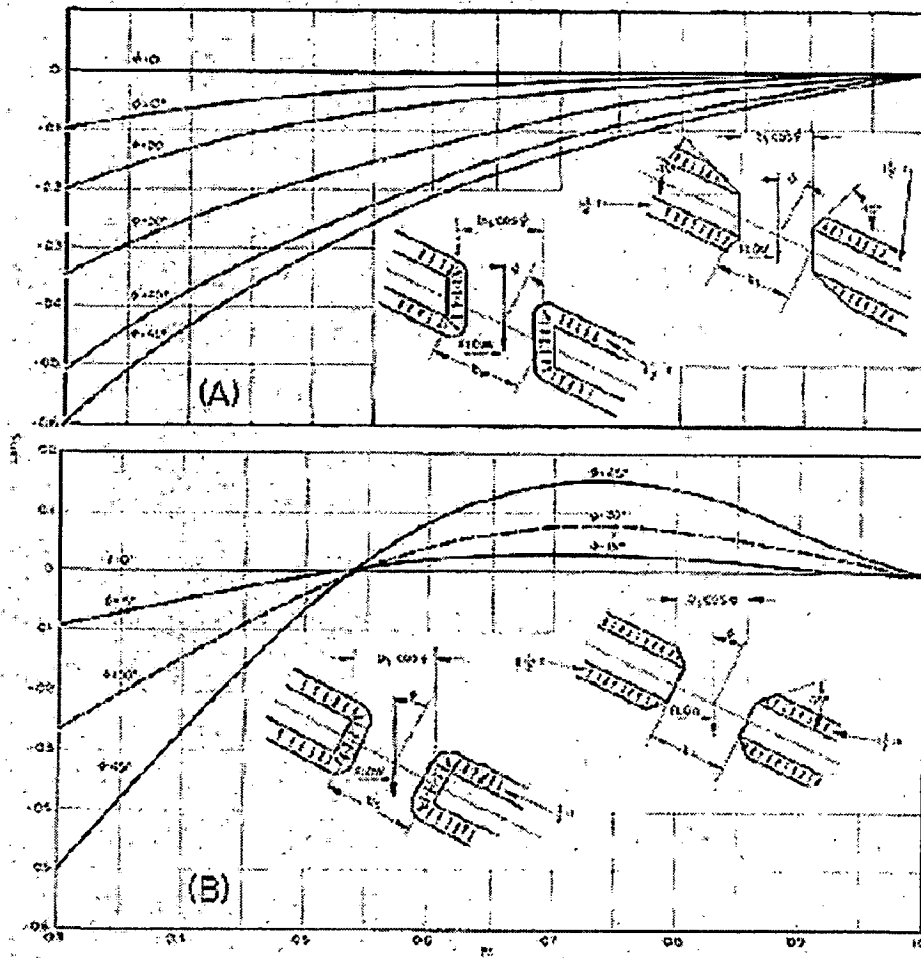


Figure 4.9. Incremental backwater coefficient for skew.

#### 4.2.2.3. Difference in Water Level across Approach Embankments

The difference in water surface elevation between the upstream and downstream side of bridge approach embankments,  $\Delta h$ , from figure 4.10

$$\Delta h = h_3^* + h_1^* + S_0 L_{1-3} \quad (4.6)$$

where

$S_0$  = natural slope of the stream

$L_{1-3}$  = distance from section 1 to 3

$h_3^*$  depend on the opening ratio,  $M$ , from Figure 4.10 we get

$$D_b = \frac{h_b^*}{h_b^* + h_3^*}$$

or 
$$h_3^* = h_b^* \left( \frac{1}{D_b} - 1 \right)$$

where  $h_b^* = K_b \frac{\alpha_2 V_{n2}^2}{2g}$  is loss head due to constriction

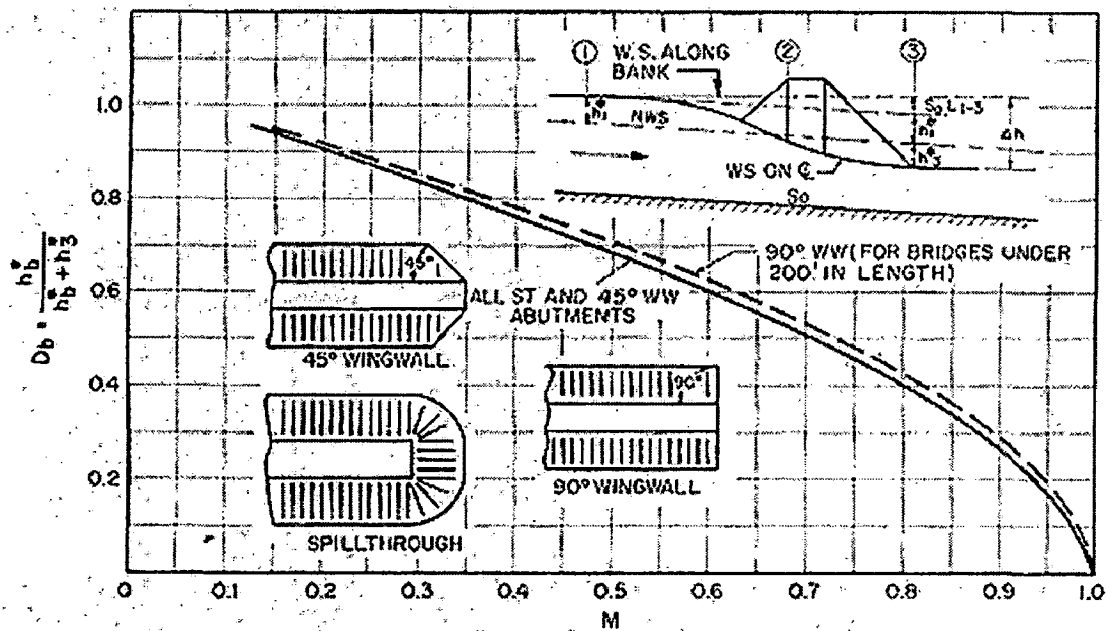


Figure 4.10. Differential water level ratio base curves.

### Effects of Piers on

As piers were introduced in the bridge constrictions in the model, it was found that the backwater increased while the value of  $h_3^*$  showed no measurable change regardless of the value of  $J$ .

### Effect of Eccentricity

In the case of severely eccentric crossings, the difference in level across the embankment considered here applies only to the side of the river having

the greater flood plain discharge. The individual values of  $h_b^*$  and  $h_3^*$  for eccentric conditions are different than for symmetrical crossings, but the ratio of one to the other, for any given value of  $M$ , remains unchanged. To obtain  $h_3^*$  for an eccentric crossing, with or without piers, enter the proper curve in Figure 10 with the value of  $M$  and read  $D_b$  as before. In this case:

$$D_b = \frac{h_b^* + \Delta h_e^*}{h_b^* + \Delta h_e^* + h_3^*}$$

or

$$h_3^* = (h_b^* + \Delta h_e^*) \left( \frac{1}{D_b} - 1 \right)$$

where  $\Delta h_e^* = \Delta K_e \frac{\alpha_2 V_{n2}^2}{2g}$

### Effect of Skewed Crossing

The differential level across roadway embankments for skewed crossings is naturally different for opposite sides of the river, the amount depending on the configuration of the stream, bends in the vicinity of the crossing, the degree of skew, etc. In this case  $h_3^*$  following:

$$h_3^* = (h_b^* + \Delta h_s^*) \left( \frac{1}{D_b} - 1 \right)$$

where  $\Delta h_s^* = \Delta K_s \frac{\alpha_2 V_{n2}^2}{2g}$

The water surface elevations along the upstream side of the embankments (Figure 4.8) from  $D$  to  $C$  were consistently higher than for the opposite upstream side  $F$  to  $G$ . Likewise, the water surface elevations along

the downstream side of the embankments were higher from  $N$  to  $O$  than for the right bank  $H$  to  $I$ .

#### **4.2.2.4. Distance to Point of Maximum Backwater**

In backwater computations, it will be found necessary in some cases to locate the point or points of maximum backwater with respect to the bridge. The maximum backwater in line with the midpoint of the bridge occurs at point  $A$  (Figure 4.11), this point being a distance,  $L^*$ , from the waterline on the upstream side of the embankment.

#### **Normal Crossings**

Figure 4.11 has been prepared for determining distance to point of maximum backwater, measured normal to centerline of bridge. Referring to Figure 4.11, the normal depth of flow under a bridge is defined here  $\bar{y} = A_{n2}/b$ , where  $A_{n2}$  is the cross sectional area under the bridge, referred to normal water surface, and  $b$  is the width of waterway. A trial solution is required for determining the differential level across embankments,  $\Delta h$ , but from the result of the backwater computation it is possible to make a fair estimate of  $\Delta h$ . To obtain distance to maximum backwater for a normal channel constriction, enter Figure 4.11 with appropriate value of  $\Delta h/\bar{y}$  and obtain the corresponding value of  $L^*/b$ . Solving for  $L^*$ , which is the distance from point of maximum backwater (point  $A$ ) to the water surface on the upstream side of embankment (Figure 4.11B).

#### **Eccentric Crossings**

Eccentric crossings with extreme asymmetry perform much like one half of a normal symmetrical crossing with a marked contraction of the jet on one side and very little contraction on the other. For cases where the value of

$e$  is greater than 0.70. From Figure 4.11C Distance to maximum backwater is then  $L^* = \epsilon b$  with eccentricity.

### Skewed Crossings

In the case of skewed crossings, to obtain the approximate distance to maximum backwater  $L^*$  for skewed crossings (Figure 4.8), the same procedure is recommended as for normal crossings except the ordinate of Figure 4.11 is read as  $L^*/b_s$ , where  $b_s$  is the full length of skewed bridge (Figure 4.8).

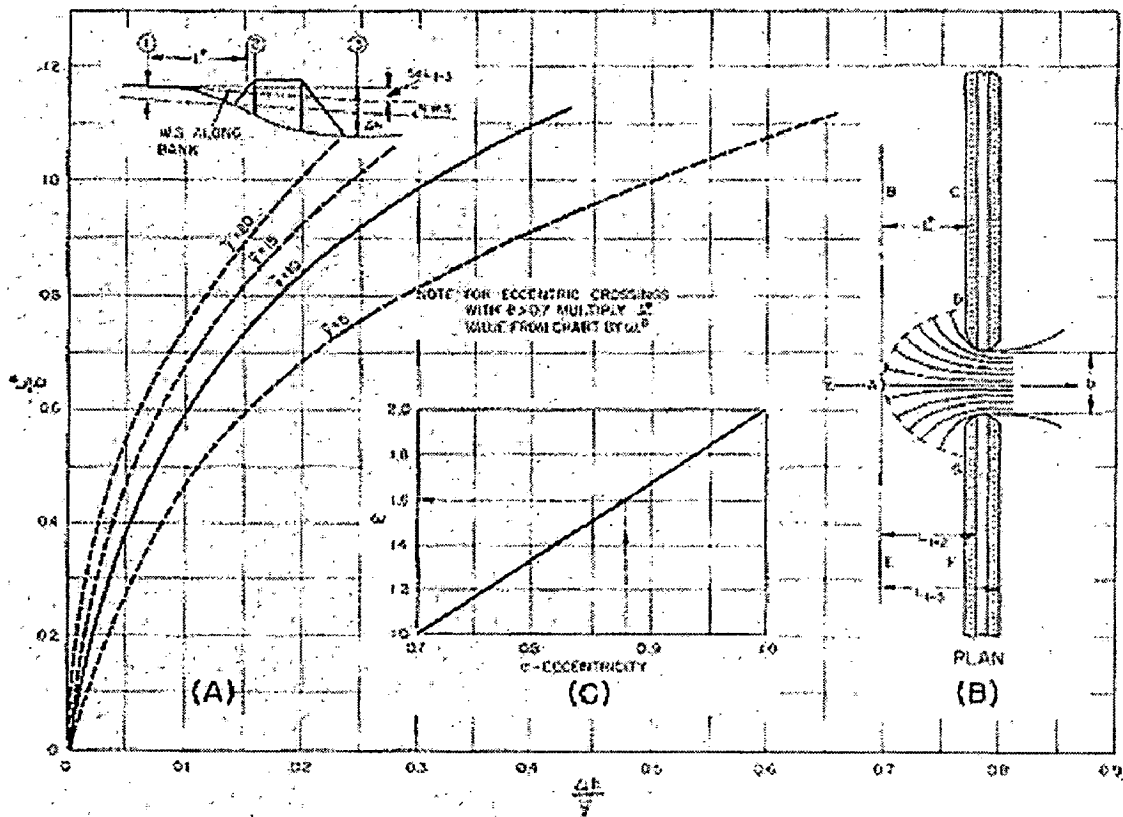


Figure 4.11. Distance to maximum backwater.

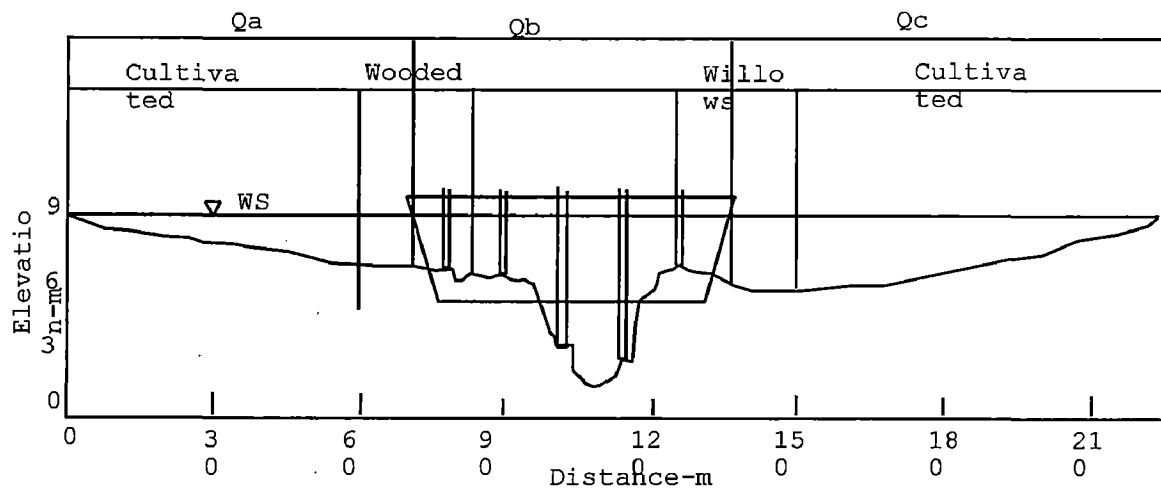
### **Example**

(Hydraulic waterway)

The channel crossing shown in Figure below with the following information: Cross section of river at bridge site showing areas, wetted perimeters, and values of Manning,  $n$ ; normal water surface for design = El.8.534 m. at bridge; average slope of river in vicinity of bridge  $S_0 = 0.00049$  ; cross section under bridge showing area below normal water surface and width of roadway = 12.2 m. The stream is essentially straight, the cross section relatively constant in the vicinity of the bridge, and the crossing is normal to the general direction of flow.

### **Find.**

- a. Conveyance at section 1. .
- b. Velocity head correction coefficient,  $\alpha_1$ .
- c. Bridge opening ratio,  $M$ .
- d. Backwater produced by the bridge.
- e. Water surface elevation on upstream side of roadway embankment.
- f. Water surface elevation on downstream side of roadway embankment.



Solution.

a. Height of backwater

Conveyance at section 1

	n	1/n	A(m <sup>2</sup> )	P(m)	R(m)	$K_i = \frac{1}{n} AR^{2/3}$	$K_i(K_i/A_i)^2$
Q <sub>a</sub>	0.045	22.2	58.29	61.02	0.955	1256.176	583.396x10 <sup>3</sup>
	0.07	14.3	26.49	12.22	2.168	633.904	363 x10 <sup>3</sup>
Q <sub>b</sub>	0.07	14.3	30.15	12.22	2.467	786.385	534.972 x10 <sup>3</sup>
	0.035	28.57	186.18	44.2	4.212	13873.64	77038.037 x10 <sup>3</sup>
	0.05	20	19.12	7.65	2.499	704.2	955.239 x10 <sup>3</sup>
Q <sub>c</sub>	0.05	20	50.11	16.79	2.984	2077.241	3569.537 x10 <sup>3</sup>
	0.045	22.2	155.84	76.5	2.037	5564.94	7096.163 x10 <sup>3</sup>
			526.18			24896.485	90140.344x10 <sup>3</sup>

$$\alpha_1 = \frac{\sum K_i(K_i/A_i)^2}{K_T(K_T/A_T)^2} = \frac{90140.344 \times 10^3}{24896.485(24896.485/526.18)^2} = 1.62$$

Discharge:  $Q = KS_0^{1/2} = 24896.485(0.00049)^{1/2} = 551.1$  cumecs

Backwater:

$$h_1^* = K^* \alpha_2 \frac{V_{n2}^2}{2g} + \alpha_1 \left[ \left( \frac{A_{n2}}{A_4} \right)^2 - \left( \frac{A_{n2}}{A_1} \right)^2 \right] \frac{V_{n2}^2}{2g}$$



Where:  $K^* = k_b + \Delta k_p$

Bridge opening ratio:

$$M = K_b / K = 15364.225 / 24896.485 = 0.62$$

$\alpha_1 = 1.62$  and  $M = 0.62$  we get  $\alpha_2 = 1.4$  from the figure 4.4

from  $M = 0.62$  we get  $k_b = 0.72$  from figure 4.5

As the bridge is supported by five solid piers. Pier 3 and 4 is 0.91 m of thick, 5.6 and 6.6 of length respectively, pier 1,2,5 is 0.76 m of thick and 2.4, 2.7, 2.3 of length respectively. The gross water area under the bridge for normal stage  $A_{n2} = 235.45$  sq.m and the area obstructed by the piers  $A_p$  is 16.72 sq.m

$$J = \frac{A_p}{A_{n2}} = \frac{16.72}{235.45} = 0.071$$

With  $J = 0.071$  and  $M = 1$   $\Delta k = 0.13$  but with  $M = 0.62$  we obtain the correction factor  $\sigma = 0.84$  for  $M = 0.62$ .

The incremental backwater coefficient for five piers,

$$\Delta k_p = \Delta k \times \sigma = 0.13 \times 0.84 = 0.11$$

The overall backwater coefficient:

$$K^* = k_b + \Delta k_p = 0.72 + 0.11 = 0.83$$

$$V_{n2} = \frac{Q}{A_{n2}} = \frac{551.1}{235.44} = 2.35 \text{ (m.p.s)}$$

$$\text{and } \frac{V_{n2}^2}{2g} = 0.28 \text{ m}$$

$$K^* \frac{\alpha_2 V_{n2}^2}{2g} = 0.83 \times 1.4 \times 0.28 = 0.325m$$

After that we find  $A_1$  (Area of water consist of backwater)

$$A_1 = 593.09 \text{sq.m}; A_4 = 526.18 \text{ sq.m}$$

Total backwater produced by the bridge is:

$$h_1^* = 0.325 + 0.019 = 0.344 \text{ m}$$

**b. Find distance to point of maximum backwater**

Width of waterway  $b = 62.48 \text{ m}$

Average depth:

$$\bar{y} = \frac{A_{n2}}{b} = \frac{235.45}{62.48} = 3.77m$$

Assume the total drop across the embankment for a first trial

$$\Delta h = 0.58 \text{ m}$$

$$\frac{\Delta h}{\bar{y}} = \frac{0.58}{3.77} = 0.154 \quad \text{from figure 4.11 we get } L^*/b = 0.78$$

And distance to point of maximum backwater

$$L^* = 0.78 \times 62.48 = 48.73 \text{ m}$$

The drop in channel gradient between section 1 and centerline of bridge is

$$S_0 L = 0.00049 (48.73 + 9.14) = 0.0284 \text{ m}$$

The water surface elevation at section 1:

$$\text{EL.}8.534 + S_0L + h_1^* = 8.534 + 0.0284 + 0.344 = 8.911 \text{ m}$$

Check: The first step is determining the water surface elevation at section 3 (downstream) is to compute the backwater for the bridge in question without piers

$$h_b^* = K_b \frac{\alpha_2 V_{n2}^2}{2g} = 0.72 \times 1.4 \times 0.28 = 0.282 \text{ m}$$

Entering with  $M=0.62$ , the differential level ratio for the bridge (without piers) is:

$$D_b = \frac{h_b^*}{h_b^* + h_3^*} = 0.58 \quad \text{enter } h_b^* = 0.282 \text{ m we get } h_3^* = 0.204 \text{ m}$$

The water surface elevation on the downstream side of the roadway embankment:

$$\text{EL.}8.534 - 0.204 = 8.33 \text{ m}$$

The drop in water surface across the embankment is :

$$\Delta h = 8.911 - 8.33 = 0.58 \text{ m}$$

So assumed  $\Delta h = 0.58 \text{ m}$  is correct

## **4.3 EVALUATING SCOUR OF BRIDGE**

### **4.3.1 General**

Scour is the result of the erosive action of flowing water, excavating and carrying away material from the bed and banks of streams. Different materials scour at different rates. Loose granular soils are rapidly eroded by flowing water, while cohesive or cemented soils are more scour resistant. However, ultimate scour in cohesive or cemented soils can be as deep as scour in sand-bed streams. Under constant flow conditions, scour will reach maximum depth in sand and gravel bed materials in hours; cohesive bed materials in days; glacial tills, sand stones and shales in months; limestones in years and dense granites in centuries. Under flow conditions more typical of actual bridge crossings, several floods will be needed to attain maximum scour.

Designers and inspectors need to carefully study site-specific subsurface information in evaluating scour potential at bridges, giving particular attention to foundations on rock. Massive rock formations with few discontinuities are highly resistant to scour during the lifetime of a typical bridge.

A factor in scour at highway crossings and encroachments is whether the scour is clear-water or live-bed scour. Clear-water scour occurs where there is no transport of bed material upstream of the crossing or encroachment and live-bed scour occurs where there is transport of bed material from the upstream reach into the crossing or encroachment.

### **4.3.2 Total Scour**

Total scour at a highway crossing is comprised of three components. These are:

- i). Long-term aggradation and degradation,
- ii). Contraction scour, and
- iii). Local scour.

In addition, lateral migration of the stream must be assessed when evaluating total scour at piers and abutments of highway crossings.

#### **Aggradation and Degradation - Long-Term Streambed Elevation Changes**

Long-term bed elevation changes may be the natural trend of the stream or may be the result of some modification to the stream or watershed. The streambed may be aggrading, degrading or in relative equilibrium in the vicinity of the bridge crossing. In this section long-term trends are considered. Long-term aggradation and degradation do not include the localized cutting and filling of the bed of the stream that might occur during a runoff event (contraction and local scour). A stream may cut and fill at specific locations during a runoff event and also have a long-term trend of an increase or decrease in bed elevation over a reach of a stream. The problem for the engineer is to estimate the long-term bed elevation changes that will occur during the life of the structure.

A long-term trend may change during the life of the bridge. These long-term changes are the result of modifications to the stream or watershed. Such changes may be the result of natural processes or human activities. The engineer must assess the present state of the stream and watershed and then

evaluate potential future changes in the river system. From this assessment, the long-term streambed changes, must be estimated. Factors that affect long-term bed elevation changes are: dams and reservoirs (upstream or downstream of the bridge), changes in watershed land use (urbanization, deforestation, etc.), channelization, cutoffs of meander bends (natural or man made), changes in the downstream channel base level (control), gravel mining from the streambed, diversion of water into or out of the stream, natural lowering of the total system, movement of a bend, bridge location with respect to stream plan form, and stream movement in relation to the crossing.

If no documented data exist or if such data require further evaluation, an assessment of long-term streambed elevation changes for riverine streams should be made using the principles of river mechanics. Such an assessment requires the consideration of all influences upon the bridge crossing; i.e., runoff from the watershed to a stream (hydrology), the sediment delivery to the channel (watershed erosion), the sediment transport capacity of a stream (hydraulics) and the response of a stream to these factors (geomorphology and river mechanics).

Significant morphologic impacts can result from human activities. The assessment of the impact of human activities requires a study of the history of the river, as well as a study of present water and land use and stream control activities.

### **Contraction Scour**

Contraction scour occurs when the flow area of a stream at flood stage is reduced, either by a natural contraction or by a bridge. From continuity, a decrease in flow area results in an increase in average velocity and bed shear stress through the contraction. Hence, there is an increase in erosive forces in the contraction and more bed material is removed from the contracted reach

than is transported into the reach. This increase in transport of bed material from the reach lowers the natural bed elevation. As the bed elevation is lowered, the flow area increases and, in the riverine situation, the velocity and shear stress decrease until relative equilibrium is reached; i.e., the quantity of bed material that is transported into the reach is equal to that removed from the reach.

Contraction scour can also be caused by short-term (daily, weekly, yearly or seasonal) changes in the downstream water surface elevation that control backwater and hence, the velocity through the bridge opening. Because this scour is reversible, it is included in contraction scour rather than in long-term aggradation/degradation.

Contraction scour is typically cyclic. That is, the bed scours during the rising stage of a runoff event, and fills on the falling stage. The contraction of flow due to a bridge can be caused by either a natural decrease in flow area of the stream channel or by abutments projecting into the channel and/or the piers blocking a large portion of the flow area. Contraction can also be caused by the approaches to a bridge cutting off the floodplain flow. This can cause clear water scour on a setback portion of a bridge section and/or a relief bridge because the floodplain flow does not normally transport significant concentrations of bed material sediments. This clear-water picks up additional sediment from the bed upon reaching the bridge opening. In addition, local scour at abutments may well be greater due to the clear-water floodplain flow returning to the main channel at the end of the abutment.

Other factors that can cause contraction scour are (1) natural stream constrictions, (2) long highway approaches over the floodplain to the bridge, (3) ice formation or jams, (4) natural berms along the banks due to sediment deposits, (5) island or bar formations upstream or downstream of the bridge

opening, (6) debris, and (7) the growth of vegetation in the channel or floodplain.

In a natural channel, the depth of flow is always greater on the outside of a bend. In fact, there may well be deposition on the inner portion of the bend at the point bar. If a bridge is located on or close to a bend, the contraction scour will be concentrated on the outer part of the bend. Also, in bends the thalweg (the part of the stream where the flow is deepest and, typically, the velocity is the greatest) may shift toward the center of the stream as the flow increases. This can increase scour and the nonuniform distribution of the scour in the bridge opening.

### **Local scour**

The basic mechanism causing local scour at piers or abutments is the formation of vortices (known as the horseshoe vortex) at their base (Figure 4.12). The horseshoe vortex results from the pileup of water on the upstream surface of the obstruction and subsequent acceleration of the flow around the nose of the pier or embankment. The action of the vortex removes bed material from around the base of the obstruction. The transport rate of sediment away from the base region is greater than the transport rate into the region, and, consequently, a scour hole develops. As the depth of scour increases, the strength of the horseshoe vortex is reduced, thereby reducing the transport rate from the base region. Eventually, for live-bed local scour, equilibrium is reestablished and scouring ceases. For clear-water scour, scouring ceases when the shear stress caused by the horseshoe vortex equals the critical shear stress of the sediment particles at the bottom of the scour hole.

In addition to the horseshoe vortex around the base of a pier, there are vertical vortices downstream of the pier called the wake vortex (Figure 4.12).



Both the horseshoe and wake vortices remove material from the pier base region. However, the intensity of wake vortices diminishes rapidly as the distance downstream of the pier increases. Therefore, immediately downstream of a long pier there is often deposition of material.

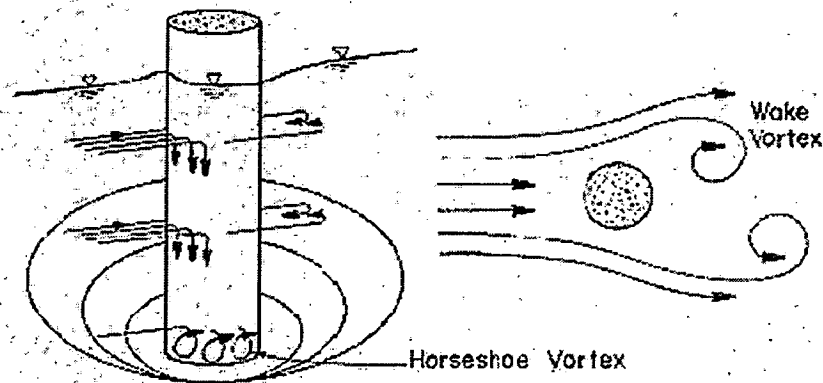


Figure 4.12. Schematic Representation of Scour at a Cylindrical Pier

Factors which affect the magnitude of local scour at piers and abutments are (1) width of the pier, (2) discharge intercepted by the abutment and returned to the main channel at the abutment, (3) length of the pier if skewed to flow, (4) depth of flow, (5) velocity of the approach flow, (6) size and gradation of bed material, (7) angle of attack of the approach flow to a pier or abutment, (8) shape of a pier or abutment, (9) bed configuration, (10) ice formation or jams, and (11) debris.

1. Pier width has a direct influence on depth of local scour. As pier width increases, there is an increase in scour depth.

2. Projected length of an abutment into the stream affects the depth of local scour.

3. Pier length has no appreciable effect on local scour depth as long as the pier is aligned with the flow. When the pier is skewed to the flow, the pier

length has a significant influence on scour depth. For example, with the same angle of attack, doubling the length of the pier increases scour depth by 33 percent.

4. Flow depth also has an influence on the depth of local scour. An increase in flow depth can increase scour depth by a factor of 2 or greater for piers. With abutments the increase is from 1.1 to 2.15 depending on the shape of the abutment.

5. Flow velocity affects scour depth. The greater the velocity, the deeper the scour. There is a high probability that scour is affected by whether the flow is subcritical or supercritical. However, most research and data are for subcritical flow (i.e., flow with a Froude Number less than one,  $Fr < 1$ ).

6. Bed material characteristics such as size, gradation, and cohesion can affect local scour. Bed material in the sand size range has little effect on local scour depth. Likewise, larger size bed material that can be moved by the flow or by the vortices and turbulence created by the pier or abutment will not affect the maximum scour, but only the time it takes to attain it. Very large particles in the bed material, such as cobbles or boulders, may armor the scour hole.

The size of the bed material also determines whether the scour at a pier or abutment is clear-water or live-bed scour. Fine bed material (silts and clays) will have scour depths as deep as sand-bed streams.

This is true even if bonded together by cohesion. The effect of cohesion is to influence the time it takes to reach the maximum scour. With sand bed material, the time to reach maximum depth of scour is measured in hours and can result from a single flood event. With cohesive bed materials it will take

much longer to reach the maximum scour depth, the result of many flood events.

7. Angle of attack of the flow to the pier or abutment has a significant effect on local scour, as was pointed out in the discussion of pier length. Abutment scour is reduced when embankments are angled downstream and increased when embankments are angled upstream. According to the work of Ahmad , the maximum depth of scour at an embankment inclined 45 degrees downstream is reduced by 20 percent; whereas, the maximum scour at an embankment inclined 45 degrees upstream is increased about 10 percent.

8. Shape of the nose of a pier or an abutment can have up to a 20 percent influence on scour depth. Streamlining the front end of a pier reduces the strength of the horseshoe vortex ,thereby reducing scour depth. Streamlining the downstream end of piers reduces the strength of the wake vortices. A square-nose pier will have maximum scour depths about 20 percent greater than a sharp-nose pier and 10 percent greater than either a cylindrical or round-nose pier. The shape effect is neglected for flow angles in excess of five degrees .Full retaining abutments with vertical walls on the streamside (parallel to the flow) will produce scour depths about double that of spill-through (sloping) abutments.

9. Bed configuration of sand-bed channels affects the magnitude of local scour. In streams with sand-bed material, the shape of the bed (bed configuration) as described by Richardson et al. may be ripples, dunes, plane bed or antidunes. The bed configuration depends on the size distribution of the sand-bed material, hydraulic characteristics, and fluid viscosity. The bed configuration may change from dunes to plane bed or antidunes during an increase in flow for a single flood event. It may change back with a decrease in flow. The bed configuration may also change with a change in water

temperature or change in suspended sediment concentration of silts and clays. The type of bed configuration and change in bed configuration will affect flow velocity, sediment transport, and scour.

10. Ice and debris can potentially increase the width of the piers, change the shape of piers and abutments, increase the projected length of an abutment and cause the flow to plunge downward against the bed. This can increase both the local and contraction scour. The magnitude of the increase is still largely undetermined. Debris can be taken into account in the scour equations by estimating how much the debris will increase the width of a pier or length of an abutment. Debris and ice effects on contraction scour can also be accounted for by estimating the amount of flow blockage (decrease in width of the bridge opening) in the equations for contraction scour. Limited field measurements of scour at ice jams indicate the scour can be as much as 10 to 20 feet.

### **Clear-Water and Live-Bed Scour**

There are two conditions for contraction and local scour. These are clear-water and live-bed scour.

Clear-water scour occurs when there is no movement of the bed material in the flow upstream of the crossing, but the acceleration of the flow and vortices created by the piers or abutments causes the material in the crossing to move. Live-bed scour occurs when the bed material upstream of the crossing is moving.

Typical clear-water scour situations include (1) coarse bed material streams, (2) flat gradient streams during low flow, (3) local deposits of larger bed materials that are larger than the biggest fraction being transported by the flow (rock riprap is a special case of this situation), (4) armored streambeds

where the only locations that tractive forces are adequate to penetrate the armor layer are at piers and/or abutments, and (5) vegetated channels where, again, the only locations that the cover is penetrated is at piers and/or abutments.

During a flood event, bridges over streams with coarse bed material are often subjected to clear-water scour at low discharges, live-bed scour at the higher discharges and then clear-water scour on the falling stages. Clear-water scour reaches its maximum over a longer period of time than live-bed scour .

### **Lateral Shifting of a Stream**

Streams are dynamic. Areas of flow concentration continually shift bank lines. In meandering stream having an "S-shaped" plan form , the channel moves both laterally and downstream. A braided stream has numerous channels which are continually changing. In a braided stream, the deepest natural scour occurs when two channels come together or when the flow comes together downstream of an island or bar. This scour depth has been observed to be 1 to 2 times the average flow depth.

A bridge is static. It fixes the stream at one place in time and space. A meandering stream whose channel moves laterally and downstream into the bridge reach can erode the approach embankment and affects contraction and local scour because of changes in flow direction. A braided stream can shift under a bridge and have two channels come together at a pier or abutment, increasing scour. Factors that affect lateral shifting of a stream and the stability of a bridge are the geomorphology of the stream, location of the crossing on the stream, flood characteristics, the characteristics of the bed and bank material and wash load. It is difficult to anticipate when a change in plan form may occur. It may be gradual with time or the result of a major flood event. Also, the direction and magnitude of the movement of the stream are

not easily determined. It is difficult to properly evaluate the vulnerability of a bridge due to changes in plan form . It is important to incorporate potential plan form changes into the design of new bridges and design of countermeasures for existing bridges. Countermeasures for lateral shifting and instability of the stream may include changes in the bridge design, construction of river control works, protection of abutments with riprap, or careful monitoring of the river in a bridge inspection program. Serious consideration should be given to placing footings/foundations located on floodplains at elevations approximating those located in the main channel.

To control lateral shifting requires river training works, bank stabilizing by riprap and/or guide banks.

#### **4.3.3. Estimating Scour at Bridges**

The seven steps recommended for estimating scour at bridges are:

Step 1: Determine scour analysis variables.

Step 2: Analyze long-term bed elevation change.

Step 3: Evaluate the scour analysis method.

Step 4: Compute the magnitude of contraction scour.

Step 5: Compute the magnitude of local scour at piers.

Step 6: Compute the magnitude of local scour at abutments.

Step 7 Plot and evaluate the total scour depths

#### **Determine Scour Analysis Variables**

1. Determine the magnitude of the discharges for the floods ,including the overtopping flood when applicable.

2. Determine if there are existing or potential future factors that will produce a combination of high discharge and low tailwater control. Are there bedrock or other controls (old diversion structures, erosion control checks, other bridges, etc.) that might be lowered or removed? Are there dams or locks downstream that would control the tailwater elevation seasonally? Are there dams upstream or downstream that could control the elevation of the water surface at the bridge?

Select the lowest reasonable downstream water-surface elevation and the largest discharge to estimate the greatest scour potential. Assess the distribution of the velocity and discharge per foot of width for the design flow and other flows through the bridge opening. Consider also the contraction and expansion of the flow in the bridge waterway. Consider present conditions and anticipated future changes in the river.

3. Determine the water-surface profiles for the discharges judged to produce the most scour. The engineer should anticipate future conditions at the bridge, in the stream's watershed, and at downstream water-surface elevation controls

4. Collect and summarize the following information as appropriate
  - a. Boring logs to define geologic substrata at the bridge site.
  - b. Bed material size and gradation distribution in the bridge reach.
  - c. Existing stream and floodplain cross section through the reach.
  - d. Stream plan form.
  - e. Watershed characteristics.
  - f. Scour data on other bridges in the area.

- g. Slope of energy grade line upstream and downstream of the bridge.
- h. History of flooding.
- i. Location of bridge site with respect to other bridges in the area, confluence with tributaries close to the site, bed rock controls, man-made controls (dams, old check structures, river training works, etc.), and downstream confluences with another stream.
- j. Geomorphology of the site (floodplain stream; crossing of a delta, youthful, mature or old age stream; crossing of an alluvial fan; meandering, straight or braided stream; etc.).
- k. Erosion history of the stream.
- l. Development history (consider present and future conditions as well) of the stream and watershed. Collect maps, ground photographs, aerial photographs; interview local residents; check for water research projects planned or contemplated.
- m. Sand and gravel mining from the streambed upstream and downstream from site.
- n. Make a qualitative evaluation of the site with an estimate of the potential for stream movement and its effect on the bridge.

### **Analysis of Long-Term Bed Elevation Change**

1. Using the information collected in Step 1 above, determine qualitatively the long-term trend in the streambed elevation.
2. If the stream is aggrading and this condition can be expected to affect the crossing, taking into account contraction scour, consider relocation of the bridge or raising the low chord of the bridge. With an aggrading stream,



use the present streambed elevation as the baseline for scour estimates because a major flood can occur prior to aggradation.

3. If the stream is degrading, use an estimate of the change in elevation in the calculations of total scour.

### **Evaluate the Scour Analysis Method**

The recommended method is based on the assumption that the scour components develop independently. Thus, the potential local scour is added to the contraction scour without considering the effects of contraction scour on the channel and bridge hydraulics

1. Estimate the natural channel hydraulics for a fixed-bed condition based on existing conditions,
2. Assess the expected profile and plan form changes,
3. Adjust the fixed-bed hydraulics to reflect any expected long-term profile or plan form changes,
4. Estimate contraction scour using the empirical contraction formula and the adjusted fixed-bed hydraulics,
5. Estimate local scour using the adjusted fixed-bed channel and bridge hydraulics and
6. Add the local scour to the contraction scour to obtain the total scour.

If contraction scour is significant, It is based on the premise that the contraction and local scour components are inter-dependent. As such, the local scour estimated with this method is determined based on the expected changes in the hydraulic variables and parameters due to contraction scour. Through an interactive process, the contraction scour and channel hydraulics

are brought into balance before local scour is computed. The general approach for this method is:

- \*Estimate the natural channel's hydraulics for a fixed bed condition based on existing site conditions;

- \*Estimate the expected profile and plan form changes based on the procedures in this manual and any historic data;

- \*Adjust the natural channel's hydraulics based on the expected profile and plan form changes;

- \*Select a trial bridge opening and compute the bridge hydraulics;

- \*Estimate contraction scour;

- \*Revise the natural channel's geometry to reflect the contraction scour and then again revise the channel's hydraulics. Repeat this iteration until there is no significant change in either the revised channel hydraulics or bed elevation changes (a significant change would be 5 percent or greater variation in velocity, flow depth, or bed elevation);

- \*Using the foregoing revised bridge and channel hydraulic variables and parameters obtained considering the contraction scour, calculate the local scour; and

- \*Extend the local scour depths below the predicted contraction scour depths in order to obtain the total scour.

### **Compute the Magnitude of Contraction Scour**

Contraction scour at bridge sites was broken down into four conditions (cases) depending on the type of contraction, overbank flow, or relief bridges. Then specific equations were presented for the different cases. However, all

conditions of contraction scour can be evaluated using two basic equations: (1) an equation for *live-bed* scour, and (2) an equation for *clear-water* scour. For any case or condition, it is only necessary to determine if the flow in the main channel or overbank area upstream of the bridge, or approaching a relief bridge, is transporting bed material (live-bed) or is not (clear-water), and then apply the appropriate equation with the variables defined according to the location of contraction scour (channel or overbank).

To determine if the flow upstream of the bridge is transporting bed material, calculate the critical velocity for beginning of motion  $V_c$  and compare it with the mean velocity  $V$  of the flow in the main channel or overbank area upstream of the bridge opening. If the critical velocity of the bed material is larger than the mean velocity ( $V_c > V$ ), then clear-water contraction scour will exist. If the critical velocity is less than the mean velocity ( $V_c < V$ ), then live-bed contraction scour will exist. To calculate the critical velocity use either Neill's or Laursen's equation .

Neill's equation

$$V_c = 1.58[(S_s - 1)gD_{50}]^{1/2}(y/D_{50})^{1/6}$$

with  $S_s$  equal to 2.65

$$V_c = 11.52y^{1/6}D_{50}^{1/3}$$

where  $V_c$  = critical velocity which will transport bed materials of size  $D_{50}$  and smaller, m/s

$S_s$  = specific gravity of bed material

$y$  = depth of upstream flow, m

Laursen's equation with  $S_s$  equal to 2.65

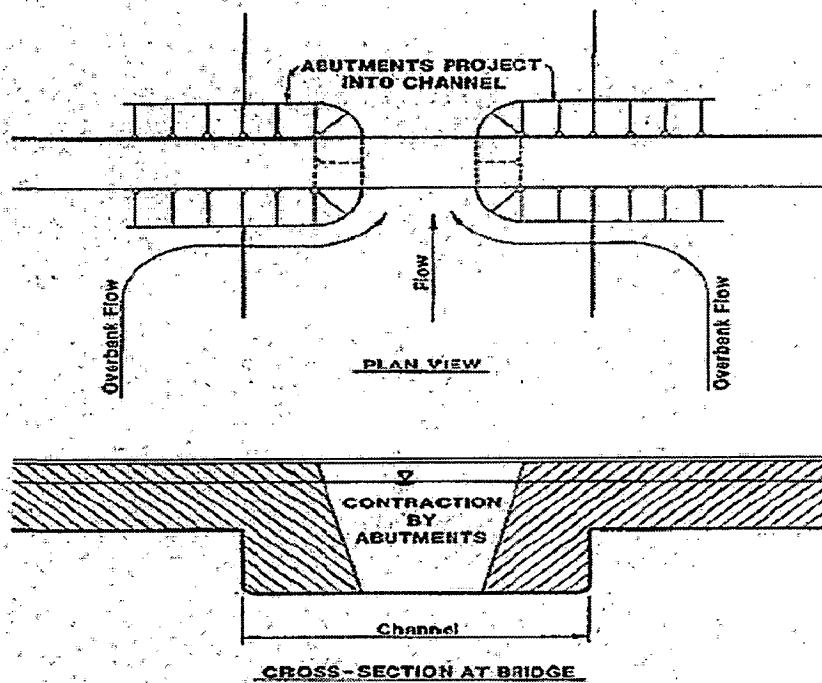
$$V_c = 10.95y^{1/6}D_{50}^{1/3}$$

Contraction Scour Conditions: Four conditions (cases) of contraction are commonly encountered:

Case 1. Involves overbank flow on a floodplain being forced back to the main channel by the approaches to the bridge.

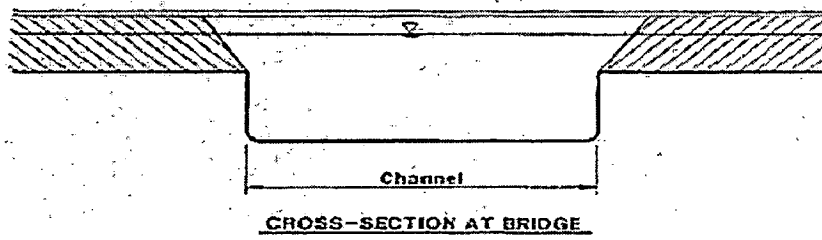
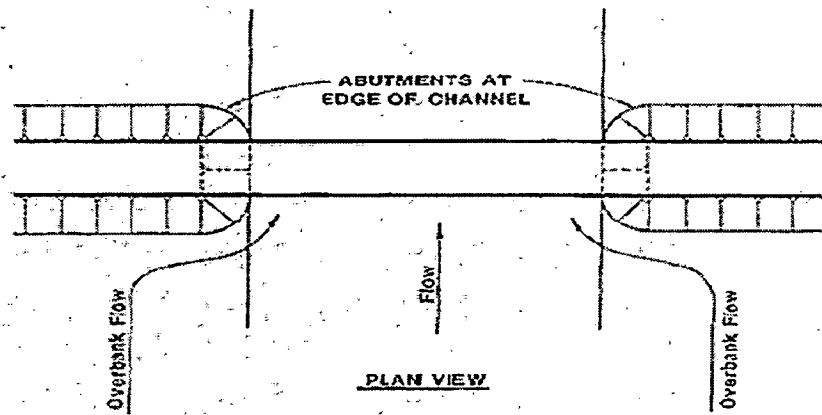
Case 1 conditions include:

a. The river channel width becomes narrower either due to the bridge abutments projecting into the channel or the bridge being located at a narrowing reach of the river;



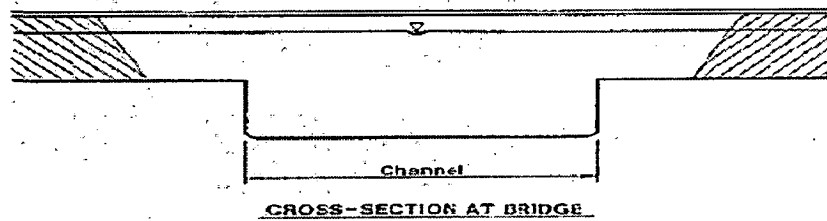
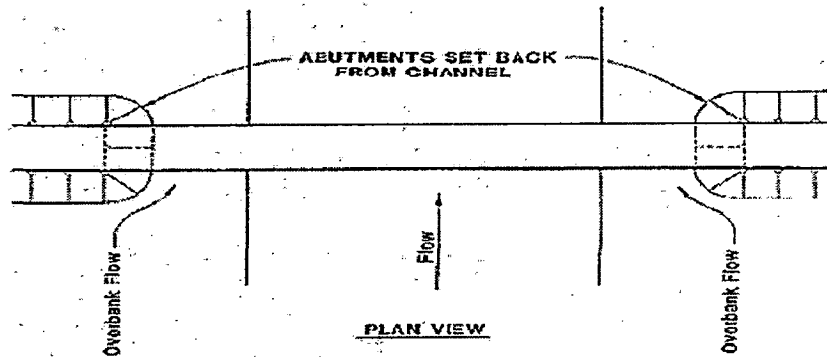
Case 1A: Abutments Project Into Channel

b. No contraction of the main channel, but the overbank flow area is completely obstructed by an embankment;



**Case 1B: Abutments at Edge of Channel**

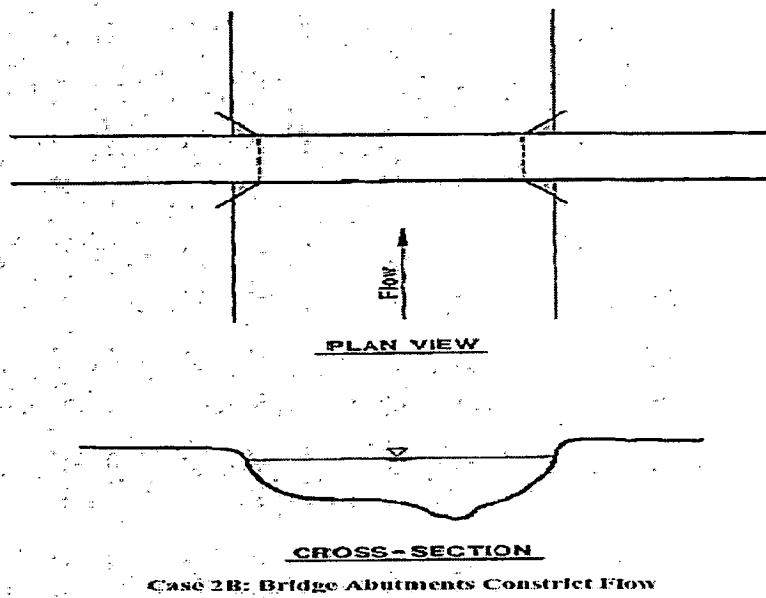
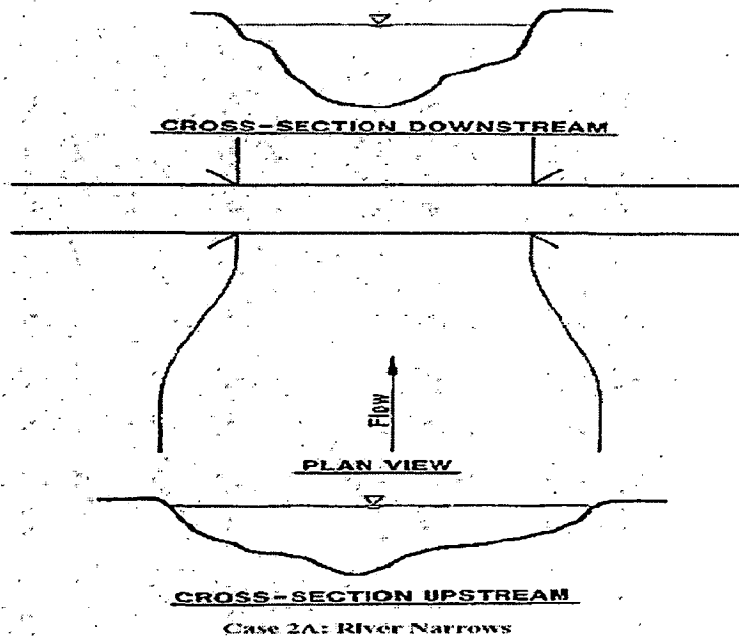
c. Abutments are set back from the stream channel.



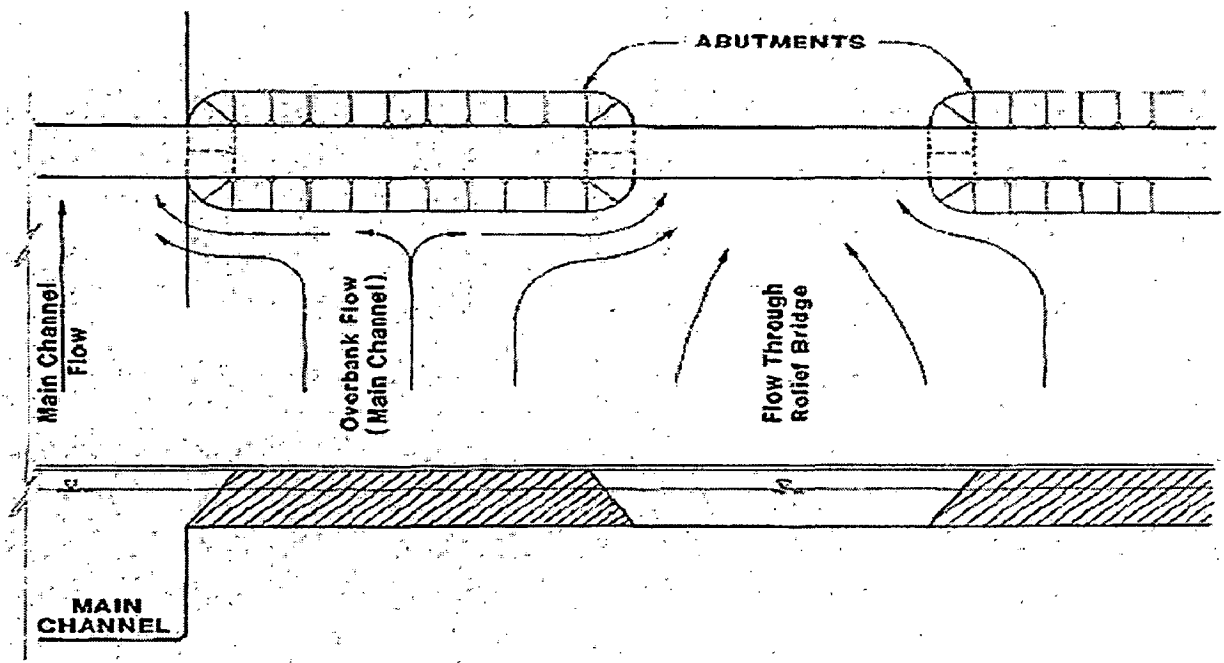
**Case 1C: Abutments Set Back From Channel**

Case 2. Flow is confined to the main channel (i.e., there is no overbank flow).

The normal river channel width becomes narrower due to the bridge itself or the bridge site is located at a narrower reach of the river.

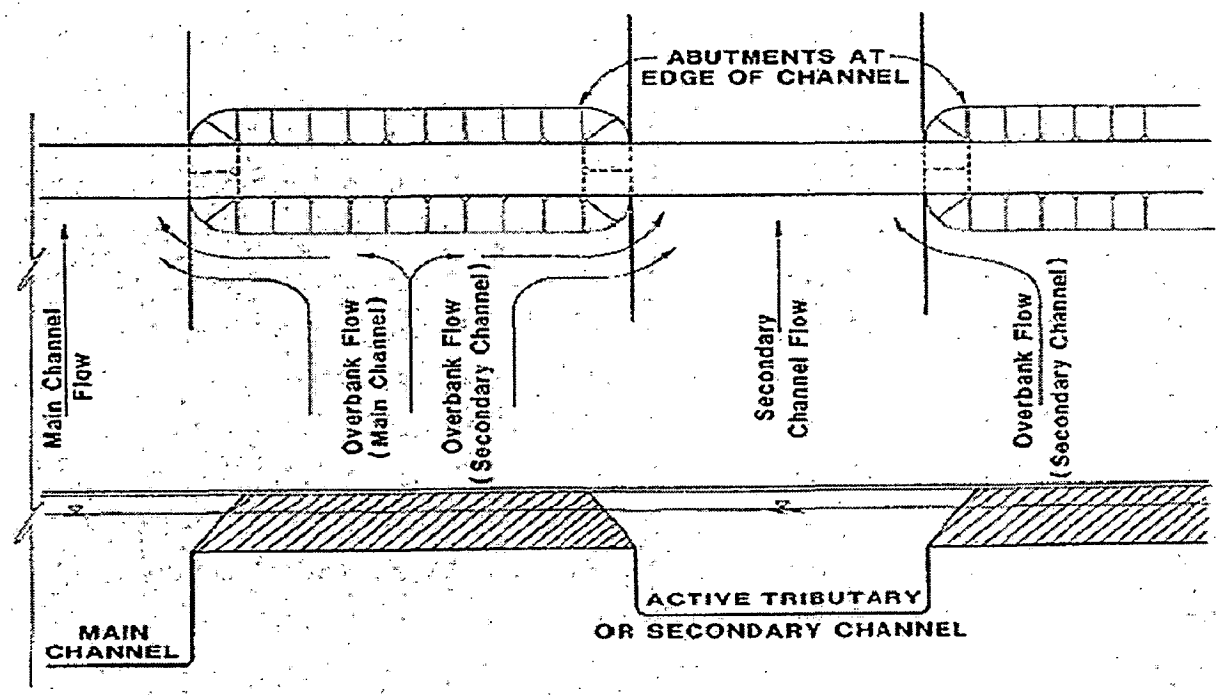


Case 3. A relief bridge in the overbank area with little or no bed material transport in the overbank area (i.e., clear-water scour).



Case 3: Relief Bridge over Floodplain

Case 4. A relief bridge over a secondary stream in the overbank area. (similar to Case 1).



Case 4: Relief Bridge over Secondary Stream

Live-Bed Contraction Scour's Equation

$$\frac{y_2}{y_1} = \left( \frac{Q_2}{Q_1} \right)^{6/7} \left( \frac{W_1}{W_2} \right)^{k_1} ; y_s = y_2 - y_1 \quad (4.7)$$

where  $y_1$  = average depth in the upstream main channel, m

$y_2$  = average depth in the contracted section, m

$W_1$  = bottom width of the upstream main channel, m

$W_2$  = bottom width of the main channel in the contracted section, m

$Q_1$  = flow in the upstream channel transporting sediment, cumec

$Q_2$  = flow in the contracted channel, cumec

$k_1$  = exponent determined below

$V^*/w$	$K_1$	Mode of bed material transport
<0.5	0.59	Mostly contact bed material discharge
0.5 to 2	0.64	Some suspended bed material discharge
>2.0	0.69	Mostly suspended bed material discharge

$V^* = (\tau / \rho)^{1/2} = (gy_1 S_1)^{1/2}$ , shear velocity in the upstream section, m/s



$w$  = fall velocity of bed material based on the  $D_{50}$ , ft/s (figure 4.13)

$g$  = acceleration of gravity ( $9.81 \text{ m/s}^2$ )

$S_1$  = slope of energy grade line of main channel,

$\tau$  = shear stress on the bed,  $\text{N/m}^2$

$\rho$  = density of water ( $1 \text{ ton /m}^3$ )

Notes:

1.  $Q_2$  may be the total flow going through the bridge opening as in Cases 1a and 1b. It is not the total for Case 1c.
2.  $Q_1$  is the flow in the main channel upstream of the bridge, not including overbank flows.
3.  $W_1$  and  $W_2$  are not always easily defined. In some cases, it is acceptable to use the top width of the main channel to define these widths. Whether top width or bottom width is used, it is important to be consistent so that  $W_1$  and  $W_2$  refer to either bottom widths or top widths.
5. The average width of the bridge opening ( $W_2$ ) is normally taken as the bottom width, with the width of the piers subtracted.

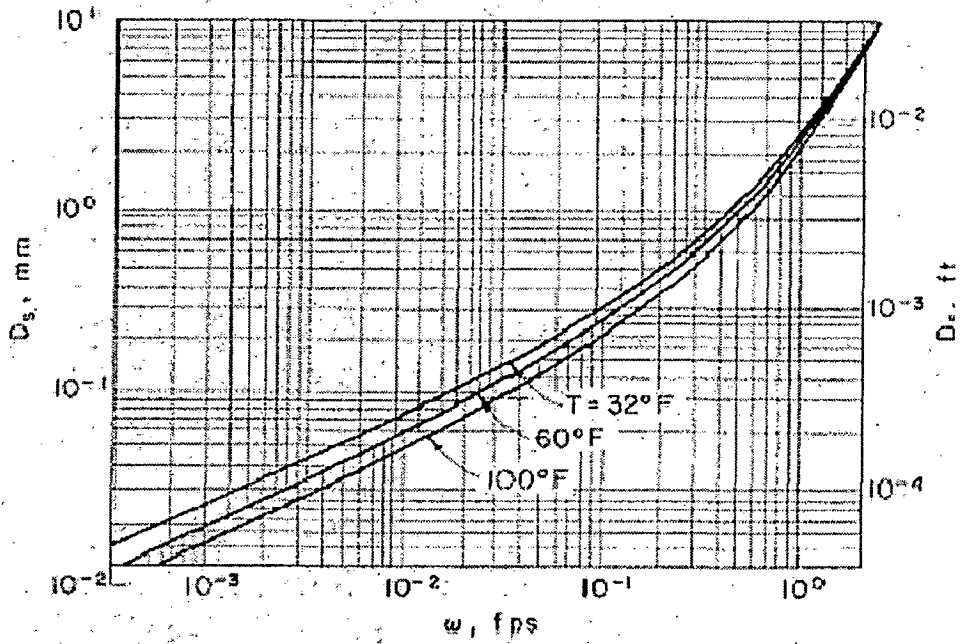


Figure 3. Fall Velocity of Sand-Sized Particles

Figure 4.13 Fall velocity of sand-sized particles

Clear-Water Contraction Scour. The recommended clear-water contraction scour equation is based on Laursen.[13] This was:

$$y_2 = \left( \frac{Q^2}{35D_m^{2/3}W^2} \right)^{3/7} ; y_s = y_2 - y_1 \quad (4.8)$$

where  $y_1$  = Depth of flow in the channel or on the floodplain prior to scour, m

$y_2$  = Depth of flow in the bridge opening or on the overbank at the bridge, m

$y_s$  = Depth of scour, m

$Q$  = Discharge through the bridge or on the overbank at the bridge, cumec

$$D_m = 1.25D_{50}$$

$D_{50}$  = Median diameter (m) of bed material in the bridge opening, or on the floodplain,

$W$  = Bottom width of the bridge less pier widths, or overbank width (set back distance), m

### **Compute the Magnitude of Local Scour at Piers**

Local scour at piers is a function of bed material size, flow characteristics, fluid properties and the geometry of the pier. The subject has been studied extensively in the laboratory, but there is limited field data. As a result of the many studies, there are many equations. In general, the equations, which give similar results, are for live-bed scour in cohesionless sand-bed streams.

To determine pier scour, the CSU equation [9] is recommended for both live-bed and clear-water pier scour. The equation predicts equilibrium pier scour depths. For plane-bed conditions, which is typical of most bridge sites for the flood frequencies employed in scour design, the maximum scour may be 10 percent greater than computed with CSU's equation. In the *unusual* situation where a dune bed configuration *with large dunes* exists at a site during flood flow, the maximum pier scour may be 30 percent greater than the predicted equation value. This may occur on very large rivers, such as the Mississippi. For smaller streams that have a dune bed configuration at flood flow, the dunes will be smaller and the maximum scour may be only 10 to 20 percent larger than equilibrium scour. For antidune bed configuration the maximum scour depth may be 10 percent greater than the computed equilibrium pier scour depth. In Table 4.1 values of the percent increase in equilibrium pier scour depths calculated with the CSU equation are given as a function of dune height  $H$ . These increases are tabulated as a correction (K3) to the CSU equation.

Table 4.1. Increase in Equilibrium Pier Scour Depths (K<sub>3</sub>) for Bed Condition

<i>Bed Condition</i>	<i>Dune Height H ft</i>	<i>K<sub>3</sub></i>
<i>Clear – water scour</i>		<i>1.1</i>
<i>Plane bed and Antidune flow</i>		<i>1.1</i>
<i>Small Dunes</i>	<i>10 &gt; H &gt; 2</i>	<i>1.1</i>
<i>Medium Dunes</i>	<i>30 &gt; H &gt; 10</i>	<i>1.1 to 1.2</i>
<i>Large Dunes</i>	<i>H &gt; 30</i>	<i>1.3</i>

Computing Pier Scour. The CSU equation for pier scour is:

$$\frac{y_s}{y_1} = 2K_1K_2K_3 \left( \frac{a}{y_1} \right)^{0.65} Fr_1^{0.43} \quad (4.9)$$

where  $y_s$  = scour depth, m

$y_1$  = flow depth directly upstream of the pier, m

$K_1$  = correction factor for pier nose shape from Table 4.2

$K_2$  = correction factor for angle of attack of flow from Table 4.3

$K_3$  = correction factor for bed condition from Table 4.1

$a$  = pier width, m

$L$  = length of pier m

$Fr_1$  = Froude Number =  $V_1/(gy_1)^{1/2}$

$V_1$  = Mean velocity of flow directly upstream of the pier, m/s

Table 4.2. Correction Factor  $K_1$  for Pier Nose Shape

Shape of pier nose	$K_1$
(a) Square nose	1.1
(b) Round nose	1.0
(c) Circular cylinder	1.0
(d) Sharp nose	0.9
(e) Group of cylinders	1.0

Table 4.3. Correction Factor  $K_2$  for Angle of Attack of the Flow

Angle	$L/a=4$	$L/a=8$	$L/a=12$
0	1	1	1
15	1.5	2	2.5
30	2	2.75	3.5
45	2.3	3.3	4.3
90	2.5	3.9	5

Note: The correction factor  $K_1$  for pier nose shape should be determined using Table 4.2 for angles of attack up to 5 degrees. For greater angles,  $K_2$  dominates and  $K_1$  should be considered as 1.0. If  $L/a$  is larger than 12, use the values for  $L/a = 12$  as a maximum.

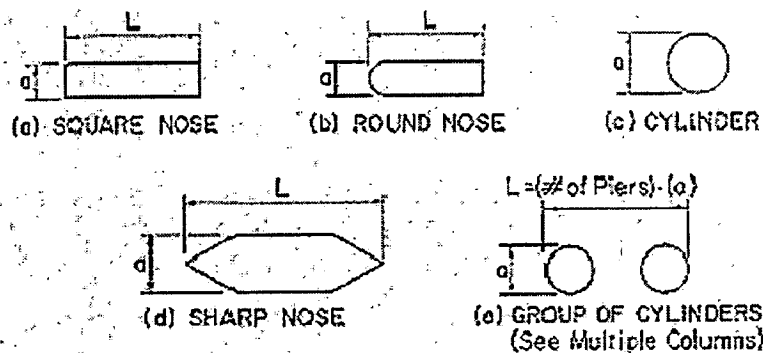


Figure 4.14. Common Pier Shapes

Multiple Columns. For multiple columns (as illustrated as a group of cylinders in Figure 4.14) skewed to the flow, the scour depth depends on the spacing

between the columns. The correction factor for angle of attack would be smaller than for a solid pier. The use of cylindrical columns would produce a shallower scour

In application of the CSU equation with multiple columns spaced less than 5 pier diameters apart, the pier width 'a' is the total projected width of all the columns in a single bent, normal to the flow angle of attack. For example, three 0.6 m cylindrical columns spaced at 3 m would have an 'a' value ranging between 0.6 and 1.8 m, depending upon the flow angle of attack. This composite pier width would be used in Equation 4.12 to determine depth of pier scour. The correction factor  $K_1$  in Equation 4.12 for the multiple column would be 1.0 regardless of column shape. The coefficient  $K_2$  would also be equal to 1.0 since the effect of skew would be accounted for by the projected area of the piers normal to the flow.

The depth of scour for a multiple column bent will be analyzed in this manner except when addressing the effect of debris lodged between columns. If debris is evaluated, it would be logical to consider the multiple columns and debris as a solid elongated pier. The appropriate  $L/a$  value and flow angle of attack would then be used to determine  $K_2$  in Table 4.3. should diminish.

Width of Scour Holes. The topwidth of a scour hole in cohesionless bed material from one side of a pier or footing can be estimated from the following equation:

$$W=y_s(K+Cot\theta) \quad (4.10)$$

where  $W$  = topwidth of the scour hole from each side of the pier or footing, m

$y_s$  = scour depth, m

$K$  = bottom width of the scour hole as a fraction of scour depth

$\phi$  = Angle of repose of the bed material and ranges from about 30 degrees to 44 degrees

If the bottom width of the scour hole is equal to the depth of scour  $y_s$  ( $K = 1$ ) the topwidth in cohesionless sand would vary from 2.07 to 2.80  $y_s$ . At the other extreme if  $K = 0$ , the topwidth would vary from 1.07 to 1.8  $y_s$ . Thus, the topwidth could range from 1.0 to 2.8  $y_s$  and will depend on the bottom width of the scour hole and composition of the bed material. In general, the deeper the scour hole, the smaller the bottom width. A topwidth of 2.8  $y_s$  is suggested for practical application.

### **Local Scour at Abutments**

Abutment scour depends on the interaction of the flow obstructed by the abutment and roadway approach and the flow in the main channel at the abutment. The discharge returned to the main channel at the abutment is not simply a function of the abutment and roadway length in the field case.

*Abutment Site Conditions.* Abutments can be set back from the natural streambank or project into the channel. They can have various shapes (vertical walls, spill-through slopes) and can be set at varying angles to the flow. Scour at abutments can be live-bed or clear-water scour. Finally, there can be varying amounts of overbank flow intercepted by the approaches to the bridge and returned to the stream at the abutment. More severe abutment scour will occur when the majority of overbank flow returns to the bridge opening directly upstream of the bridge crossing. Less severe abutment scour will occur when overbank flows gradually return to the main channel upstream of the bridge crossing.

Abutment Shape. There are three general shapes for abutments: (1) spill-through abutments, (2) vertical-wall abutments with wing walls (Figure 4.15), and (3) vertical walls without wing walls. Depth of scour is approximately double for vertical-wall abutments as compared with spill-through abutments.

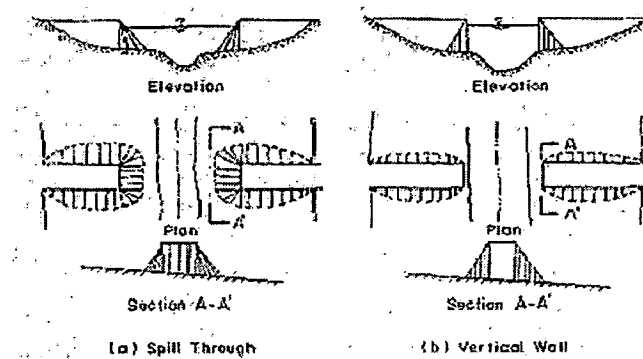


Figure 4.15. Abutment Shapes

Design for Scour at Abutments. The potential for lateral channel migration, long term degradation and contraction scour should be considered in setting abutment foundation depths near the main channel. It is recommended that foundation depths for abutments be set at least 1.8 m below the streambed, including long-term degradation, contraction scour, and lateral stream migration. Normally, protection is provided using rock riprap and/or guide banks. Scour at abutments is divided into its various cases and equations are given for each case is tabulated below

Table 4.4. Abutment scour cases

Case	Abutment location	Overbank Flow	Value of $a/y_1$	Bed load Condition	Abutment Type	Equation Number
1	Projects into Channel	No	$a/y_1 < 25$	Live bed	Vertical wall	4.13,4.15,4.17
					Spill-through	4.11,4.15,4.17
				Clear water	Vertical wall	4.14,4.16,4.18
					Spill-through	4.12,4.16,4.18
2	Projects into Channel	yes	$a/y_1 < 25$	Live bed	Vertical wall	4.15,4.19
				Clear water	Vertical wall	4.16,4.19
3	Set back from main channel	yes	$a/y_1 < 25$	Clear water	Vertical wall	4.16
4	Relief bridge on floodplain	yes	$a/y_1 < 25$	Clear water	Vertical wall	4.16



5	Set at edge of main channel	yes	$a/y_1 < 25$	Live bed	Vertical wall	4.15
6	Not designated	yes	$a/y_1 > 25$	Not designated	Spill-through	4.20
7	Skewed to stream	-	-	-	-	-

**Case 1. Abutments Project into Channel, No Overbank Flow**

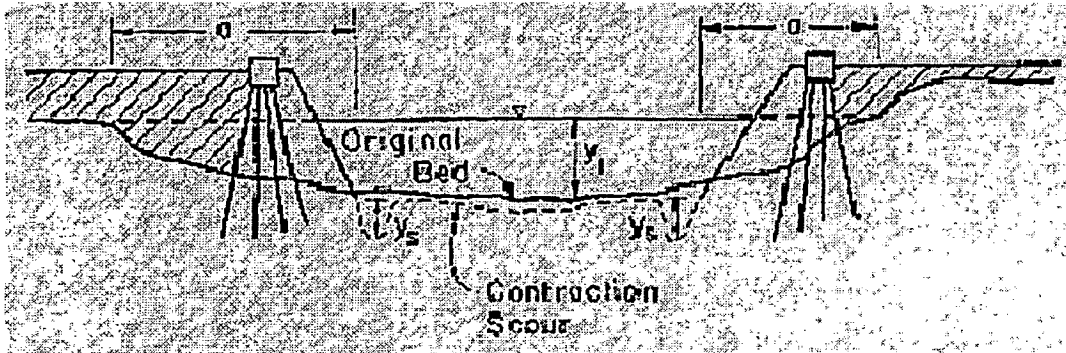


Figure 4.16. Abutments Project into Channel, No Overbank Flow

Six equations are given for this case. Two by Liu, et al (1), two by Laursen (2) and two by Froehlich (3).

**Liu, et. al.'s, Case 1 Equations**

Equation 1: Liu et al's (1) equation for live-bed scour at a spill through abutment.

According to the 1961 studies of Liu, et al., (1) the equilibrium scour depth for local live-bed scour in sand at a stable spill through slope with no overbank flow when the flow is subcritical is determined by Equation 4.11.

$$\frac{y_s}{y_1} = 1.1 \left( \frac{a}{y_1} \right)^{0.4} Fr_1^{0.33} \quad (4.11)$$

where  $y_s$  = equilibrium depth of scour (measured from the mean bed level to the bottom of the scour hole)

$y_1$  = average upstream flow depth

$a$  = abutment and embankment length (measured at the top of the water surface and normal to the side of the channel from where the top of the design flood hits the bank to the outer edge of the abutment)

$Fr_1$  = upstream Froude number

$$Fr_1 = \frac{v_1}{(gy_1)^{0.5}}$$

Equation 2: Liu et al's (1) equation for clear water scour at a spill through abutment.

$$\frac{y_s}{y_1} = 1.1 \left( \frac{a}{y_1} \right)^{0.4} Fr_1^{0.33} + 0.3 \quad (4.12)$$

Equation 3: Lui, et al's (1) equation for live bed scour at a vertical wall abutment.

$$\frac{y_s}{y_1} = 2.15 \left( \frac{a}{y_1} \right)^{0.4} Fr_1^{0.33} \quad (4.13)$$

Equation 3: Lui, et al's (1) equation for live bed scour at a vertical wall abutment.

$$\frac{y_s}{y_1} = 2.15 \left( \frac{a}{y_1} \right)^{0.4} Fr_1^{0.33} + 0.3 \quad (4.14)$$

### **Laursen's case 1 Equations**

Laursen's equation for live bed scour at a vertical wall abutment.

$$\frac{a}{y_1} = 2.75 \frac{y_s}{y_1} \left[ \left( \frac{y_s}{11.5y_1} + 1 \right)^{1.7} - 1 \right] \quad (4.15)$$

Laursen's equation for clear water scour at a vertical wall abutment.

$$\frac{a}{y_1} = 2.75 \frac{y_s}{y_1} \left( \frac{\left( \frac{y_s}{11.5y_1} + 1 \right)^{7/6}}{\left( \frac{\tau_1}{\tau_c} \right)^{0.5}} - 1 \right) \quad (4.16)$$

where  $\tau_1$  = shear stress on the bed upstream

$\tau_c$  = critical shear stress of the  $D_{50}$  of the upstream bed material.

Laursen's (1) scour depths for other abutment shapes.

Scour values given by Laursen's equations are for vertical wall abutments. He suggests the following multiplying factors for other abutment types for small encroachment lengths:

Abutment Type	Multiplying Factor
45 degree wing wall	0.9
Spill-Through	0.8

Froehlich's case 1 Equations

1. Live bed scour at an abutment.

$$\frac{y_s}{y_1} = 2.27 K_1 K_2 \left( \frac{a}{y_1} \right)^{0.43} Fr_e^{0.61} + 1 \quad (4.17)$$

where  $K_1$  = coefficient for abutment shape

$K_2$  = coefficient for angle of embankment to flow

$$K_2 = (\theta/90)^{0.13}$$

$\theta < 90^\circ$  if embankment points downstream

$\theta > 90^\circ$  if embankment points upstream

$a'$  = the length of abutment projected normal to flow, m

$A_e$  = the flow area of the approach cross section obstructed by the embankment,  $m^2$

$Fr_e$  = Froude Number of approach flow upstream of the abutment

$$Fr_e = V_e / (gy_a)^{1/2}$$

$$V_e = Q_e / A_e$$

$Q_e$  = the flow obstructed by the abutment and approach embankment, cumec

$y_1$  = average depth of approach flow, m

$y_s$  = scour depth, m

## 2. Clear-water scour at an abutment.

Froehlich (3) using dimensional analysis and multiple regression analysis of 164 clear-water scour measurements in laboratory flumes developed an equation for clear water scour. It is as follows:

$$\frac{y_s}{y_1} = 0.78 K_1 K_2 \left( \frac{a'}{y_1} \right)^{0.63} Fr_e^{1.16} \left( \frac{y_1}{D_{50}} \right)^{0.43} G^{-1.87} + 1 \quad (4.18)$$

where:  $K_1$  = coefficient for abutment shape

$G$  = geometric standard deviation of bed material

$$= (D_{84}/D_{16})^{0.5}$$

Description	$K_1$
Vertical abutment	1.00
Vertical abutment with wing walls	0.82
Spill through abutment	0.55

$D_{84}$ ,  $D_{16}$  = grain sizes of the bed material. The subscript indicates the percent finer at which the grain size is determined.

In using Froehlich's clear water scour equation the  $D_{50}$  of the bed and foundation material should be equal to or larger than 0.076m and  $G$  should be equal to or larger than 1.5.

### Comments on Case 1 Equations

1. These equations are limited to cases where  $a/y_1 < 25$ . For  $a/y_1 > 25$  go to Case 6.
2. Laursen's (2) equations are based on sediment transport relations. They give maximum scour and include contraction scour. For these equations, do not add contraction scour to obtain total scour at the abutment
3. Liu, et al's (1) equations are for a dune bed configuration. Therefore, for a dune bed configuration in the natural stream the scour given by their equations are for equilibrium scour and for maximum scour the values must be increased by 30 percent. For plane bed and antidune flow there are no equations given, but it is suggested that Liu, et al's equations could be used as given unless the antidunes would be occurring at the abutment.

### Case 2. Abutment Projects into Channel, Overbank Flow

No bed material is transported in the overbank area and  $a/y_1 < 25$ .

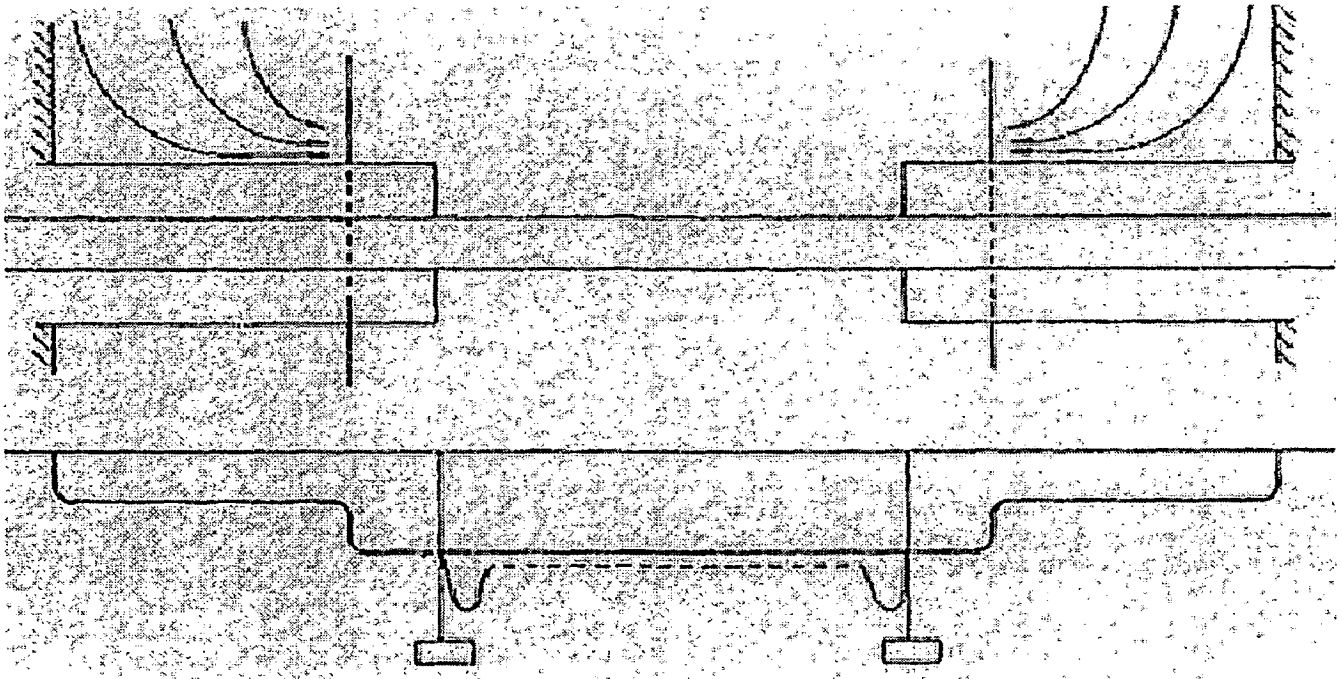


Figure 4.17. Bridge Abutment in Main Channel and Overbank Flow

Laursen's Equation 4.15 or Equation 4.16 should be used to calculate the scour depth with abutment length  $a$  determined by Equation 4.19

$$a = \frac{Q_o}{v_1 y_1} \quad (4.19)$$

where  $Q_o$  = Flow obstructed by abutment and bridge approach.

$y_1$  = Average upstream flow depth in the main channel.

$V_1$  = Average velocity in the main channel.

It is assumed that there is no bed material transported by the overbank flow or that the transport is so small that it will not decrease abutment scour.

**Case 3. Abutment Is Set Back from Main Channel More Than 2.75  $y_s$**

There is overbank flow with no bed material transport (clear water scour).

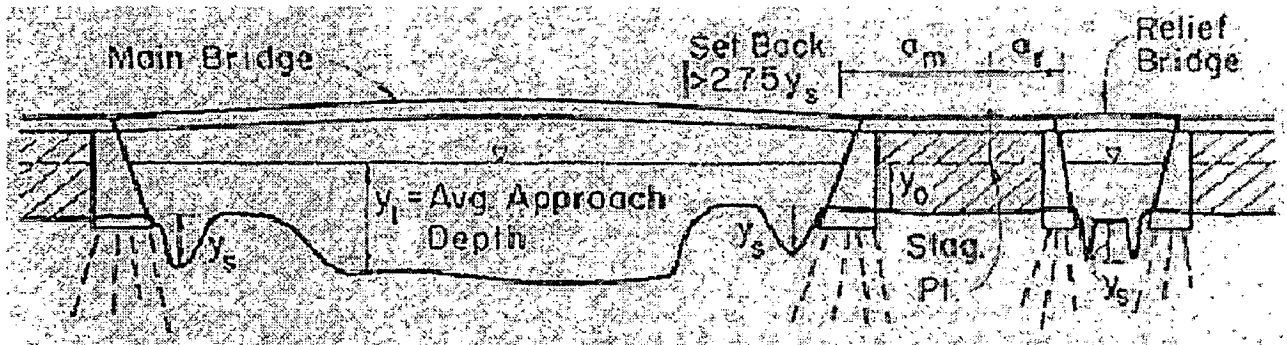


Figure 4.18. Bridge Abutment Set Back from Main Channel Bank and Relief Bridge

With no bed material transport in overbank flow, scour at a bridge abutment, set back more than 2.75 times the scour depth from the main channel bank line, can be calculated using Equation 4.16 from Laursen

#### Case 4. Abutment Scour at Relief Bridge

Scour depth for a relief bridge on the overbank flow area having no bed material transport is calculated using Equation 4.16 where  $y_1$  is average flow depth on the flood plain. If on the flood plain  $\tau_o > \tau_c$ , but there is no sediment transport or the sediment transported in the judgement of the engineer will not effect the scour, use Equation 4.16 with the shear ratio set to 1. Use  $a_r$  for  $a$  in the equation.

#### Case 5. Abutment Set at Edge of Channel

The case of scour around a vertical wall abutment set right at the edge of the main channel as sketched in Figure 4.19 can be calculated with Equation 4.15 proposed by Laursen when  $\tau_o < \tau_c$  on the flood plain or there is no appreciable bed material transport by the overbank flow.

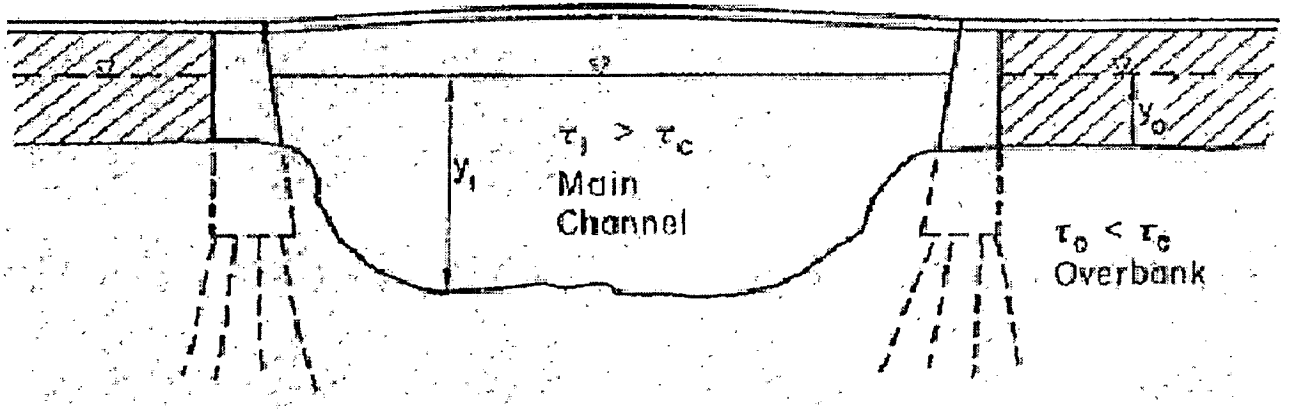


Figure 4.19. Abutment Set at Edge of Main Channel

**Case 6. Scour at Abutments when  $a/y_1 > 25$**

Field data for scour at abutments for various size streams are scarce, but data collected at rock dikes on the Mississippi indicate the equilibrium scour depth for large  $a/y_1$  values can be estimated by following equation:

$$\frac{y_s}{y_1} = 4Fr^{0.43} \tag{4.20}$$

**Case 7. Abutments Skewed to the Stream**

With skewed crossings, the approach embankment that is angled downstream has the depth of scour reduced because of the streamlining effect. Conversely, the approach embankment which is angled upstream will have a deeper scour hole. The calculated scour depth should be adjusted in accordance with the curve of Figure 4.20 which is patterned after Ahmad.



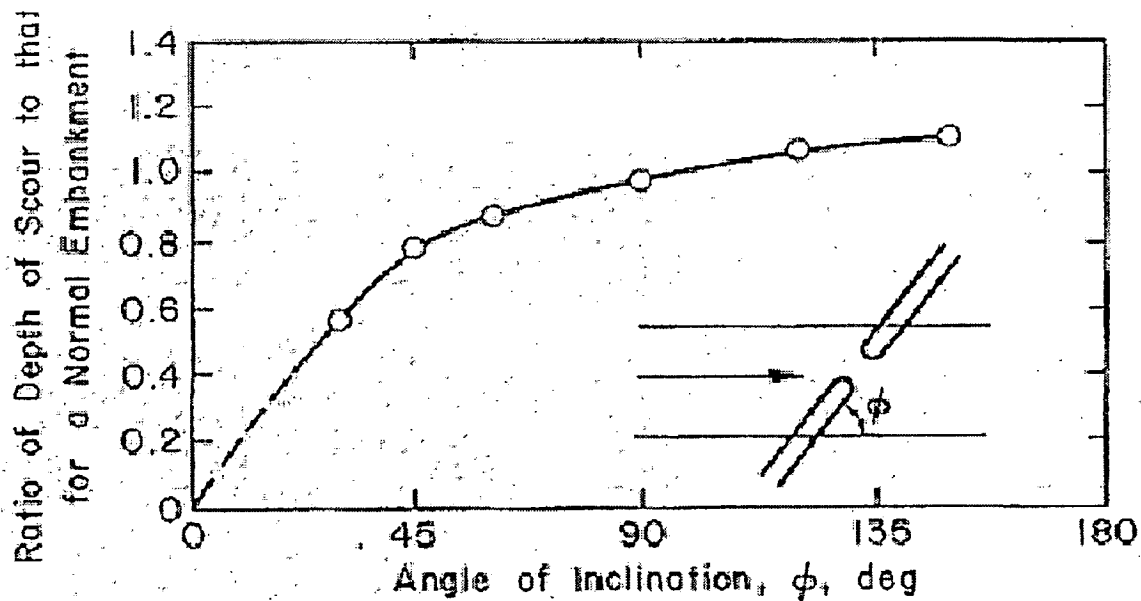


Figure 4.20. Scour Estimate Adjustment for Skew

### Example 2

(Scour Example Problem)

A 198 m long bridge is to be constructed over a channel with spill-through abutments (slope of 2H:1V). The left abutment is set approximately 64 m back from the channel bank. The right abutment is set at the channel bank. Six round-nose piers are evenly spaced in the bridge opening. The piers are 1.5 m thick, 12 m long, and are aligned with the flow.

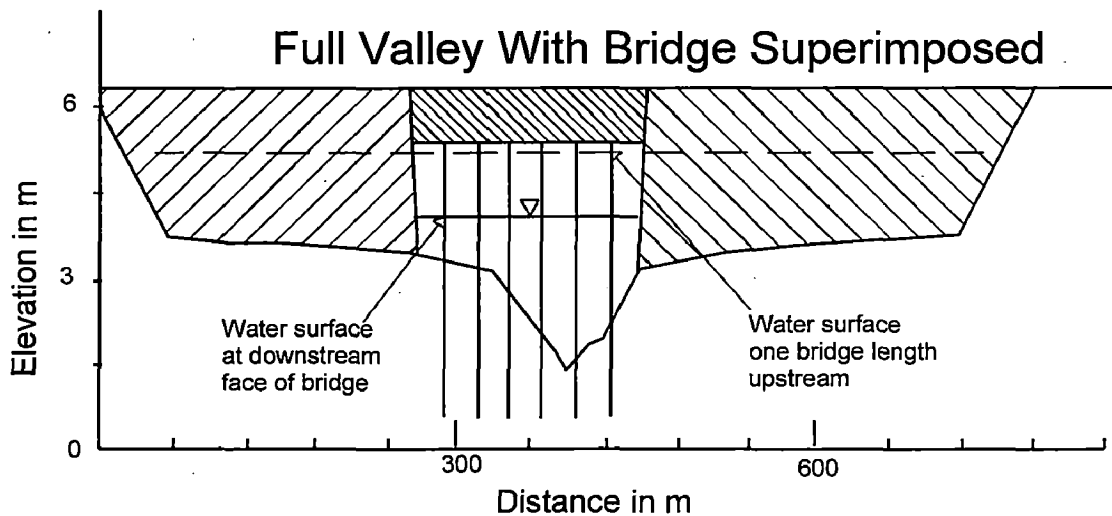
The 100-year design discharge is 850 cumecs.

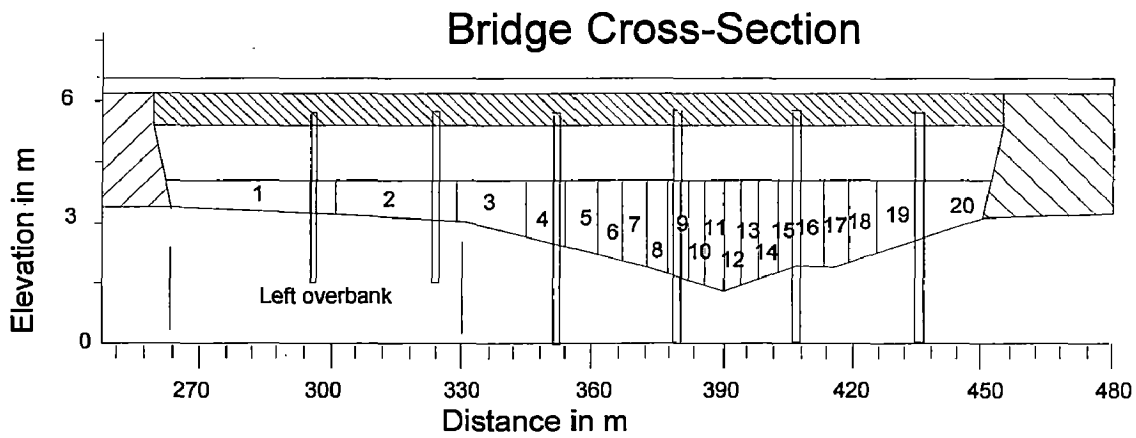
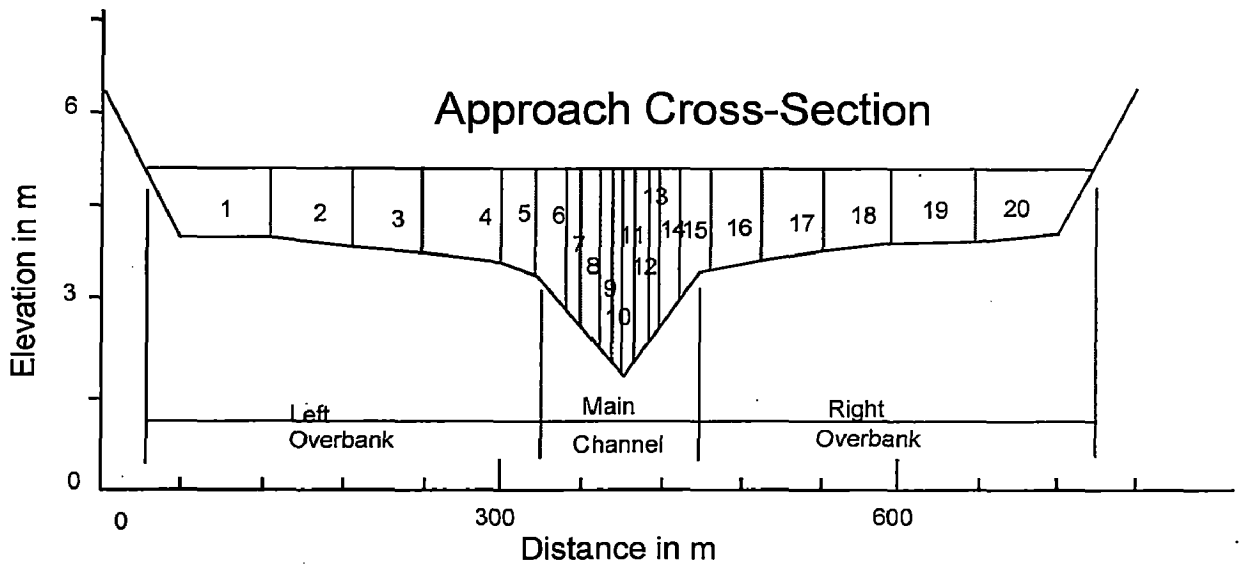
#### Step 1: Determine Scour Analysis Variables

Evaluation of the site indicates that the river has a relatively wide floodplain. The floodplain is well vegetated with grass and trees. However, the presence of remnant channels indicates that there is a potential for lateral shifting of the channel. The bridge crossing is located on a relatively straight reach of channel. The channel geometry is relatively the same for

approximately 1,000 feet upstream and downstream of the bridge crossing. The  $D_{50}$  of the bed material, and overbank material is approximately 2 mm. The maximum grain size of the bed material is approximately 8 mm. The river and crossing are located in a rural area with the primary land use consisting of agriculture and forest. Rock outcrops have been identified in the valley bottom approximately 914 m upstream and downstream of the bridge crossing; however, at the bridge site, bedrock is approximately 45 m below the channel bed.

Since this is a sand-bed channel, no armoring potential is expected. Furthermore, the bed for this channel at low flow consists of dunes which are approximately 0.3 to 0.45 m high. At higher flows, above the  $Q_5$ , the bed will be either plane bed or antidunes.





$$Q_c = Q(K_c/K_{total}) = 850(19283/40066) = 409 \text{ cumecs}$$

Critical velocity  $V_c = 11.52y^{1/6}D_{50}^{1/3}$

Where  $y = A_c/W = 322/122 = 2.64 \text{ m} = 8.67 \text{ ft}$ ;  $D_{50} = 0.002 \text{ m} = 0.0066 \text{ ft}$

$$V_c = 11.52 * (8.67)^{1/6} * (0.0066)^{1/3} = 3.1 \text{ ft/s} = 0.94 \text{ m/s}$$

Velocity through approach cross section

$$V = Q_c/A_c = 409/322 = 1.27 \text{ m/s}$$

Comparing  $V > V_c$  so condition for contraction scour and local scour computation is live – bed condition in main channel. On floodplain is covered by vegetation and grass so it is clear water condition

**Contraction scour for main channel**

Q(cumecs)	850
$K_c(\text{Approach})$	19283
$K_{\text{total}}(\text{Approach})$	40066
$W_1(\text{Approach})(\text{m})$	122
$A_c(\text{Approach})(\text{m}^2)$	322
TopW(Approach)(m)	122
WetP(Approach)(m)	122
$K_c(\text{Bridge})$	11119
$K_{\text{total}}(\text{Bridge})$	12274
$W_2(\text{Bridge})(\text{m})$	114
$S_f$	0.002

The hydraulic radius of the approach channel is:

$$R = A_c/P = 322/122 = 2.64 \text{ m}$$

The average shear stress on the channel bed is:

$$\tau = \gamma RS = 9.81 \times 2.64 \times 0.002 = 0.052 \text{ KN/m}^2$$

The shear velocity in the approach channel is:

$$V_* = (\tau/\rho)^{0.5} = (0.052/1)^{0.5} = 0.228 \text{ m/s}$$

$$D_{50} = 0.002 \text{ m we get fall velocity } (w) = 0.9 \text{ ft/s} = 0.274 \text{ m/s}$$

Therefore

$$V_*/w = 0.228/0.274 = 0.83$$

From table we get  $K_1 = 0.64$

$$Q_1 = Q(K_c/K_{\text{total}}) = 850(19283/40066) = 409 \text{ cumecs}$$

$$Q_2 = Q(K_c/K_{\text{total}}) = 850(11119/12274) = 770 \text{ cumecs}$$

Laursen's live-bed equation :

$$\frac{y_2}{y_1} = \left( \frac{Q_2}{Q_1} \right)^{6/7} \left( \frac{W_1}{W_2} \right)^{k_1}$$

$$\frac{y_2}{2.64} = \left( \frac{770}{409} \right)^{6/7} \left( \frac{122}{114} \right)^{0.64} = 1.8$$

So  $y_2 = 4.75 \text{ m}$  ;  $y_s = y_2 - y_1 = 4.75 - 2.64 = 2.11 \text{ m}$

### Contraction scour for left overbank

Q(cumecs)	850
Qchan(Bridge)(cumecs)	770
Q <sub>2</sub> Bridge)(cumecs)	80
D <sub>50</sub> (Bridge overbank)(m)	0.0022
Wsetback(Bridge)(m)	64
TopW <sub>left</sub> (Approach)(m)	302
A <sub>left</sub> (approach)(m <sup>2</sup> )	376

$Q = 850 - 770 = 80 \text{ cumecs}$  ;  $D_m = 1.25D_{50} = 0.0025 \text{ m}$

$$y_2 = \left[ \frac{Q^2}{35D_m^{2/3}W_{setback}^2} \right]^{3/7} = \left[ \frac{80^2}{35(0.0025)^{2/3}64^2} \right]^{3/7} = 1.46m$$

Flow depth in left overbank approach section  $y_1$ :

$$y_1 = A / \text{TopW} = 376 / 302 = 1.24 \text{ m}$$

$$y_s = y_2 - y_1 = 1.46 - 1.24 = 0.22 \text{ m}$$

### Compute the magnitude of local scour at piers

Area(m <sup>2</sup> ) (tube 12)	11.2
V <sub>1</sub> (m/s) (tube 12)	3.79
Topwidth(m)(tube 12)	4
Y <sub>1</sub> (m) (tube 12)	2.8

Using CSU's equation

$$\frac{y_s}{y_1} = 2K_1K_2K_3 \left( \frac{a}{y_1} \right)^{0.65} Fr_1^{0.43}$$

For a round nose pier aligned with the flow:

$$K_1=K_2=1$$

For plane-bed condition:

$$K_3=1.1$$

$$Fr_1 = V / (gy_1)^{0.5} = 3.79 / (9.81 \times 2.8)^{0.5} = 0.72$$

$$\frac{y_s}{2.8} = 2 \times 1 \times 1 \times 1.1 \left( \frac{1.5}{2.8} \right)^{0.65} 0.72^{0.43} = 1.28$$

$$y_s = 3.6 \text{ m and width of hole } W = 2.8 y_s = 10 \text{ m}$$

### Scour at left abutment

Q(cumecs)	850
$Q_{\text{tube}}$ (cumecs)	42.5
$A_{\text{tube}}$ (m <sup>2</sup> ) (Bridge)	32.2
$V_{\text{tube}}$ (m/s)	1.32
Top $W_{\text{tube}}$ (m)	39.5
$y_1$ (m)	0.82

$a/y_1 = 233/0.82 = 285 > 25$  therefore we use Hire's equation

$$\frac{y_s}{y_1} = 4Fr_1^{0.33}$$

Where  $Fr_1 = V / (gy_1)^{0.5} = 1.32 / (9.81 \times 0.82)^{0.5} = 0.47$

$$\frac{y_s}{y_1} = 4Fr_1^{0.33} = 3.12$$

$y_s=2.56$  m and width of hole  $W= 2.8 y_s = 7.2$  m

**Scour at right abutment**

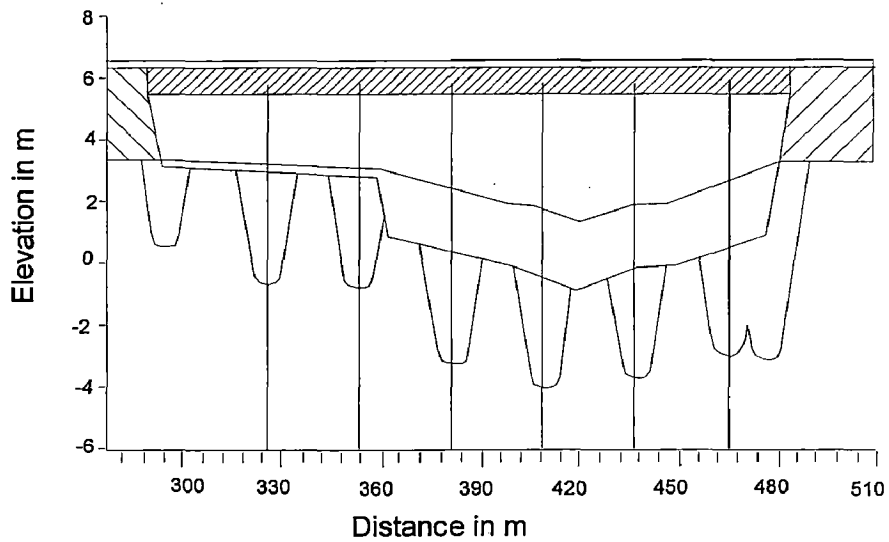
Q(cumecs)	850
$Q_{tube}$ (cumecs)	42.5
$A_{tube20}$ ( $m^2$ ) (Bridge)	22.78
$V_{tube20}$ (m/s)	1.86
Top $W_{tube1}$ (m)	18.2
$y_1$ (m)	1.25

$a/y_1 = 291/1.25 = 233 > 25$  therefore we use Hire's equation

$$Fr_1 = V/(gy_1)^{0.5} = 1.86/(9.81 \times 1.25)^{0.5} = 0.53$$

$$\frac{y_s}{y_1} = 4Fr_1^{0.33} = 3.25$$

$y_s=4.06$  m and width of hole  $W= 2.8 y_s = 11.4$  m



Plot of Total Scour

## Discussion of results

Three components of bridge scour are estimated which are Long-term aggradation and degradation, Contraction scour and Local scour. In this example, due to the lack of other possible impacts to the river reach, it is determined that the channel will be relatively stable vertically at the bridge crossing and long term aggradation or degradation potential is considered to be minimal. Hydraulic variables for performing the various scour computations were determined from the WSPRO(water surface profile computation) output is tabulated in tables above.

The contraction scour for main channel is computed by using the formula

$$\frac{y_2}{y_1} = \left( \frac{Q_2}{Q_1} \right)^{6/7} \left( \frac{W_1}{W_2} \right)^{k_1}$$

The depth of contraction scour for main channel  $y_s = 2.11$  m. The contraction scour for left bank is computed by using the formula

$$y_2 = \left[ \frac{Q^2}{120 D_m^{2/3} W_{setback}^2} \right]^{3/7}$$

The depth of contraction scour for left bank  $y_s = 0.22$  m

Local scour consist of pier scour and abutment scour. In computation pier scour , it is anticipated that any pier under the bridge could potentially be subject to the maximum flow depths and velocities Therefore, only one computation for pier scour is conducted and assumed to apply to each of the six piers for the bridge. This assumption is appropriate based on the fact that the thalweg is prone to shifting and because there is a possibility of lateral channel migration.

Computation pier scour by using the formula



$$\frac{y_s}{y_1} = 2K_1 K_2 K_3 \left( \frac{a}{y_1} \right)^{0.65} Fr_1^{0.43}$$

The depth of pier scour  $y_s = 3.6$  m ,width of hole  $W = 2.8 y_s = 10$  m

The formula use to compute abutment

$$\frac{y_s}{y_1} = 4Fr_1^{0.33}$$

The depth of left abutment scour  $y_s = 2.56$  m ,width of hole  $W = 2.8 y_s = 7.2$  m ,the depth of right abutment scour  $y_s = 4.06$  m and width of hole  $W = 2.8 y_s = 11.4$  m. Total depth scour is plotted in fig above.

It is important to carefully evaluate the results of the scour computations. For example, although the total scour plot indicates that the total scour at the overbank piers is less than for the channel piers, this does not indicate that the foundations for the overbank piers can be set at a higher elevation. Due to the possibility of channel and thalweg shifting, all of the piers should be set to account for the maximum total scour. The plot of the total scour also indicates that there is a possibility of overlapping scour holes between the sixth pier and the right abutment. During the plotting process, it is unclear where the right abutment scour should be measured from, since the abutment is located at the channel bank. Both of these uncertainties should be avoided for replacement and new bridges whenever possible. As such, it would be advisable to set the right abutment back from the main channel. This would also tend to reduce the magnitude of contraction scour in the main channel. The possibility of lateral migration of the channel will have an adverse effect on the magnitude of the pier scour. This is because lateral migration will most likely skew the flow to the piers. This problem could be minimized by using circular piers. An alternative approach would be to install guide banks to align the flow through the bridge opening. The usage of guide

banks would also minimize abutment scour. A final concern relates to the location and depth of contraction scour in the main channel near the second pier and near toe of the right abutment. At these locations, contraction scour in the main channel could increase the bank height to a point where bank failure and sloughing would occur. It is recommended that the existing bank lines be protected with revetment (i.e., riprap, gabions, etc.).

### **Conclusion**

In this chapter, we discuss hydraulic design of bridges. In hydraulic design of bridges typically include hydraulics of bridge waterway and evaluation scour of bridge. Due to bridge constriction, backwater is made and may inundate upstream of bridge. How much total depth of backwater, distance to point of maximum backwater and difference in water level across approach embankments are estimated in hydraulics of bridge waterway. Backwater also affect depth of bridge scour, difference in water level across approach embankments is large will make more depth scour of bridge. Bridge scour normally consist of long-term aggradation and degradation, contraction scour, and local scour. The recommended method is based on the assumption that three components scour of bridge develop independently. Thus, the potential local scour is added to the contraction scour without considering the effects of contraction scour on the channel and bridge hydraulics

## **CONCLUSION**

Culverts and bridges in any road project are so large that, together, they account for a considerable portion of the total expenditure. In the present study, hydrologic and hydraulic aspects of culvert and bridge design are studied and discussed. In the hydrologic design, the aim is to estimate the peak flood discharge that the structure is desired to pass safely. In this study, two methods, i.e., SCS-CN and Kinematics methods are discussed in detail. The SCS-CN method has several advantages over other methods. It is a simple conceptual method for estimation of the direct runoff amount from a storm rainfall amount and is well supported by empirical data. It can reliably be applied to small, mid or large size catchments upto 250 sq.km. But there are several problems associated with the SCS-CN method, such as it does not contain any expression for time and ignores the impact of rainfall intensity and its temporal distribution. The kinematic wave model of the rainfall-runoff process offers the advantage over the unit hydrograph method that it is a solution of the physical equations governing the surface flow, but the solution is only for one-dimensional flow, whereas the actual watershed surface flow is two-dimensional as the water follows the land surface contour. As a consequence, the kinematic wave parameters, such as Manning's roughness coefficient, must be adjusted to produce a realistic outflow hydrograph.

Computers have very wide applications in the design of hydrologic Engineering. Two computer programs are written to solve problems in hydrologic study. It can be used on any personal computer and the language used is C++.

In the hydraulic design of culverts, velocities of less than about 0.5 m/s usually results into faster deposition of sediment and therefore 0.5 m/s is recommended as a minimum velocity for culvert design and operation. For economy and hydraulic efficiency, engineers should design culverts to operate with the inlet submerged during flood flows.

In the hydraulic design of bridges, backwater effects and scour are the two main parameters that are required to be considered. The method of computing backwater as presented is intended to be used for relatively straight reaches of streams having sub-critical flow and approximately uniform slope.

Design the bridge waterway opening to provide a flow area sufficient to maintain the through-bridge velocity at no greater than the allowable through-bridge velocity under the circumstances of design discharge. Generally, the waterway opening defined by the following should cause an average through bridge velocity of 6 fps (1.8 m/s) or less.

If the intrusion of either or both roadway headers into the stream floodplains is more than about 800 ft. (240 m), consider including either relief openings or guide banks.

One foot of backwater may be an upper limit. On the other hand, for sites with stable river channels, the backwater can be increased accordingly.

Total depth of scour due to bridge constriction, may make loss of bridge, so we should found foundation of piers and abutments below line profile of total scour depth a minimum depth of 2 meter. When bridge constrict river, velocity through bridge will increase , make bank failure and sloughing would occur. We should provide revetment (i.e., riprap, gabions, etc) to protect the existing bank lines. An alternative approach would be to

install guide banks to align the flow through the bridge opening. The usage of guide banks would also minimize abutment scour.

### **Scope for future work**

Debris accumulation at culvert and bridge structures openings is a widespread problem. The accumulation of debris at inlets of highway culverts and bridge structures is a frequent cause of unsatisfactory performance and malfunction. This accumulation may result in erosion at culvert entrances, overtopping and failure of roadway embankments and damage to adjacent properties, increased local scour at piers and/or abutments, and the formation of pressure flow scour. Consideration of debris accumulations and the need for debris-control structures should be an essential part of the design of all drainage structures.

Pier and abutment scour has been extensively studied in the past for uniform and graded sediment mixtures. In general, pier scour equations account for the variation in sediment properties by either including a correction factor for sediment gradation or by using median size and the gradation coefficient in developing the experimental regression equations.

The scour of cohesive materials is fundamentally different from that of noncohesive materials. It involves not only complex mechanical phenomena, including shear stress and shear strength of soils, but also the chemical and physical bonding of individual particles and properties of the eroding fluid. Cohesive materials, once eroded, remain in suspension such that clear-water scour conditions always prevail. So we should apply the knowledge gained in the past in cohesive material scour to local pier and abutment scour.

## REFERENCES

1. Arora, K.R. ,(2002), “*Irrigation Water Power and Water Resources Engineering*”, A book published by Standard Publishers and Distributors, Delhi, pp 107-132.
2. Dr. E.V. Richardson, L.J. Harrison, Dr. J.R. Richardson & S.R.Davis., (1993). “*Evaluating Scour at Bridges*”, A manual published by Hydraulics & Geotech Br.FHWA, HNG-31 Washington, D.C, pp 10-77
3. Department of Main Roads,(2002), “*Road Drainage Design Manual*”, Published by Queensland Government ,pp 4.10-4.28.
4. Edward Kuiper, (1965), “*Water Resources Development*”, Butterworth & Co. (Publishers) Ltd, London, pp 123-132.
5. Hydrologic Engineering Center, (1998), “*Flood Hydrograph Package*”, US Army Corps of Engineers Hydrologic Engineering Center (Hec), pp 8-24.
6. Joseph N. Bradley ,(1978) , “*Hydraulics of Bridge Waterways*”, A manual published by Bridge Division of U.S. Federal Highway Administration, pp 23-43.
7. Jerome M. Normann, Robert J. Houghtalen, (2001), “*Hydraulic Design of Highway Culverts*”, Ayres Associates Ft. Collins, CO, pp 1-70
8. Kanhu Charan Patra, (2002), “*Hydrology and Water Resources Engineering*”, Published by Narosa Publishing House, pp 324-408
9. Ken Bohuslav, P.E, (2004), “*Hydraulic Design Manual*”, Published by the Texas Department of Transportation, Design Division ,pp 259-374.

10. Kent E. Cotdes and Rollin H. Hotchkiss, (1993), "*Design Discharge of Culverts*", A Research Report by Department of Civil Engineering University of Nebraska-Lincoln, pp 36-52.
11. Predwojsk, B. I, R.Blazejewski and Pilarczyk, K.W.,(1995), "*River Training Techniques*", A.A.Balkema Publishers, Netherlands, pp 405-409.
12. Pierre Y.Julien. ,(2002), "*River mechanics*", Published by University of Cambridge Press, United Kingdom, pp 310-315.
13. Subramanian, K ,(2003), "*Engineering Hydrology*" ,Tata McGraw-Hill, New Delhi , pp 193-219
14. Soil Conservation Service (1986), "*Urban Hydrology for small watersheds*", Revised Technical release 55. U.S.Deptt. of Agriculture, Washington D.C ,pp 85-129
15. Santosh Kumar Garg, (2005), "*Irrigation Engineering and Hydraulic Structures*", Khanna Publishers, Delhi, pp 775-788.
16. Tideman, E.M, (1996). "*Watershed Management*"- Guidelines for Indian Conditions, A book published by Omega Scientific Publishers, New Delhi, pp 79-100.
17. Ven Te Chow, David R.Maidment and Larry W.Mays (1988), "*Applied Hydrology*", McGraw Hill Book Co., New York, pp 140-154.
18. Vijay P. Singh, (1997), "*Kinematic Wave Modeling In Water Resources*" , Published by John Wiley& Sons, Inc, pp 226-233.
19. W.F.Chen, (1995), "*Civil Engineering Handbook*", Published by CRC Press,Inc, pp 1124-1129.